A DETAILED ANALYSIS OF THE HELICAL ARRAY AS A HIGH PERFORMANCE PORTABLE GROUND STATION ANTENNA

by

Neil D. Fox

Thesis Submitted to the Faculty of the

Virginia Polytechnic Institute and State University

in partial fulfillment of the requirements for the degree of

MASTER OF SCIENCE

in

ELECTRICAL ENGINEERING

APPROVED:

Dr. F. Ricci, Chairman

Dr. D.A. de Wolf

Dr. W. Stutzman

March, 1988

Blacksburg, Virginia

A DETAILED ANALYSIS OF THE HELICAL ARRAY AS A HIGH PERFORMANCE PORTABLE GROUND STATION ANTENNA

by

Neil D. Fox

Committee Chairman: Dr. Fred Ricci

Electrical Engineering

(ABSTRACT)

Modern satellite operations often require a portable ground station capability. However, the traditional large parabolic dish solidly mounted in concrete is not conducive to portable operation. This work offers the helical array as a viable alternative. A critical literature survey shows what work has been performed by others, and what issues must be addressed so that a feasible helical array design may be put forth. Analysis was performed using data from experiments and from a computer simulation.

ACKNOWLEDGEMENT

I would like to thank my advisors, Dr. Fred Ricci, Dr. Warren Stutzman, and Dr. David de Wolf for their cooperation thoughout the course of my work. I would also like to thank

for their assistance at the antenna test range facility. Finally, I would like to thank my wife and parents for helping me keep a proper perspective.

I dedicate this work to my wonderful wife, who I thank for her support and understanding throughout the course of my education.

TABLE OF CONTENTS

Chapter 1: Introduction

1.0 Introduction

Modern satellite communications systems often require a portable ground station capability. Portable ground stations afford a system flexibility not possible with fixed ground stations. For instance, it is sometimes desirable for downlink information (the satellite to earth link) to reach a specific location in a timely manner. This location is often not in the vicinity of a fixed ground station. One solution is to simply build a fixed ground station when and where needed. This option is expensive and requires months of construction. However, a portable ground station can be transported from site to site. Since construction only occurs once, set-up time at a site can be as short as a few hours.

Unfortunately, there exists a serious barrier to portable operation for high performance satellite systems. The ground station antenna is traditionally a large parabolic dish solidly mounted in concrete; obviously not a portable antenna. Therefore, it is necessary to develop new antennas amenable to portable ground station operation. This work addresses this issue by examining the helical array as a candidate antenna.

1.1 Objective

The primary objective of this work is to characterize the figure-of-merit, G/T, for a prototype helical array. A graph of G/T versus elevation angle (angle the satellite is above the horizon) is sufficient to determine communications windows, given the corresponding link budgets. Therefore, given the results of this work, one can easily evaluate the helical array for a given satellite system. Figure 1.1-1 shows this process. The secondary objective is to design a small, lightweight, portable antenna that maximizes G/T. This antenna is a helical array. Although the helix is a well-known antenna, not much work has been performed with high-gain helices in an array. Methods of improving performance of the helical element and the helical array are presented. This work also examines the behavior of the helix itself.

1.2 Scope

The scope of this work is the design and analysis of helices and helical array antennas. There are a variety of ways to examine the helical antenna. This work is limited by finite resources.

1.2.1 Frequency

The experiments were performed at 1.3 GHz. This frequency was chosen because it lies in the so-called "L-band," which is a commonly

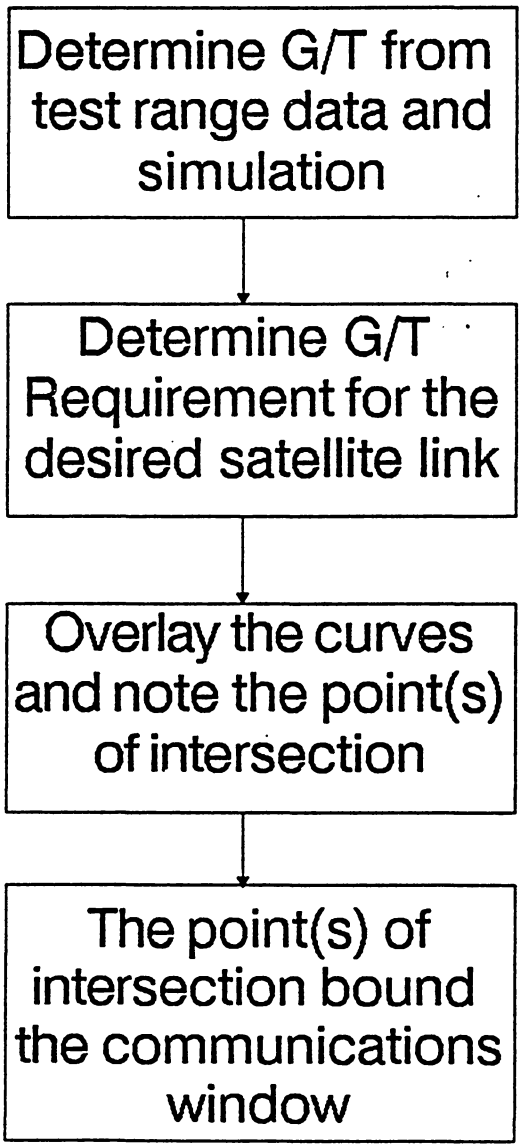

Figure 1.1 – 1 :The Communications Window Can Be Determined

used band for satellite downlinks. Also, much previous work has been done in this frequency range. Background work in the form of a literature survey, however, deals with the entire frequency range in which the helix is a practical antenna; roughly 400 MHZ to 10 GHz.

1.2.2 Experimentation

The number of tests was limited by available time at an antenna test range. Also, material cost and construction was a factor. To simplify matters, the "uniform" (cylindrical) helix was the elementary test item. This inexpensive helix was easy to construct. Although there is some evidence that multiple winding helices exhibit superior gain characteristics[1,37], they are not considered in this work because of the somewhat complicated feed assembly.

Each test was designed to produce the maximum useful data. For example, the effect of phasing two elements was examined as part of the prototype helical array test. Laboratory equipment was used to perform testing (impedance measurements) to minimize the number of adjustments performed at the test range.

Chapter 2: Problem Statement and Approach

2.0 Problem Statement and Approach

This work addresses a unique space system problem: how to implement a portable ground station. As stated earlier, the primary barrier to portable operation is the antenna. This section shows how satellite communications requirements drive antenna requirements, and introduces the approach of this work.

2.1 Link Budget

The communication link budget drives antenna requirements. Good link budget design, whenever possible:

- Maximizes Transmitter Effective Isotropic Radiated Power (EIRP)
- Maximizes Antenna Gain on the Receive Side, G_{rec}
- Minimizes Receive System Noise Temperature, T_{sys}
- Minimizes Channel Bandwidth (or equivalently, the data rate), BW
- Minimizes Space and Atmospheric Losses (Frequency and Orbit Selection), L_s and L_a, respectively
- Minimizes Polarization Loss, L_p

The link budget equation (2.1-1) shows the interaction of these parameters.

$$EIRP = L_a + L_s + L_p + k_{dB} + BW_{dB} - G/T + S/N \qquad (2.1\text{-}1)$$

where

BW_{dB} is 10log(BW), BW in Hz
S/N is the required signal-to-noise ratio in dB
k_{dB} is Boltzmann's constant (-226.6 dBW/K/Hz)
Note: L_a, L_s, L_p, and G/T are in dB

The goal of link budget design is to maximize the signal-to-noise ratio at the receiver. If the satellite has already been placed in orbit, the only variable link parameter is the so-called figure-of-merit, G/T. (The potential use of signal-processing techniques is neglected). This means that the designer is constrained to maximizing antenna gain and minimizing receive system noise, T_{sys}. With the signal-to-noise ratio required for detection defined, the figure-of-merit threshold is set. Since L_s and L_a are a function of elevation angle (angle of the satellite above the horizon), so is G/T. Therefore, it is informative to construct a curve of required G/T versus elevation angle for a particular satellite link. If a curve representing the actual G/T as a function of elevation is drawn over the "threshold" curve, then it is easy to identify the communications window; this is, the angle at which the signal is acquired and the angle at which the signal is lost. This threshold curve is derived from equation (2.1-1) for elevation angles between 0 and 90^{o}. Figure 2.1-1 shows the signal acquisition point for a hypothetical satellite link. The link budget for the threshold curve assumes that only the factors given in equation (2.1-1) are significant, and not other factors such as interference from

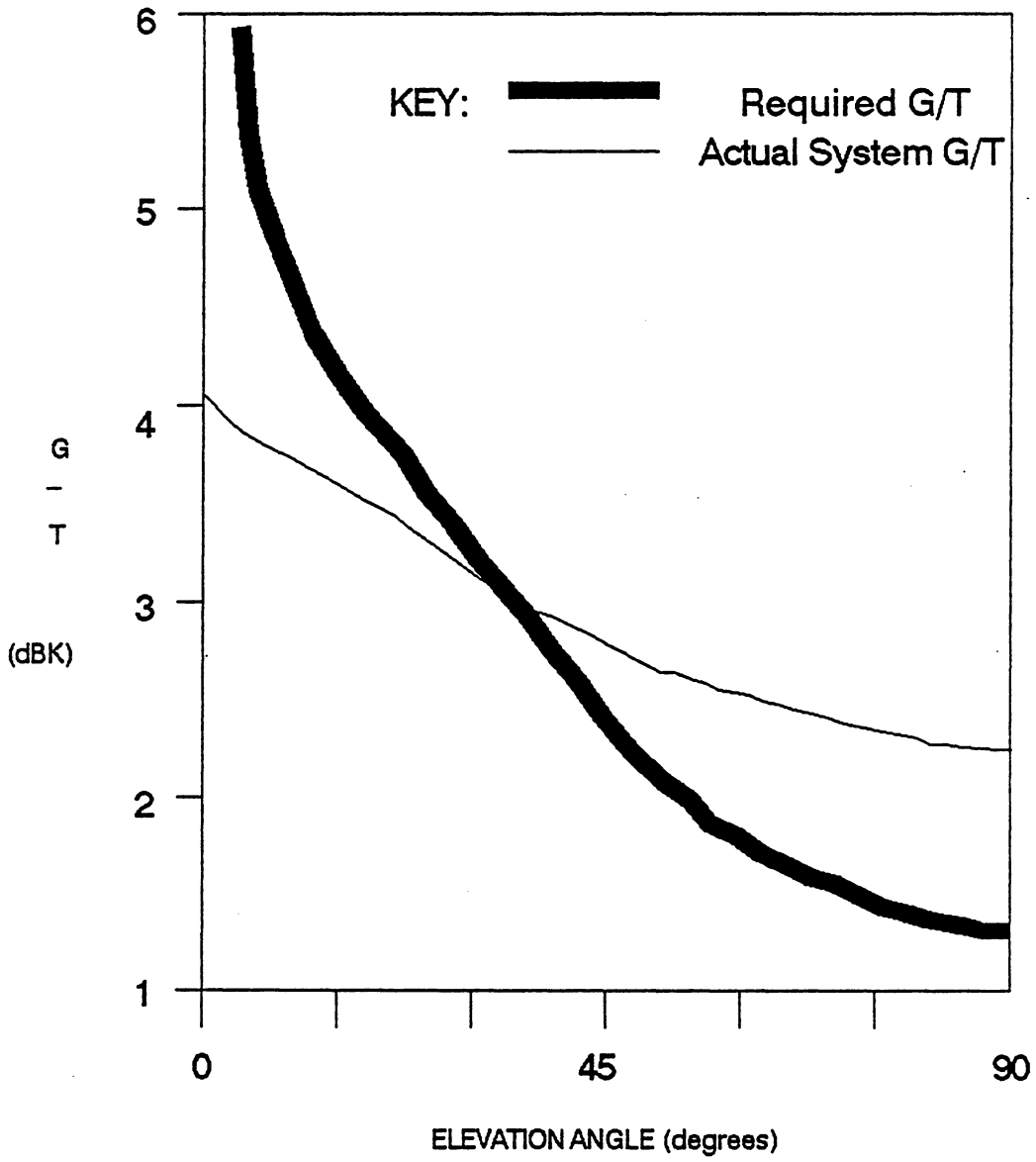

Figure 2.1 – 2 : Communication Window is 40 to 90 Degrees Elevation

various transmitters. Several sources contribute to the system noise temperature:

- o Sky Noise, T_{sky}
- o Ground Noise, T_{ground}
- o Internal (Electronic) Noise, T_{RF}

If the noise figures of the ground station equipment are known, it is a simple matter to calculate the RF equipment noise.

The noise contribution from the sky, T_{sky}, and ground, T_{ground}, is computed by integrating the antenna pattern times the noise temperature distribution as shown in equation (2.1-2)[39].

$$T_A(\Theta,\phi) = \frac{1}{4\pi}\int_0^{\pi}\int_0^{2\pi} G(\theta,\phi)T'(\theta-\Theta_0,\phi-\phi_0)\sin\theta\, d\phi\, d\theta \qquad (2.1\text{-}2)$$

where

$T_A(\Theta,\phi)$ is the antenna noise temperature (Kelvin)
$T(\Theta-\Theta_O,\phi-\phi_O)$ is the environmental noise temperature (Kelvin)
$G(\Theta,\phi)$ is the (gain) pattern of the antenna

This relationship can include the effects of scattering and reflection if $T(\Theta-\Theta_O,\phi-\phi_O)$ includes these effects.

With other sources of noise neglected, the total noise temperature is simply the sum of the antenna noise temperature, T_A, the feed and

cable noise temperature, T_{insert}, and the effective noise temperature of the RF electronics, T_{RF}.

Obviously, if the designer is given an infinite volume in which to operate, antenna size is not an issue. This is certainly not true for portable operation. Restricting size places an upper bound on gain.

So the problem of increasing G/T reduces to one of decreasing the noise temperature and increasing antenna efficiency. However, there are physical antenna requirements in addition to G/T. These requirements are discussed in the following section.

2.2 Portable Ground Station Requirements

Portable ground station operation imposes stringent electrical and mechanical requirements. Pointing accuracy is important, particularly if open loop tracking is used. The effects of wind and vibration are minimal for a fixed site antenna mounted in concrete. However, the portable antenna must have provisions to ensure proper track even under vibration and in wind. The beamwidth can be increased to compensate for this effect (assuming satellite isolation is not an issue).

The physical size and weight of the antenna is also important. The antenna must be transportable and amenable to some transportation (plane, train, ship, or towed). Also, the antenna cannot be unwieldy. Set-up time is often important, so the antenna must not be so cumbersome

that a few people (five or less) have difficulty preparing the antenna for operation.

2.3 The Helical Array

The helical array is a viable portable ground station antenna. It is "volumetrically efficient"; that is, it provides considerable gain per unit of swept volume. It is a circularly polarized antenna which is important for nearly all space communications systems to overcome the problem of Faraday rotation. The axial ratio is low and the array gain is high over a large frequency range. Simple construction of the helical elements makes reproducibility of performance parameters likely. Lightweight materials can be used to reduce overall antenna weight without degrading electrical performance.

2.4 Unanswered Questions

Several questions must be addressed before the helical array can fully satisfy portable ground station requirements. The type of helix must be determined. For example, the element spacing in the array must be optimized. This is done by reducing the mutual coupling between helical elements and finding the best array factor for desired pattern characteristics. Reference [46] gives a detailed discussion of mutual coupling and the array factor.

An efficient design procedure is needed. Time on an antenna test range is expensive and should be minimized. However, accuracy must not be sacrificed to the point where the designer has little confidence that the resulting antenna will meet requirements.

The helix can be tapered or be made conical and can be wound with either wire or conductive tape of varying thickness. The different deviations from the "uniform" helix change:

- Bandwidth, BW
- Axial Ratio, AR
- Gain, G
- Sidelobe Level

Antenna bandwidth, for this work, is defined as:

$$BW = f_{3\ dB,high} - f_{3\ dB,low}\ [Hz]$$

where

$f_{3\ dB,low}$ is the frequency on the low side of the center frequency, f_o, where the gain is 3 dB below the maximum gain (the gain at f_o)

$f_{3\ dB,high}$ is the frequency on the high side of the center frequency, f_o, where the gain is 3 dB below the maximum gain (the gain at f_o).

Some researchers in the literature have expressed bandwidth as a percentage of the center frequency:

$$BW_{\%} = BW_{Hz}/f_o \times 100\ \%$$

Unless otherwise specified, bandwidth shall refer to the 3 dB bandwidth. If the bandwidth is defined as the 1 dB bandwidth, the above definition applies, but $f_{3\ dB,low}$ and $f_{3\ dB,high}$ are replaced by the corresponding 1 dB frequencies.

The feed network must be low-loss and low-noise. Also, it should be designed to minimize crosstalk and thereby reduce mutual coupling.

Sidelobe level must be minimized to reduce T_{sky} and T_{ground} contributions. Many sidelobe reduction techniques exist. This is a major issue since the uniform helix tends to have a rather high sidelobe level. These minor lobes also contribute to mutual coupling between helical elements in the array.

Finally, the exact physical dimensions of the helix and the helical array must be determined. Some key dimensions requiring specification are:

- o Helix Diameter, D
- o Helix Length, L
- o Pitch Angle, α
- o Conductor Width, W
- o General Helix Shape

2.5 Approach

Three efforts were used to resolve important issues:

- o Critical Literature Survey
- o Experimentation
- o Computer Simulation

The results of each are compared so that reasonable qualitative and quantitative conclusions can be drawn. Specifically, helical array gain as a function of element spacing will be determined as will the effects of mutual coupling on array gain. Information will also be given on the helix, itself. These results are given in the following chapters.

Chapter 3: Critical Literature Survey

3.0 Critical Literature Survey

A critical literature survey was performed to gather and evaluate pertinent information. This information concerns both the helix and the helical array. While a good deal of the open literature deals with the more theoretical aspects of this topic, much information exists regarding practical applications. This literature survey is comprehensive in that it includes information for the various types of helices over the time period, 1947-1987.

3.1 Background Information

General information regarding the helix was collected as background information. The physical dimensions, operational modes, and pattern characteristics have been exhaustively researched. The results given in the following sections characterize helix properties.

3.1.1 Physical Dimensions

Figure 3.1.1-1 illustrates the four physical parameters of the uniform helix:

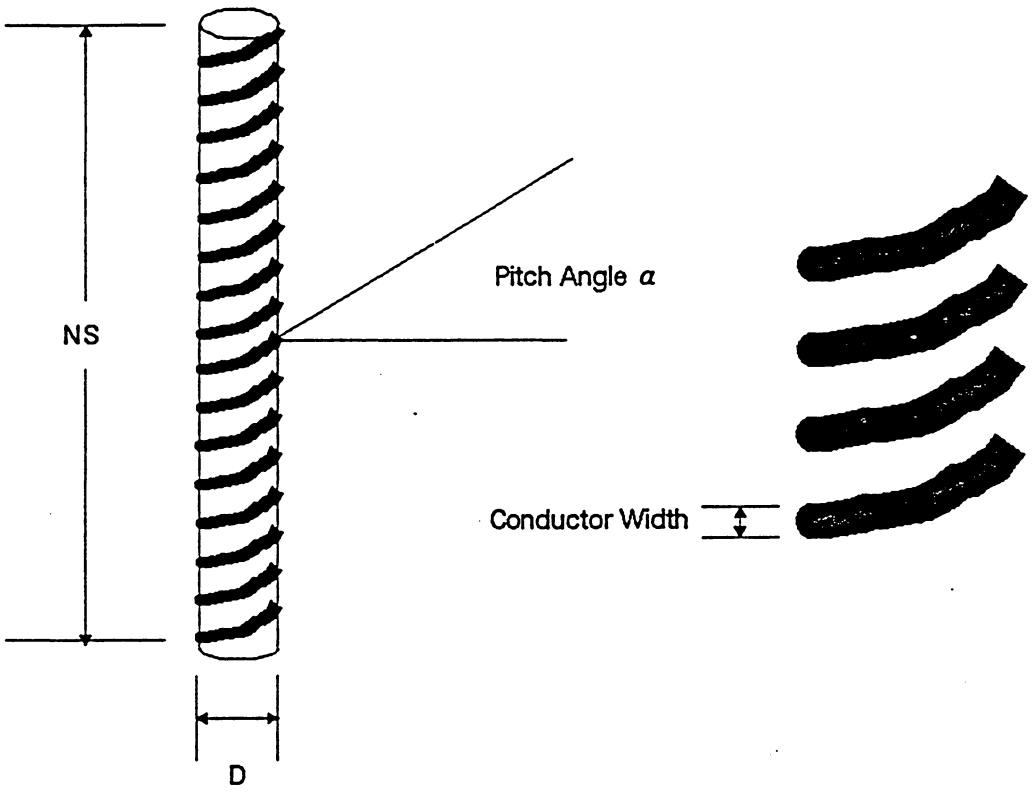

N is number of turns

D is the diameter

S is the spacing between turns

Figure 3.1.1 – 1: Dimensions of the Standard Helix

- o Pitch Angle, α
- o Conductor Width, W
- o Number of Turns, N
- o Helix Diameter, D

As will be shown in the next section, the parameters must be constrained for the helix to produce high forward gain. The helix circumference must be on the order of one wavelength. Some have found the optimal value of the circumference to be 1.1 wavelengths[2,3].

Some experiments have shown that a pitch angle of 12.5^{o} maximizes the forward gain[4,5]. Figure 3.1.1-2 [6], however, shows gain to vary inversely with pitch angle. This indicates that the smallest pitch angle for which the helix operates in the axial mode, 11^{o}, should be used. Nevertheless, most researchers have preferred a pitch angle near 12.5^{o} for axial mode helices.

For short helices, (length less than 4 wavelengths) gain, G, varies linearly with length. Figure 3.1.1-3 shows the relationship[7]. Note the saturation effect for long (greater than 4 wavelengths) helices.This curve was generated for a modified (tapered) helix, but the general characteristic is the same for the uniform helix. Figure 3.1.1-3 also shows that the helix circumference for maximum gain decreases toward one wavelength as the number of turns increases.

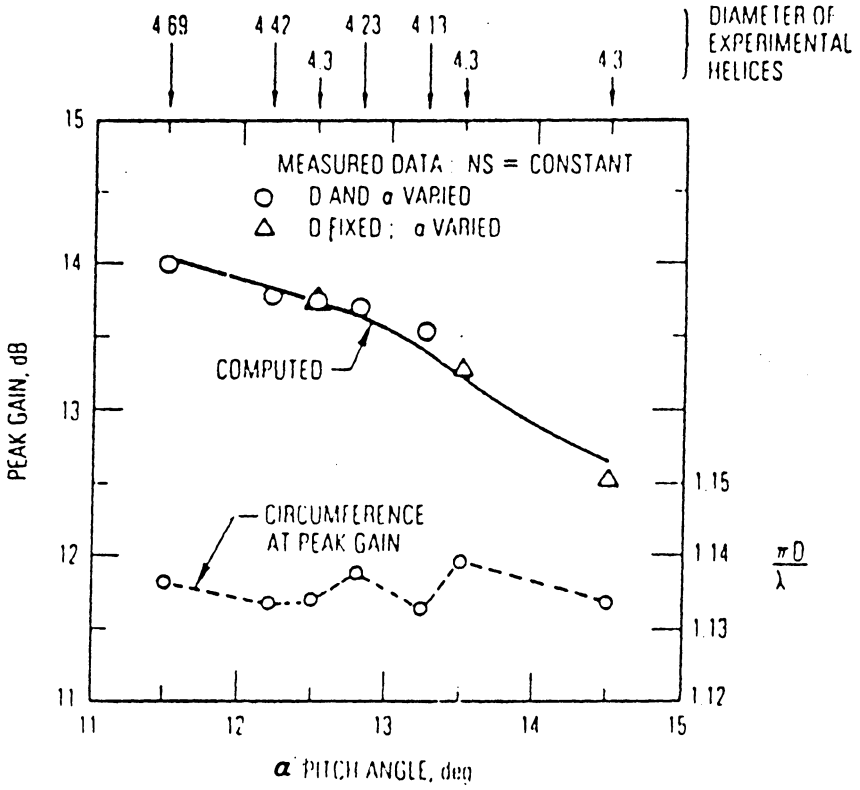

Peak gain of fixed length helix (NS = 30 in) as function of pitch angle.

Figure 3.1.1 – 2: Gain Varies with Pitch Angle [6]

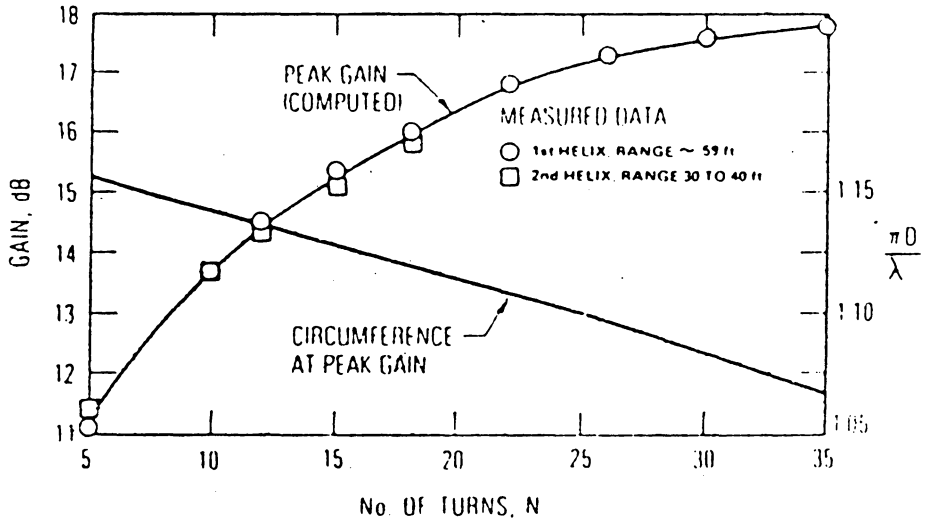

Peak gain characteristics of 4.23-in diameter helix; $\alpha = 12.8^{\circ}$

Figure 3.1.1 – 3: Gain Saturation Occurs for Long Helixes [6]

The conductor width, W, has theoretically and experimentally been shown to be not critical to helix performance[8].

3.1.2 Operating Modes

Although the helix has many modes of operation, only two, the so-called normal and axial modes, are of any practical interest.[4] Figure 3.1.2-1 shows the basic radiation pattern shapes for these modes. Quite obviously, the normal mode is not a suitable array element for an endfire array. In addition, it is a very narrow-band antenna [40] and its physical dimensions are very restrictive[45]. The circumference must be less than approximately 0.5 wavelengths and the number of windings must be less than three[4,45].

When operating in the axial mode, the helix provides high forward gain over a broad bandwidth. The pitch angle, circumference, and length of the helix must meet the restrictions given in Table 3.1.2-1 [4,45].

The traveling-wave model of the helix is often considered to explain the behavior of the helix in the axial and normal modes. In the simplified model, there are three traveling-wave modes on the helix[9]. Figure 3.1.2-2 shows each of these modes as well as the associated phase velocities, P. The T_0 mode is characterized by, "an appreciable axial distance" between positive and negative charges whereas the charge polarity reverses over only one turn in the T_1 mode [4].

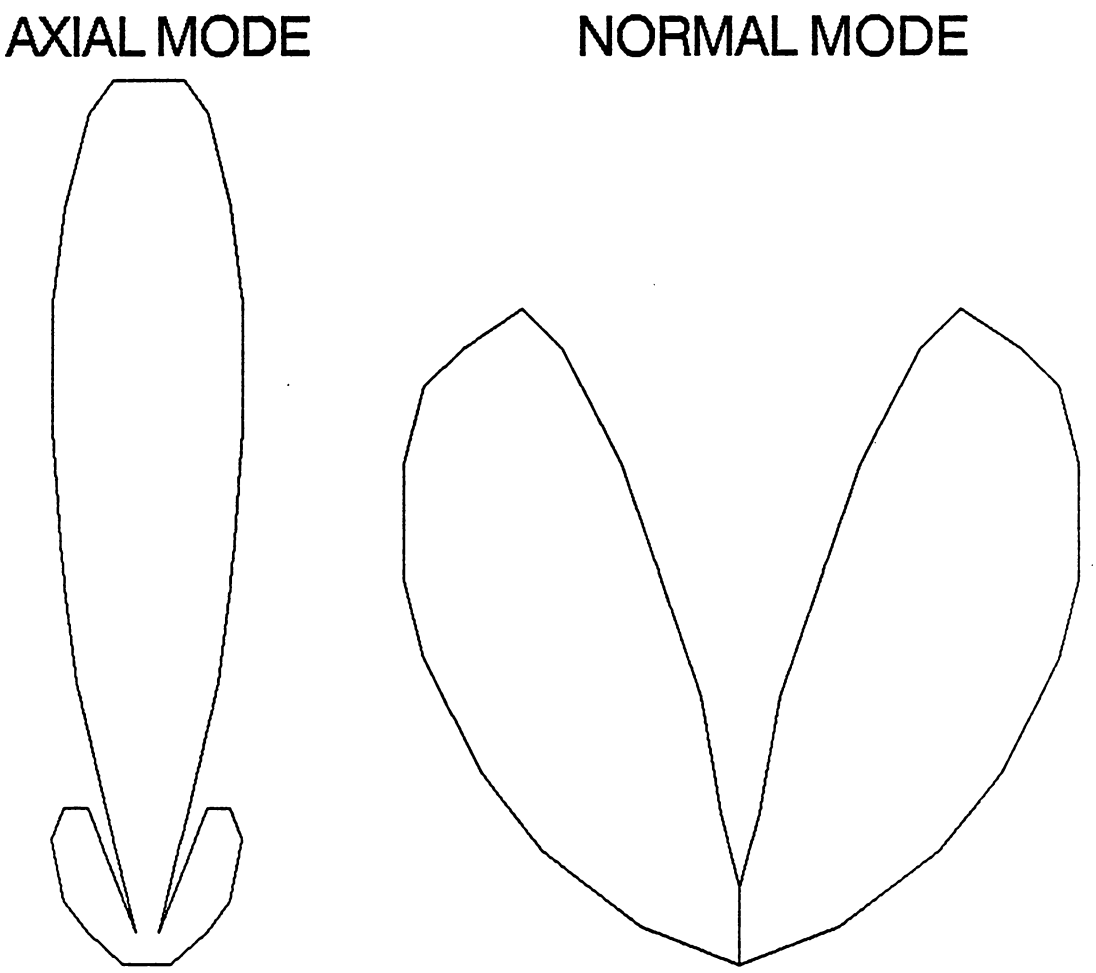

Figure 3.1.2 – 1: The Two Primary Modes

Table 3.1.2 – 1: The Axial Mode Helix Must Meet These Restrictions

Length: Less than 10 wavelengths
Pitch Angle: 11 to 14 degrees
Turns: At least two
Circumference: Between 0.75 and 1.3 wavelengths

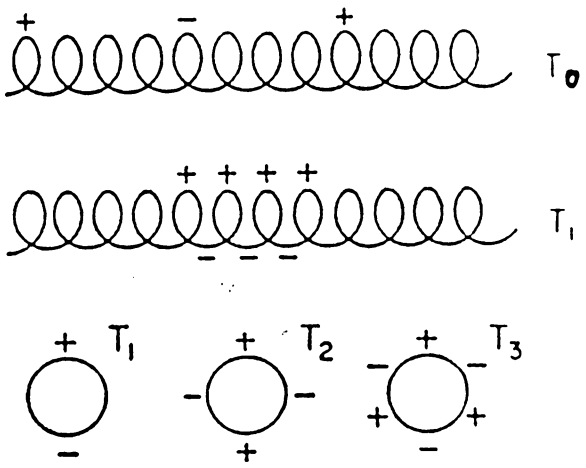

Approximate instantaneous charge distributions on helices for different transmission modes.

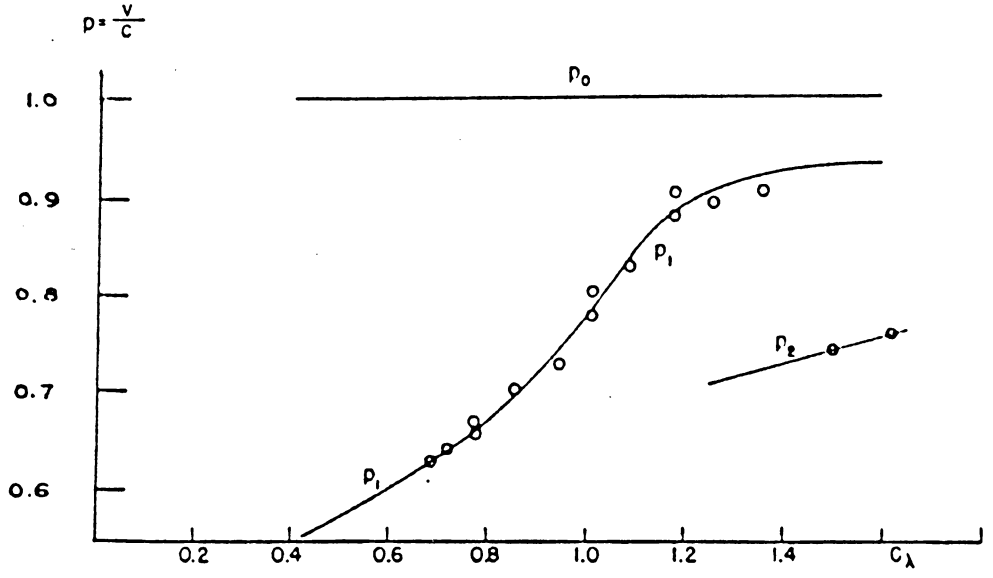

-p versus C_λ curves for the T_0, T_1, and T_2 modes on the helix

Figure 3.1.2 – 2: Charge Distributions [4] and Phase Velocities [9] for Helix Modes

The phase velocity in equation (3.1.2-2) is defined from equation (3.1.2-1) which is Marsh's approximation for current along a helix due to a single traveling wave[9].

$$I = I_o e^{-ax+j(wt\pm Bx)} \quad (3.1.2\text{-}1)$$

where

a is the attenuation constant
w is the angular frequency
B is the phase constant
x is the position
t is time
I_o is a constant

$$P = w/B \quad (3.1.2\text{-}2)$$

The normal mode results from the T_0 traveling wave whereas the T_1 wave is the only one contributing to operation in the axial mode[9]. Therefore, the T_0 and T_2 waves are completely undesirable.

Even though the T_1 wave dominates, the T_0 traveling wave exists in the axial mode[9]. In fact it is the T_0 wave that produces the rather large sidelobes[10]. Figure 3.1.2-3 shows the current along a uniform helix. The large decaying current is due to the T_0 wave and the more uniform current is due to the T_1 wave[10]. The figure shows that for the axial mode of propagation, the decaying current is restricted to the feed region (the first one to three turns on the helix). The bulk of the helix is dominated by the uniform current distribution[1,10]. Unless the helix length exceeds 10 wavelengths, the T_2 wave will have

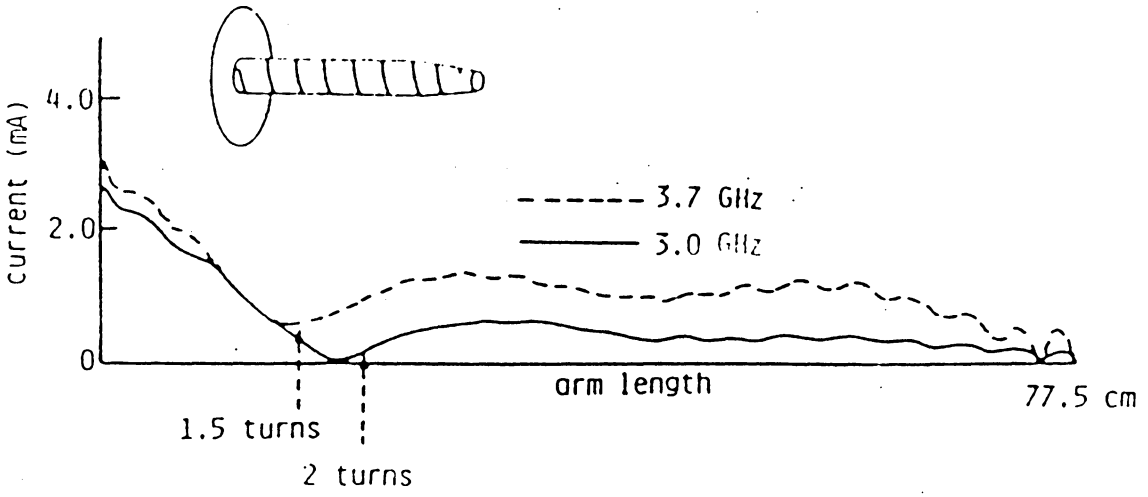

Frequency characteristic of the current distribution of a monofilar helical antenna. The number of helical turns n = eight, pitch angle α = 12.5°, circumference C = 10 cm, and wire radius ρ = 0.5 mm.

Figure 3.1.2 – 3: Current Along the Helix [1]

little contribution. Therefore, the effect of T_2 will be neglected throughout most of this work.

3.1.3 Pattern Characteristics

The pattern characteristics of interest are:

- o Forward Gain/Beamwidth
- o Sidelobe Level
- o Bandwidth
- o Axial Ratio
- o General Pattern Shape

Antenna beamwidth, $\theta_{3\ dB}$, for this work, is defined as

$$\theta_{3\ dB} = \theta_{3\ dB,high} - \theta_{3\ dB,low}$$

where

$\theta_{3\ dB,low}$ is the angle on the low side of the center angle, θ_o, where the gain is 3 dB below the boresite gain (θ_o is defined as 0^o),

$\theta_{3\ dB,high}$ is the angle on the high side of the center angle, θ_o, where the gain is 3 dB below the boresite gain.

Unless otherwise specified, beamwidth shall refer to the 3 dB beamwidth. If the beamwidth is defined as the 1 dB beamwidth, the above definition applies, but $\theta_{3\ dB,low}$ and $\theta_{3\ dB,high}$ are replaced by the corresponding 1 dB angles.

3.1.3.1 **Gain**

The general expression for axial mode gain has been a subject of debate for a number of years. There are two popular gain expressions. The first gain equation (3.1.3.1-1) was given by Kraus[4].

$$G = 15C_{\lambda}^{2} L_{\lambda} \quad (3.1.3.1\text{-}1)$$

where

C_{λ} is the normalized helix circumference
L_{λ} is the normalized helix length
Note: Normalized to the free space wavelength

This was an empirical equation based on many measurements by Kraus[4]. The work of others has shown this equation to be quite optimistic. King and Wong [6,7] have shown that the gain is well approximated by equation (3.1.3.1-2)[6].

$$G_p = 8.3\left(\frac{\pi D}{\lambda_p}\right)^{\sqrt{N+2}-1}\left(\frac{NS}{\lambda_p}\right)^{0.8}\left[\frac{\tan 12.5^{\circ}}{\tan \alpha}\right]^{\sqrt{N}/2} \quad (3.1.3.1\text{-}2)$$

where

G_p is the peak gain
λ_p is the wavelength at peak gain
N is the number of turns
S is the spacing between turns
α is the pitch angle
D is the diameter

At present, this is the best gain prediction equation available. Like Kraus's equation, equation (3.1.3.1-2) is empirical and was derived

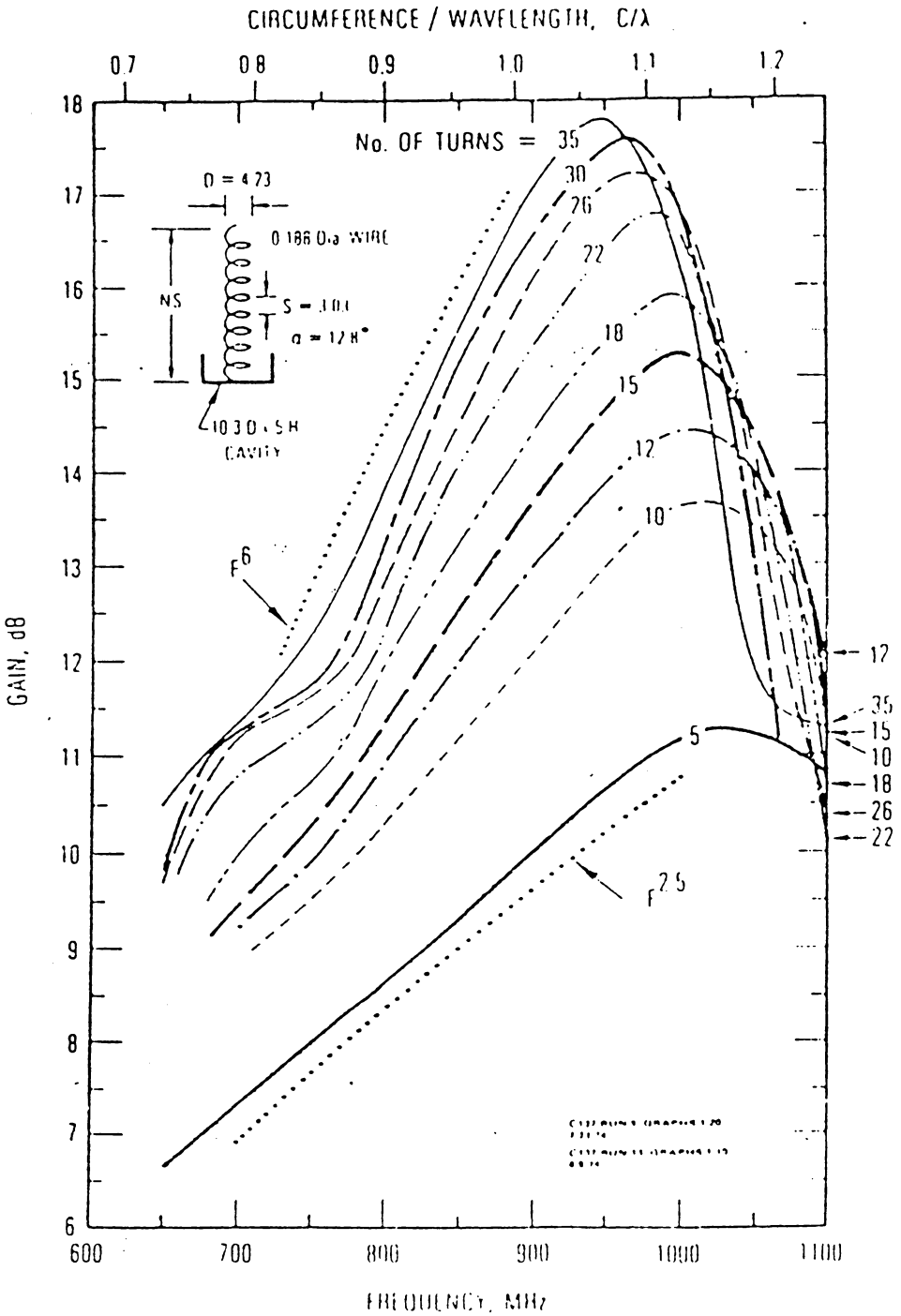

Figure 3.1.3.1 – 1: Gain as a Function of Normalized Circumference [6]

through many measurements. Figure 3.1.3.1-1 shows the gain versus C characteristic found by King and Wong. Still, work by others has shown the measured gain to differ by 1 or 2 dB from this expression[11]. Additionally, all the preceding expressions are specifically for the uniform helix, and are not necessarily valid for more exotic helices.

Figure 3.1.3.1-2 shows typical half-power beamwidths for the helix. King and Wong [7] have formulated a beamwidth formula, equation (3.1.3.1-1), from experiments.

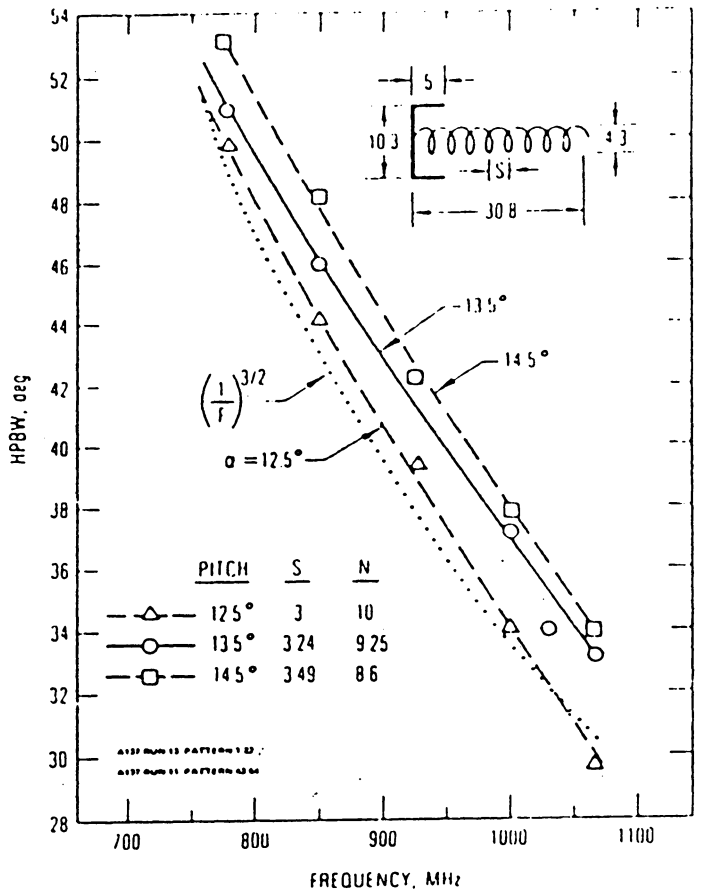

Half-power beamwidths of 30.8-in length and 4.3-in diameter helix for pitch angles = 12.5°, 13.5°, and 14.5°.

Figure 3.1.3.1 – 2: Typical Half – Power Beamwidths of the Helix [6]

$$\theta_{3\ dB} \approx \frac{K_B \left(\frac{2N}{N+5}\right)^{0.6}}{\left(\frac{\pi D}{\lambda}\right)^{\sqrt{N}/4} \left(\frac{NS}{\lambda}\right)^{0.7}} \left(\frac{\tan \alpha}{\tan 12.5^\circ}\right)^{\sqrt{N}/4} \qquad (3.1.3.1\text{-}1)$$

where

N is the number of turns
D is the helix conductor
S is the spacing between turns
λ is the free-space wavelength
$\theta_{3\ dB}$ is as previously defined
$K_B \cong 61.5^\circ$
α is the pitch angle

3.1.3.2 Sidelobe Level

The sidelobe level of a helix is typically 10 dB below the main lobe[6]. Careful feed design can help reduce sidelobes. The end of the helix is of great importance as well[12,13,14]. Methods of reducing sidelobes will be presented later.

3.1.3.3 Bandwidth

One desirable feature of the axial mode helix is the large bandwidth as previously defined in Section 2.4. It has been shown that $BW_\%$=70 % is possible[1,2,6,15,17].

Maclean and Kouyoumjian [2] have shown that bandwidth decreases with increasing length. They claim that as the length increases to an extreme (10 wavelengths, for instance) the pattern becomes distorted.

King and Wong [7] later empirically derived the bandwidth expression shown in Figure 3.1.3.3-1.

3.1.3.4 Axial Ratio

Axial ratio is a measure of polarization circularity[4]. The axial ratio of a helix operating in the axial mode is usually less than 1 or 2 dB[4,8]. As will be shown later, techniques exist that reduce the axial ratio. The general expression for the main lobe axial ratio is given by equation (3.1.3.4-1)[4,16].

$$AR \cong (2N+1)/2N \qquad (3.1.3.4\text{-}1)$$

where N is the number of turns on the helix.

This formula has been criticized for its inaccuracy and should be used only as a rough estimate[10,16]. The reason for this inaccuracy is that the expression is derived from the Hansen-Woodyard condition for increased directivity (see [16] for this derivation). Maclean and Kouyoumjian [2] have shown that Sensiper's solution for an infinite helix is more exact. Figure 3.1.3.4-1 shows the phase velocities as

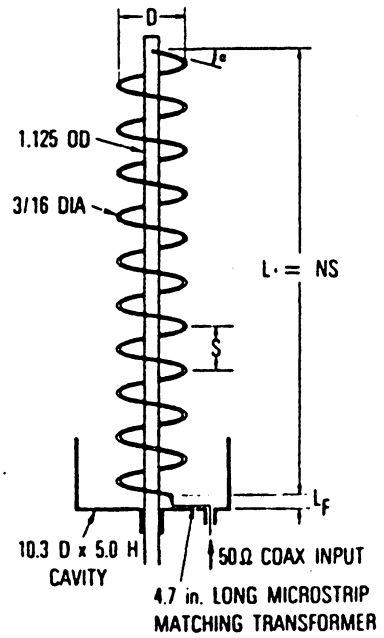

Helix Configuration

$$\frac{f_h}{f_l} \approx 1.07 \left(\frac{0.91}{G/G_p}\right)^{4/(3\sqrt{N})}$$

Where: N is the number of turns
f_h is the upper frequency limit
f_l is the lower frequency limit
G_p is the peak gain
G is the gain lower limit (usually – 3dB from G_p)

Figure 3.1.3.3 – 1: King and Wong's Bandwidth Relationship [7]

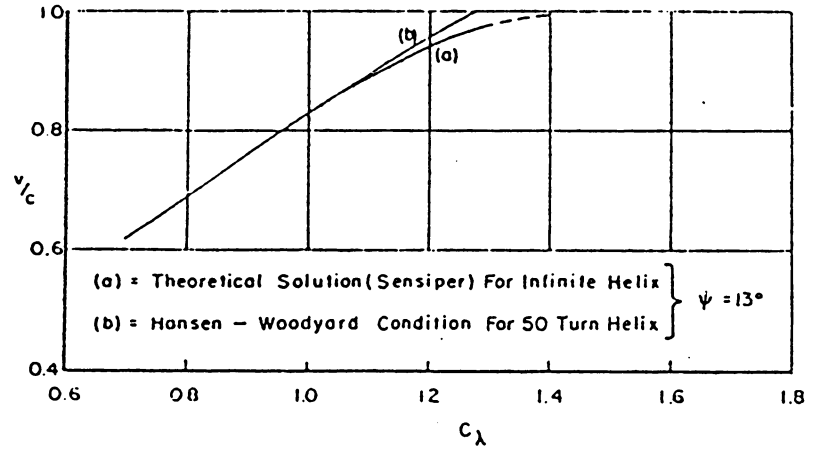

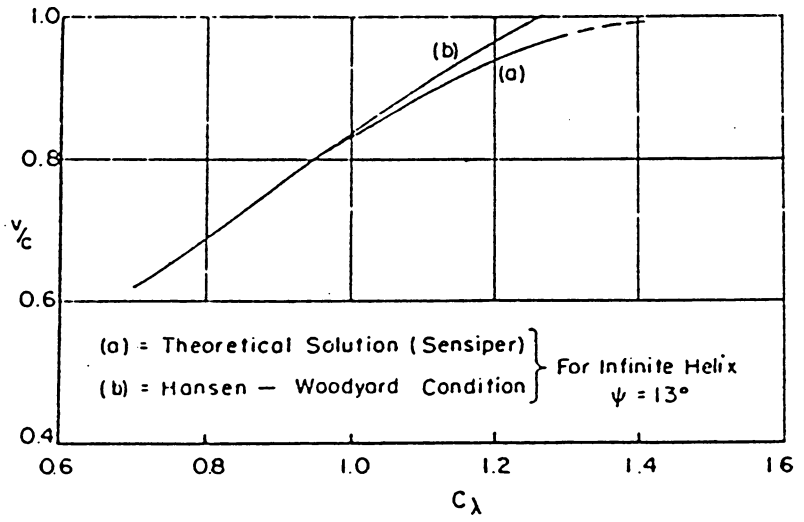

Figure 3.1.3.4 – 1: Phase Velocities from Sensiper and H/W Solutions [2]

predicted by both Sensiper and H/W methods. The solution is identical for values of C_λ less than 1.1. Therefore, it is logical to assume that the axial ratio formula given above is most accurate in this region. Lee [16] bounds C_λ between 0.75 and 1.1 for axial mode operation.

Figure 3.1.3.4-2 shows that the axial ratio varies with the number of turns along the uniform helix [2]. The amplitude of the oscillations decrease for helices with many (N>10) turns. Often, the axial ratio can be improved by simply trimming the end of the helix. This technique was used successfully in the experimental portion of this work.

3.1.3.5 Field Pattern

Figure 3.1.3.5-1 shows the effect of the T_0, T_1, and T_2 traveling waves on the field pattern [3]. Note that as C_λ increases the sidelobe level likewise increases. Also illustrated is the large bandwidth that characterizes the axial mode.

3.2 Feeds

Many feed methods exist for the helix[17,18,19,20,21]. The feed design should minimize VSWR over a large bandwidth. The feed should also be mechanically stable. Adjustment to the feed should be simple and fast. The methods presented in this section satisfy all of these requirements.

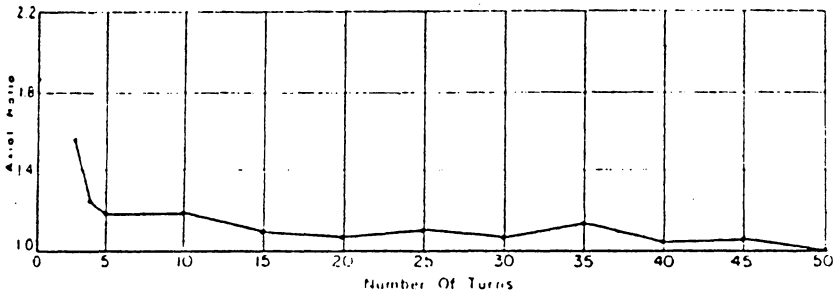

Voltage axial ratio vs number of turns, 13° helix; $f = 8$ kmc.

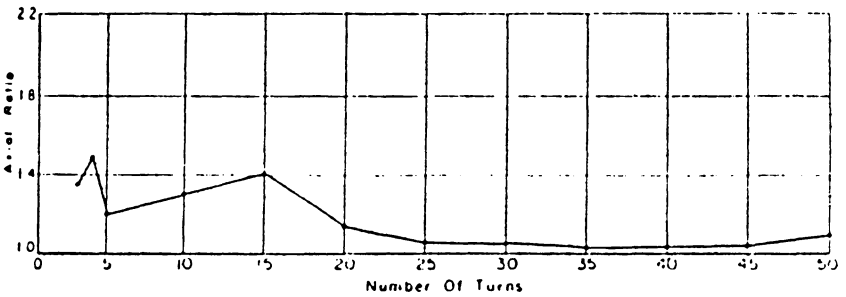

Figure 3.1.3.4 – 2: The Axial Ratio is a Function of the Number of Turns [2]

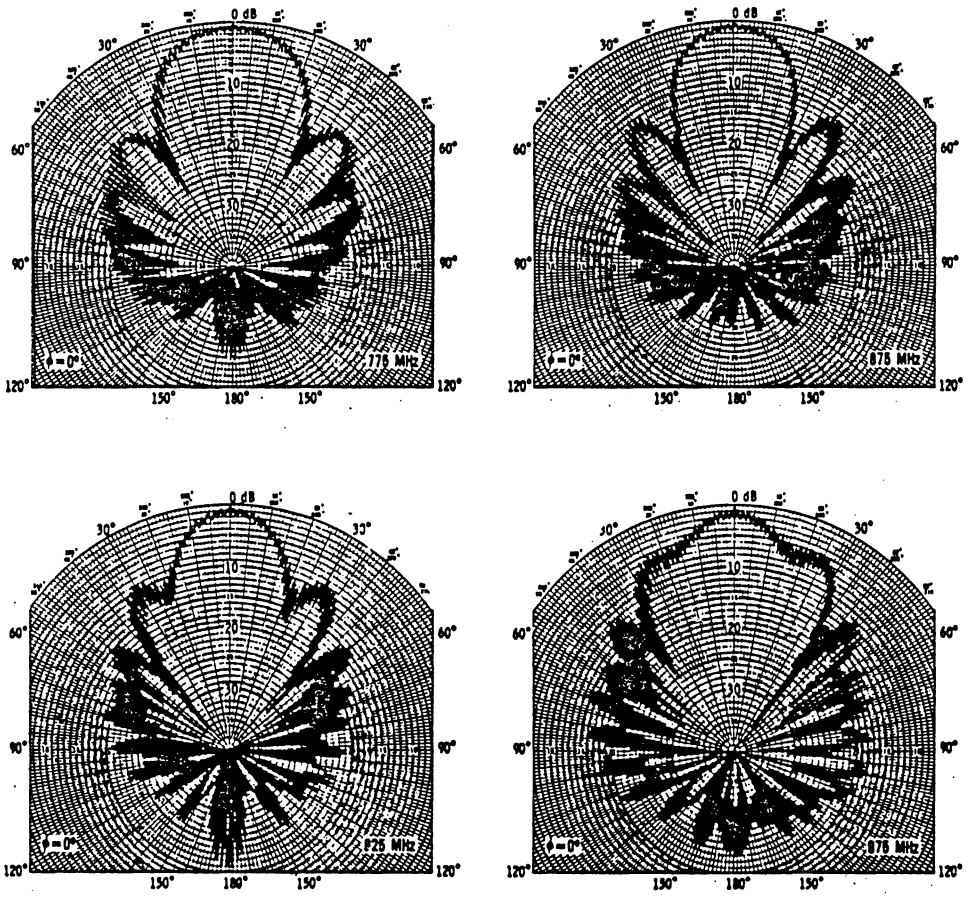

Radiation patterns of an 18-turn uniform helix

Figure 3.1.3.5 – 1: Effect of Traveling Waves on Helix Field Pattern [3]

3.2.1 Impedance Characteristics

The standard impedance formula used for the uniform helix, is somewhat suspect. The popular impedance formula is [17]

$$Z_o = 140\ C_\lambda \qquad (3.2.1\text{-}1)$$

where

Z_o is the (real) impedance of the wire in Ohms
C_λ is the normalized circumference

This is based on the theoretical impedance of a wire over a perfect ground (equation (3.2.1-2)[17]).

$$Z_o = 138\ \mathrm{Log}_{10}\ (4h/d) \qquad (3.2.1\text{-}2)$$

where

Z_o is the (real) impedance of the wire in Ohms
h is the height of the wire above the ground
d is the diameter of the wire

At present, no equation accurately describes the impedance of the axial mode helix. Hence, the often quoted 140 Ohm terminal impedance should at best be considered a first order approximation. However, the impedance of the helix has been clearly shown to be nearly constant over a wide bandwidth[4,17]. This bandwidth can be as large as 70 % of the center frequency, f_o. Figure 3.2.1-1 shows a typical impedance spiral.

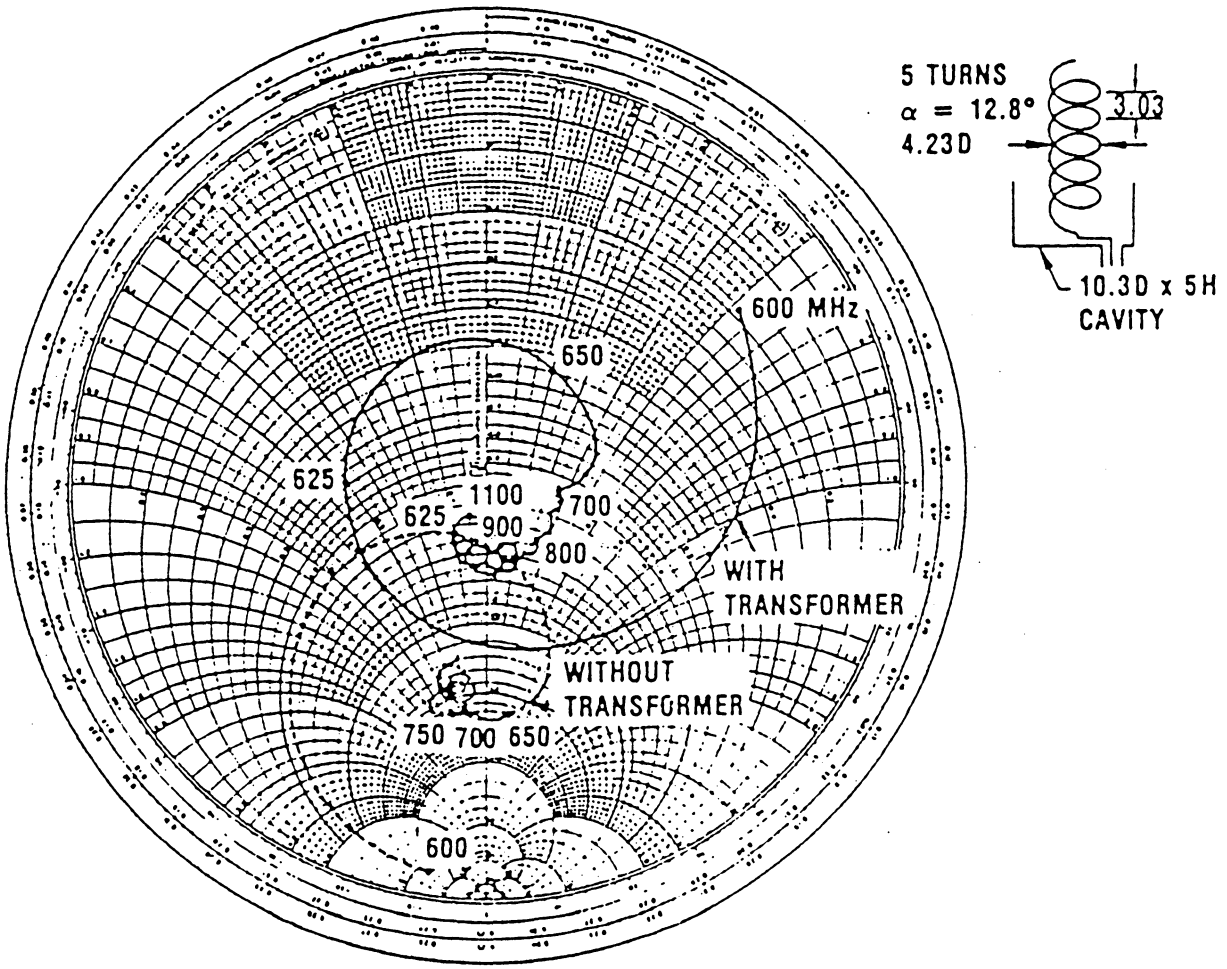

Impedance characteristics of a five-turn helix with and without an impedance-matching transformer.

Figure 3.2.1 – 1: Typical Helix Impedance Spiral [40]

Table 3.2.2 – 1: There are Several Viable Ways to Match Impedance

Method	Description
Transformer	Microstrip or stripline techniques are used to fabricate. Matches a known impedance such as 140 ohms to desired output impedance, usually 50 ohms.
Waveguide Feed	Eliminates the need for feed lines. Generally used for frequencies near 10 GHZ. Many be used for an array feed if the helixes are properly phased by mechanical rotation
Tin Snip	A small metal disk is soldered to the feed end of the helix. This disk is cut by tin snips until the output impedance is 50 Ohms or some other desired value.
Last Turn	The distance from the last turn to the ground plane is increased or decreased to modify the output impedance. Generally, the smaller the distance, the lower the impedance. Also, a metal strip may be attached to the ground plane an adjusted by a screw to make fine adjustments.
"Fox Method"	The method used in this work. A wire is soldered to the first turn on the helix. This wire is covered by teflon tubing for insulation. It runs near the ground plane to an N – type coaxial connector. The orientation of the wire is changed until impdeance characteristics are as desired.

The distance between the feed wire and the bottom of the cylindrical reflector, s, is ~ 1 to 2 cm

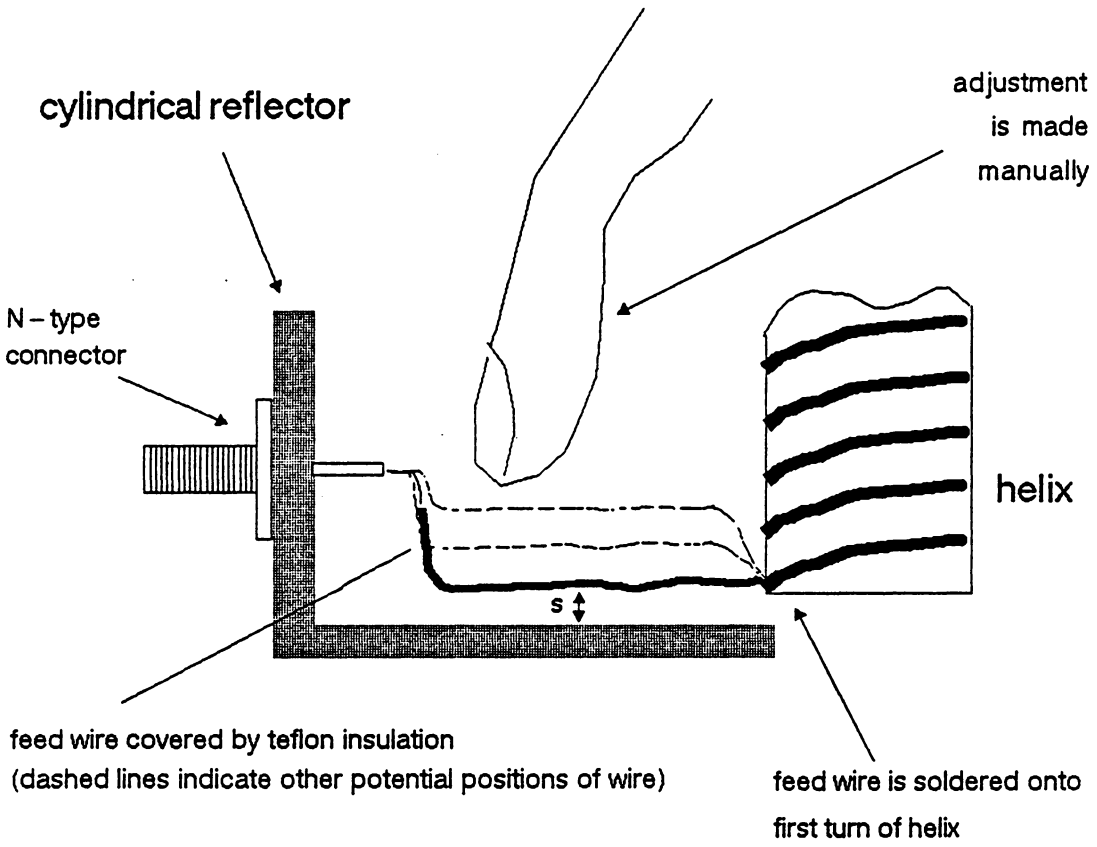

Figure 3.2.2 – 1: The "Fox Feed Method"

3.2.2 Impedance Matching

Table 3.2.2-1 gives the various methods of matching the impedance of the helix to 50 Ohms. Work has been done that shows each of these methods to be convenient and effective. The author's "Fox Method", shown in Figure 3.2.2-1, was selected for use in the experimental portion of this work because of its simplicity. This method consists of adjusting the height of an insulated feed wire above the side and base of the cylindrical reflector. In general, the real part of the impedance, R, decreases as the wire is moved closer to the surface of the reflector.

3.3 Modifications

Certain modifications to the helix improve performance. The mechanisms by which these improvements are made can be described in terms of the traveling waves T_0 and T_1 and the corresponding phase velocities, P_0 and P_1. These modified helices are described in the following paragraphs.

3.3.1 Reflectors

For the purpose of this work, the term "reflector" will refer to the metal section at the base of a single helix. The terms "backplane" and "ground plane" will refer to the large square metal sheet that

supports an entire array of helices. A helix can be backed by a reflector to improve performance [6,22,43]. More specifically, the reflector suppresses the T_0 wave. As mentioned earlier, the T_0 wave contributes to sidelobe level. In addition, experimental work has been performed which shows the reflector increases the forward gain of the helix[6]. Figure 3.3.1-1 gives cylindrical reflector dimensions used by several researchers.

Figure 3.3.1-2 shows several reflector geometries. The cylindrical reflector has been popular for many years. However, the conical reflector can be used to form what has been termed a "helicone" antenna. The helicone has an impressively low sidelobe level (-33 dB for a 10 turn helix) and high forward gain[43].

3.3.2 Tapered End

One of the common techniques used to improve the VSWR, axial ratio, and bandwidth of the helix is to taper the end of the helix. Figure 3.3.2-1 shows this simple modification. The taper angle, α, is usually taken to be the same as the pitch angle[12,13]. Tapering reduces the amount of reflected energy by making the helix/free-space transition more gradual[13,36].

Reference	Frequency	Cylindrical Refector Dimensions (in Wavelengths) Height	Diameter
[12]	2.3 GHz	0.20	0.90
[3]	900 MHz	0.29	0.87
[21]	9.375 GHz	0.25	0.75
[6]	900 MHz	0.38	0.78
[7]	900 MHz	0.38	0.80
[22]	2.3 GHz	1.00	1.22
[32]	1.55 GHz	0.25	0.70

Figure 3.3.1 – 1: Cylindrical Reflector Dimensions Used by Several Researchers

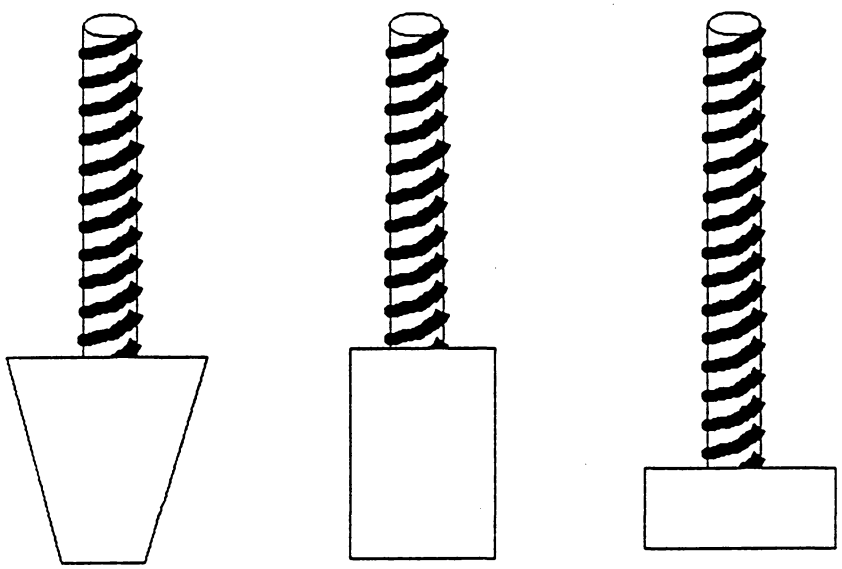

Conical Long Cylindrical Short Cylindrical

(Profiles Shown)

Figure 3.3.1 – 2: Typical Reflector Geometries

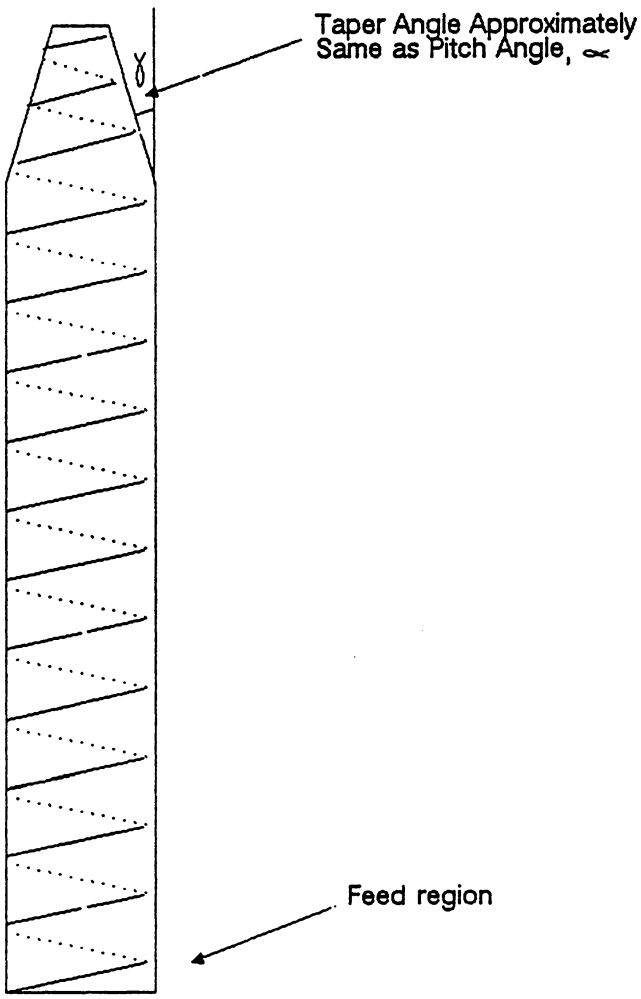

Figure 3.3.2 – 1: Tapering the Helix Improves Performance

3.3.3 Dielectric Core

Aside from changing the physical dimensions of the helix, performance characteristics can also be modified through the insertion of a dielectric core. Introduction of a core into a helix produces the following effects:

- o Reducing the current in the helix conductor
- o Decreasing the bandwidth
- o Improving polarization purity (decreases axial ratio)

Vaughn [10] asserts that insertion of a core with a relative emissivity of 5 improves the axial ratio to the point where tapering the end becomes unnecessary.

3.3.4 Double Pitch Helix

Sultan [23] has used a "double pitch" winding to improve gain, axial ratio, and bandwidth. Figure 3.3.4-1 shows the geometry based on this concept. Helices A and E are standard (uniform) single pitch helices. Helices B, C, and E are double pitch helices. He suggests that this technique can be used to design a helix which has a particular gain-frequency characteristic. Apparently, the frequency at which maximum gain occurs decreases as the pitch angle decreases[6,23]. Therefore, combining two pitch angles on one helix effectively broadens the bandwidth as Figure 3.3.4-2 shows graphically. The gain versus

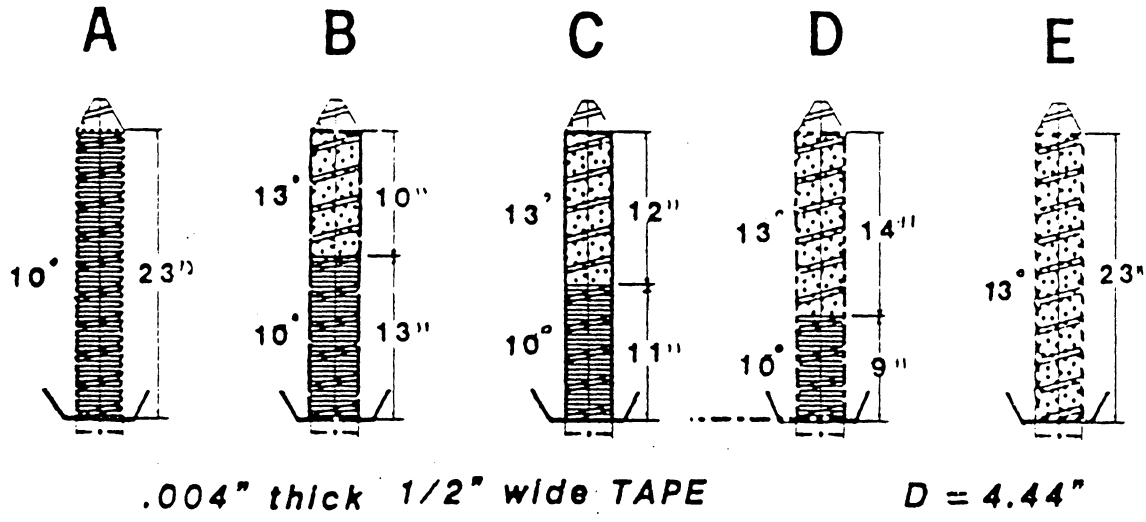

Concept of double pitch cyclindrical helical antenna.

Figure 3.3.4 – 1: The Double Pitch Helix [23]

frequency graph for helix C can be interpreted as the approximate average of the gain versus frequency graphs for uniform helices A and E. This makes intuitive sense since helix C has pitch angles of 10^{o} (same as helix A) and 13^{o} (same as helix E).

3.3.5 Non-uniform Helix

Figure 3.3.5-1 shows the non-uniform helix designed by King and Wong to increase bandwidth, decrease axial ratio, and improve the field pattern. This type of helix has a uniform section from the base of the helix to approximately one-third up the length of the helix where it is then tapered down to a smaller circumference over two turns. The remainder of the helix is uniform except for the last two turns which are tapered. So there are not one, but two tapers on the non-uniform helix. The technique of "quasi-tapering" a helix has been used to improve the 1 dB bandwidth from 26% to 55 % [3].

3.3.6 Conical Helix

The logical extension of the tapered end is to taper the entire helix. Figure 3.3.6-1 shows an example of a conical helix. While some gain is lost by doing this, the axial ratio and bandwidth of the helix further improves. Also, the sidelobe level is particularly low[3,24]. Figure 3.3.6-2 shows the field pattern of a conical helix.

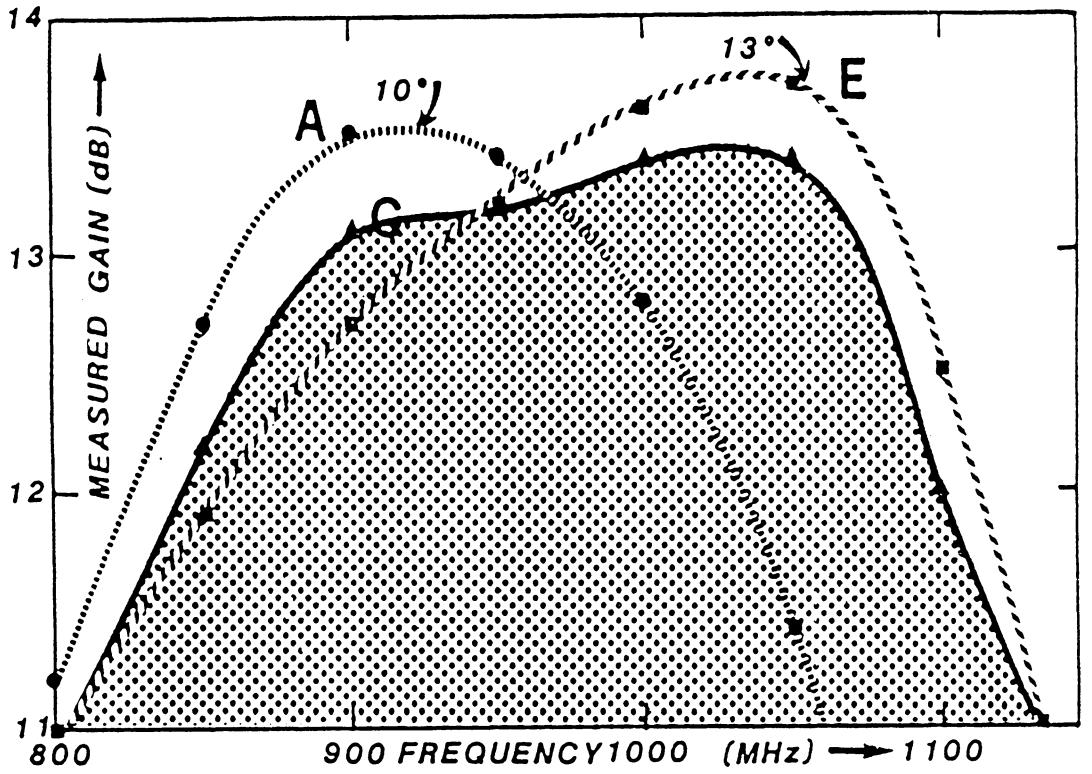

Measured gain frequency response for cylindrical helices of Fig. 1: "single pitch" A:10° & E:13°, "double pitch" C: (10° + 13°)

Figure 3.3.4 – 2: The Double Pitch Helix can be Used to Alter Gain Performance [23]

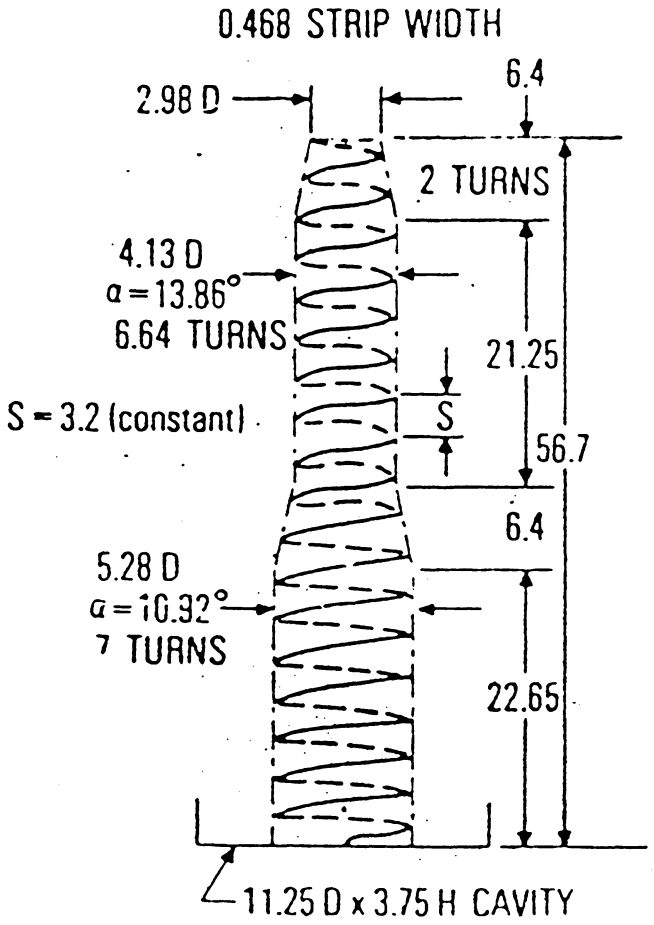

Figure 3.3.5 – 1: The Quasi – Taper Helix can be Used to Improve Performance [3]

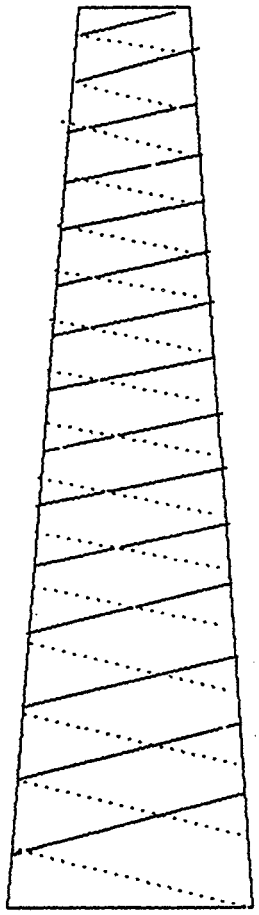

Figure 3.3.6 – 1: The Conical Helix Provides Low Sidelobe Level

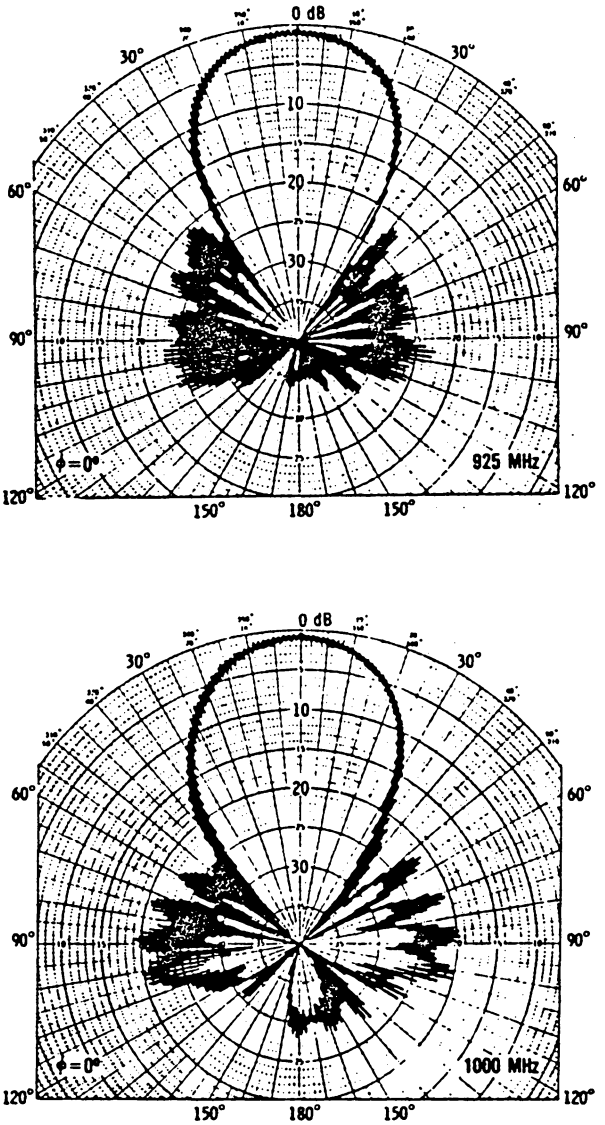

Radiation patterns of a 17.64-turn conical helix

Figure 3.3.6 – 2: Field Patterns of the Conical Helix [3]

Since the antenna noise temperature is a function of sidelobe level, G/T for an array of conical helices should be relatively high. An additional benefit of reducing sidelobe level is the reduction of mutual coupling between elements.

3.3.7 Parasitic Winding

Recently, a new method to increase the forward gain of the helix has been successfully demonstrated. Figure 3.3.7-1 shows this method. A second, "parasitic", winding has been added. This winding starts after the second turn of the primary helix on the opposing side. This technique has been shown to increase gain of L-band helices by about 1 dB[5]. Figure 3.3.7-2 shows the results reported by Nakano. The parasitic winding is said not to affect the axial ratio[5].

Parasitic windings can be implemented in other ways [25], but not much work has been done using them.

3.3.8 Discontinuous Ground Plane

The field set up by the helix induces small eddy currents in the ground plane. These currents in turn can produce unwanted fields and degrade array performance by increasing mutual coupling. By breaking up the ground plane (or using a wire mesh) the eddy currents are diminished[26].

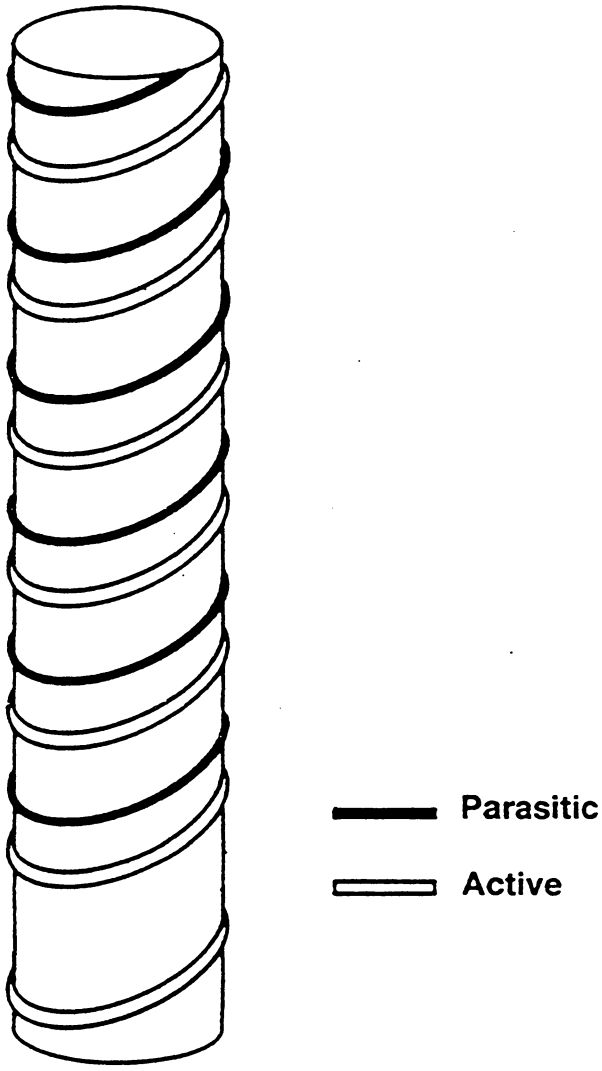

Figure 3.3.7 – 1: The Parasitic Helix Exhibits an Increase in Forward Gain

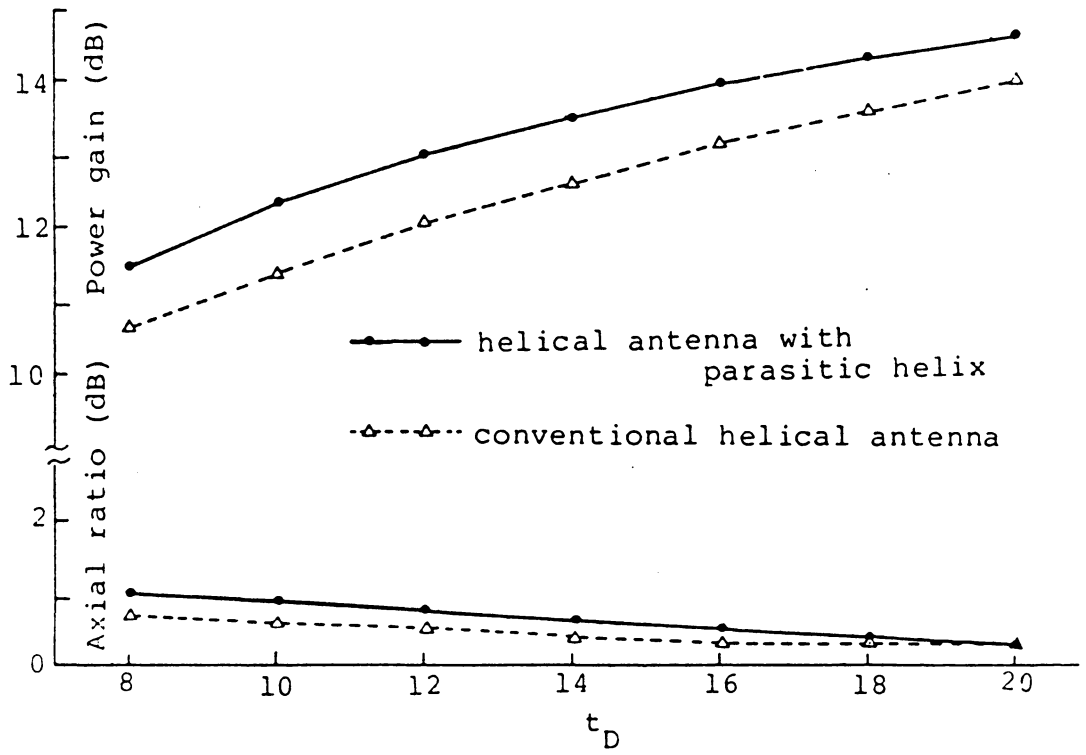

Figure 3.3.7 – 2: Gain versus Frequency for Parasitic Helix [5]

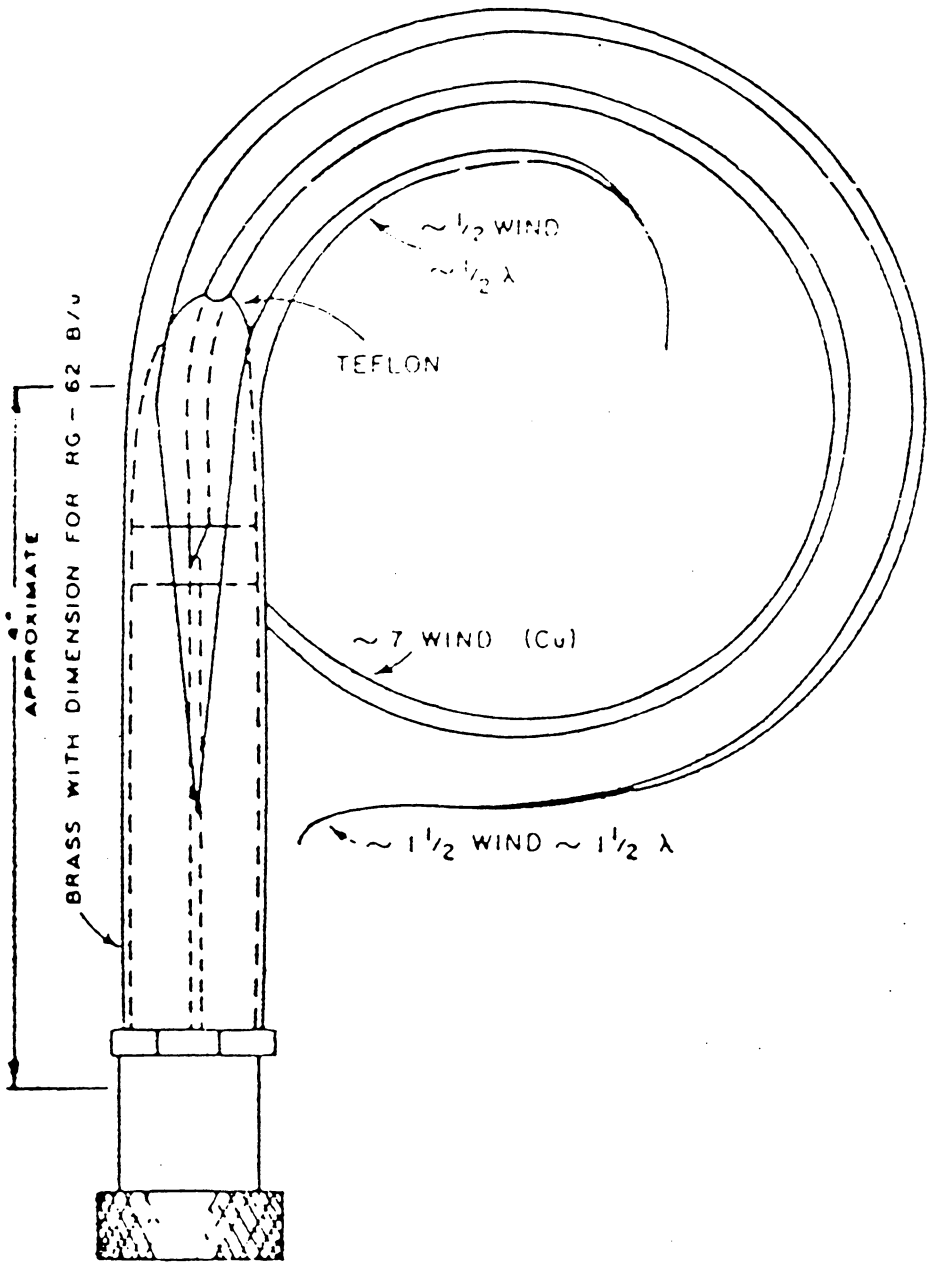

Figure 3.3.8 – 1: The Helical Launcher Eliminates the Backplane [20]

Figure 3.3.8-1 shows a feed method designed to eliminate completely the need for a ground plane [20]. However, it is likely that the resulting field pattern will have a large backlobe.

3.3.9 Conductor Width

Many researchers have concluded that helix performance is virtually independent of conductor thickness and width [8,38]. Either tape or wire may be used. Tape helices seem preferred because of weight considerations and ease of construction (tape with an adhesive backing can be purchased at reasonable cost).

3.4 Previous Work On Helical Arrays

Some work has been performed on arrays of helices. These are arrays of low gain helix elements, but it is possible that some results can be extrapolated for use with high-gain elements. Table 3.4-1 summarizes the significant work on helical arrays. Most work was performed for arrays of two turn helices, with the notable exception of Agrawal's [22] who used one wavelength long helices at S-Band (2.1 GHz) and Kraus' [35] who tested a high-gain four element array.

Table 3.4 – 1: Previous Work on Helical Array

Worker	Physical Description	Findings
Sultan [23]	Flaired reflector, tapered end, varied pitch angle	1. Bandwidth and gain can be controlled by varying pitch angle
Stratoti [29]	Two turn axial mode helixes, resistor placed in series with helix, elements rotated	1. Coupling between helices is smaller than between dipoles for a given element spacing 2. A resistor in series with the helix reduces mutual coupling and axial ratio 3. The effect of "passive" array elements cannot be neglected 4. Elements can be rotated up to 180 degrees with respect to each other to reduce mutual coupling
Nakano [21]	Cylindrical reflector, waveguide feed, two turn axial mode helixes	1. The feed arrangement can be greatly simplified by using a waveguide at 10 GHz 2. Mechanical rotation can be used instead of phase shifters

Table 3.4 – 1: Previous Work on Helical Array (continued)

Worker	Physical Description	Findings
Agrawal [22]	Cylindrical reflector, matching transformer, tapered end, hexigonal ground plane	1. Mutual coupling is small for element spacings of 2.1 wavelengths 2. Cylindrical reflector dimensions were optimized: diameter was 1.22 wavelengths, height was 0.9 wavelengths
Shiokawa [32]	Cylindrical reflector, two turn axial mode helixes	1. Best axial ratio of array occurs for reflector dimensions: diameter of 1.7 wavelengths, height of 0.25 wavelengths 2. Reflector reduces mutual coupling and axial ratio of array 3. Quantified many parameters in graphs
Kraus [4]	No reflector, tapered feed lines, 1.5 wavelength spacing between elements	1. Square four element array produced 16 dB gain at 600 MHz; 20 dB at 1000 MHz 2. SWR, beamwidth, and axial ratio were plotted as a function of frequency

Chapter 4: Experiments

4.0 Experimentation

Experimental tests to determine helical array gain as a function of element spacing and to quantify mutual coupling were performed in the laboratory and radiation pattern and gain measurements were made at an antenna test range. Tests were also performed on single helices to determine bandwidth, gain, and radiation pattern characteristics. This chapter describes the results of these tests.

4.1 Purpose

The experimental program serves several purposes. The testing of a prototype helical array (four elements) addresses the major assertion of this work: that the helical array performs well as a high-gain ground station antenna. Other testing was performed to provide more quantitative information relating to element spacing, mutual coupling, forward gain, beamwidth, axial ratio, and bandwidth.

4.1.1 Validate/Refute Literature

The data were designed to validate, refute, or supplement the literature with respect to the following areas:

- o Gain as a Function of Array Element Spacing
- o Mutual Coupling
- o Impedance Characteristics
- o Element Performance Parameters (Gain, Axial Ratio, Bandwidth)
- o Sidelobe Level
- o Element Phasing
- o Interaction of Traveling Waves
- o General Field Pattern

Information regarding helical arrays is sparse, and literature concerning high-gain helical arrays is all but non-existent as was shown in Section 3.4. Therefore, experimentation was deemed necessary so that eventually a high-performance ground station antenna can be realized.

4.1.2 Evaluation of Array Performance

Theoretically, a doubling of the number of array elements should result in approximately a 3 dB increase in gain. However, in reality, this is not the case. The effective apertures of the elements overlap if the elements are too close together. Figure 4.1.2-1 illustrates this phenomenon. (This is explained in terms of the "space factor" in [44]).

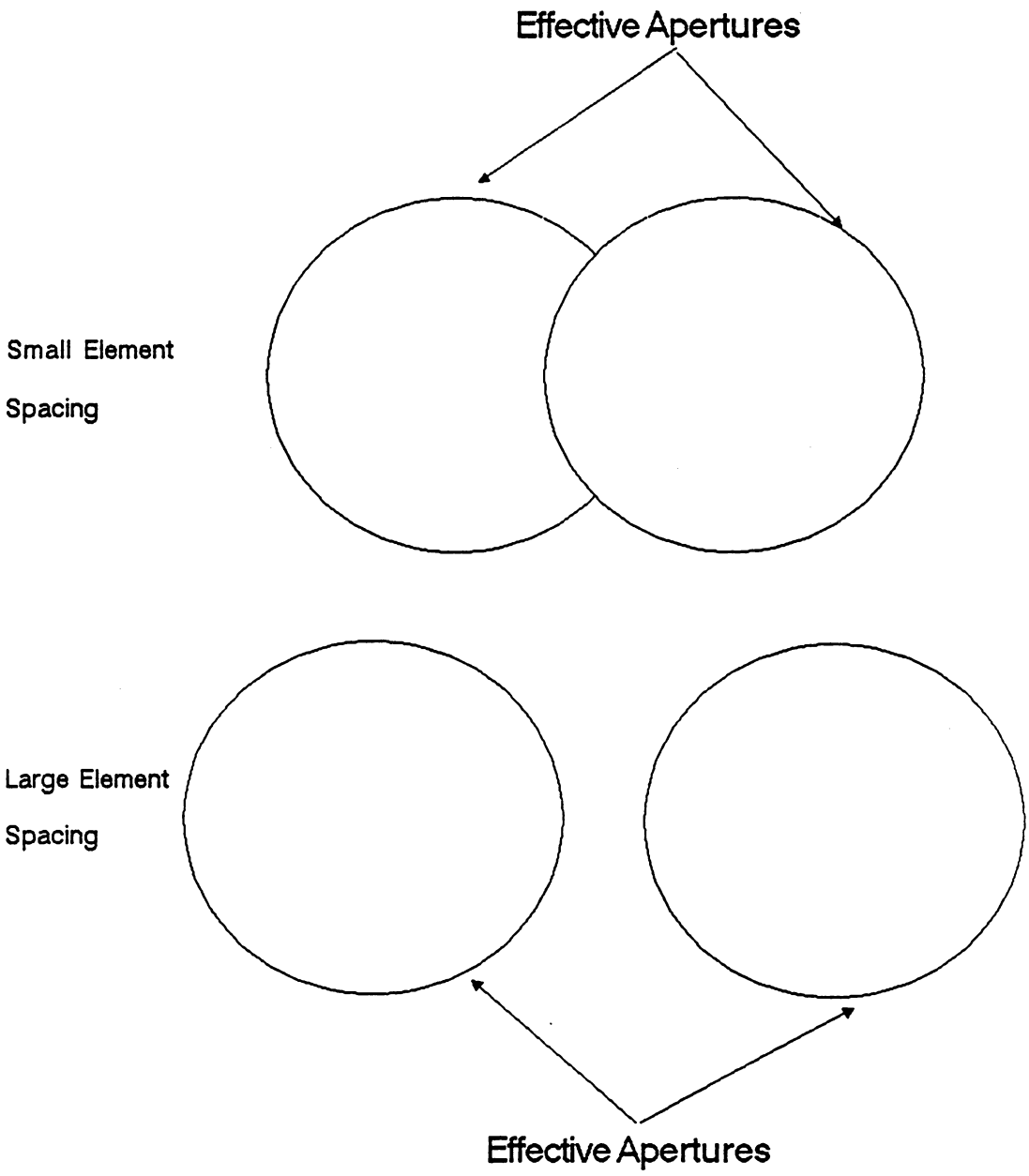

Figure 4.1.2 – 1 Effective Aperture Overlap as a Function of Electrical Spacing

As previously mentioned, mutual coupling, which is also a function of element spacing, also reduces the actual array gain [27,28,29,30,31,32]. So the issue to be resolved is; for a given element spacing, what "gain per doubling" can be expected? Some experiments were designed to answer this question.

The sensitivity of the array to errors in phasing the elements was also in question. (The elements were phased by visually aligning the helices by rotating them in the ground plane). The effect of small phase errors has not been reported in the literature. Also, the effect of the environment and handling needed to be evaluated.

4.1.3 Data Collection

The last, but perhaps most important, purpose was to collect data for use in the computer simulation, program HEMAN, discussed in chapter 5. The importance stems from the fact that the experiments performed do not yield the noise temperature of the antenna, hence the figure-of-merit, G/T, could not be calculated without the use of simulation.

The data collected includes:

- o Field Patterns
- o Axial Ratio
- o Sidelobe Level
- o Gain
- o Bandwidth

4.2 Design

The helical element and backplane were designed to facilitate fast, but meaningful, testing. The physical layout and experimental procedures were designed to support this approach. Figure 4.2-1 shows the four test configurations and Figure 4.2-2 gives the physical dimensions of the test helices. All testing of configuration II, III, and IV were performed at 1.3 GHz.

4.2.1 Physical Description

Figure 4.2.1-1 shows the backplane used in testing. Holes were drilled so that the elements could be easily positioned at various spacings. The holes also allow the rotation of the helices for "proper phase matching" which is discussed in more detail in Section 4.3.4. The helices must have identical rotational orientations so that the respective currents add in-phase in the power combiner. The center hole was drilled to allow single element testing and the mutual coupling experiment.

A bracket was made to connect the test-bed antenna to the test range pedestal.

Figure 4.2.1-2 shows the structure of the test helices. Paper with a spiral template was taped onto the cylindrical form. Thin copper tape

BACKPLANES

I. Single element measurements

active elements: 1 (also 2 – 10)
passive elements: none

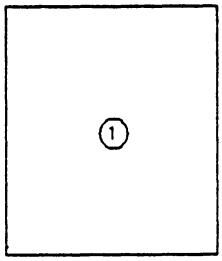

Element spacings in wavelengths: N/A

II. Phasing two elements

active elements: 1,2
passive elements: none

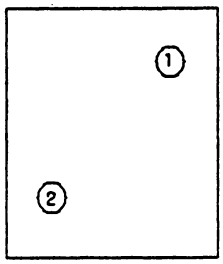

Element spacings in wavelengths: 1.92

III. 4 element (2x2) array (gain as a function of element spacing)

active elements: 1,2,3,4
passive elements: none

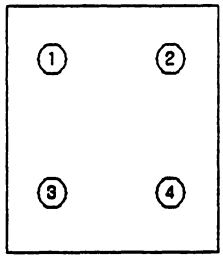

Element spacings in wavelengths

1.00
1.18
1.37
1.55
1.73
1.92
2.18
2.46

IV. Mutual coupling as a function of element spacing

active elements: 5
passive elements: 1,2,3,4

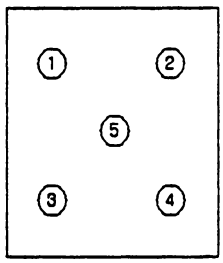

Element spacings in wavelengths

1.27
1.32
1.61
1.87

Figure 4.2 – 1: Test Configurations

All helices are wound with 18 turns of adhesive copper tape

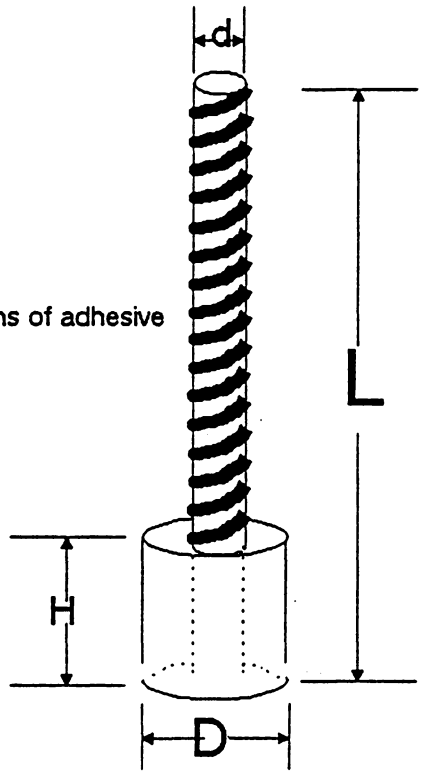

Test Helix	L	H	D	d	pitch angle
1 – 8	1.0 meters	21 cm	21 cm	7.62 cm	12.5 degrees
9	2.0 meters	21 cm	21 cm	7.62 cm	12.5 degrees
10	1.0 meters	42 cm	21 cm	7.62 cm	12.5 degrees

Figure 4.2 – 2: Test Helices

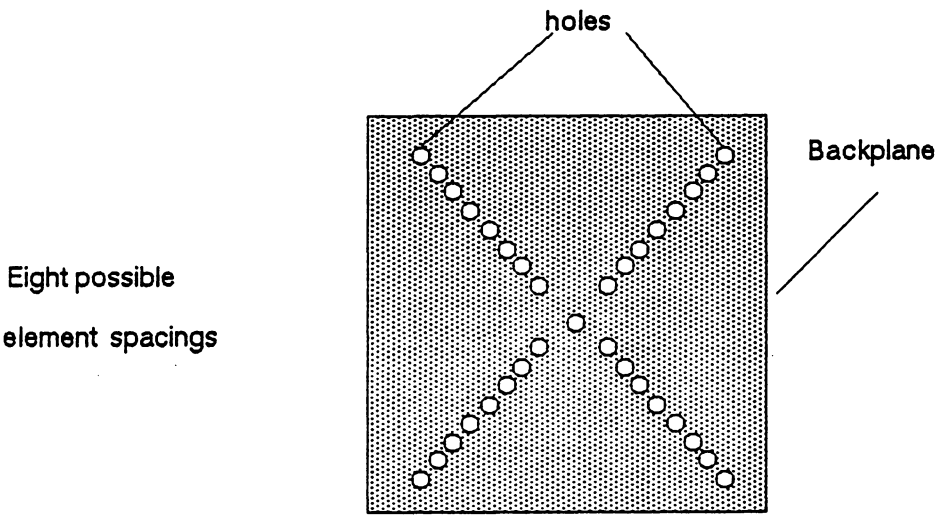

Figure 4.2.1 – 1: The Back Plane Used for Testing

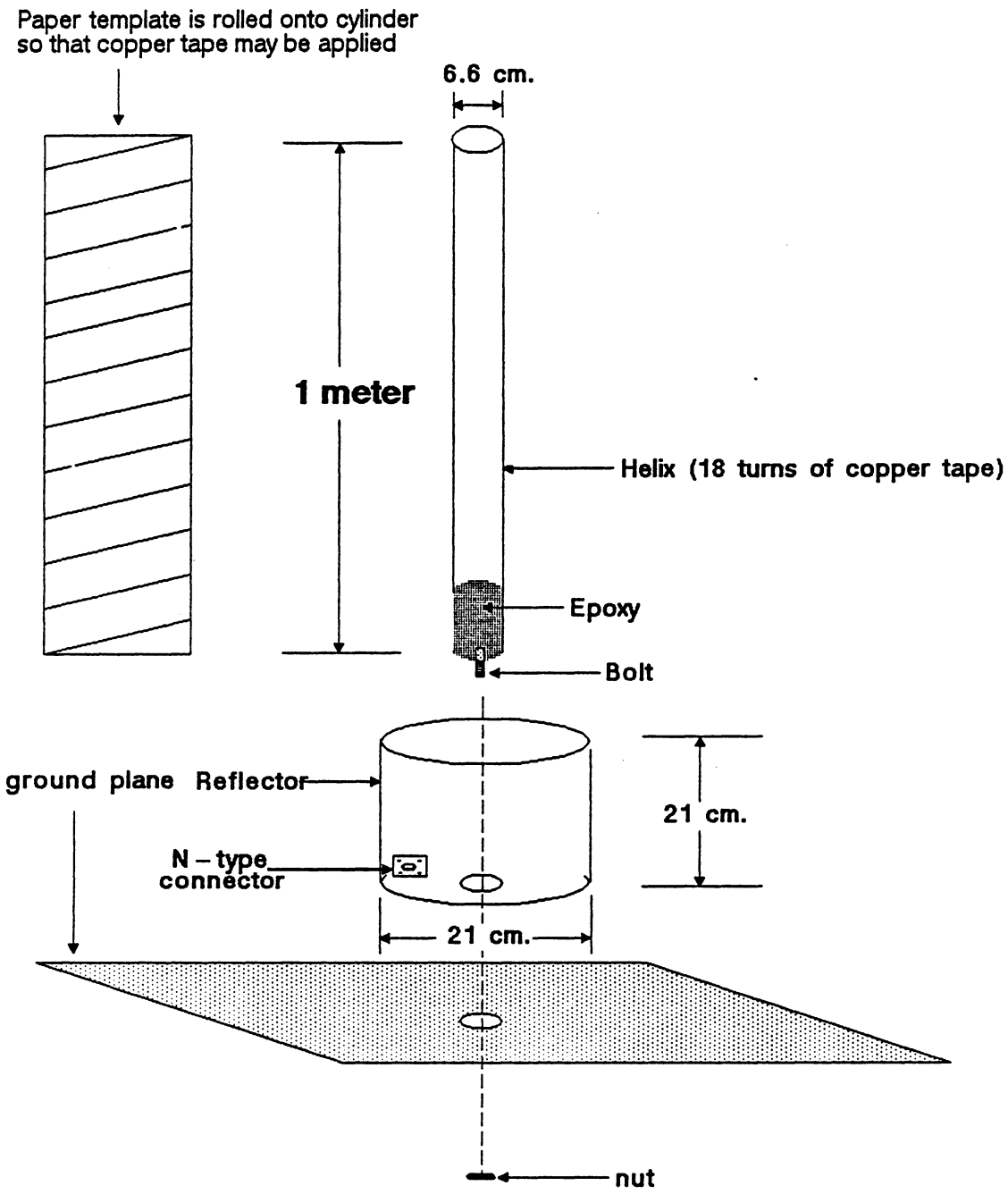

Figure 4.2.1 – 2: Test Helixes

with an adhesive backing was then wound on the template at a pitch angle of 12.5^{o} for N=18 turns. The lightweight cylinder around which the tape is wound is made of a polycarbonate. A metal bolt was fixed in epoxy at the base of the helix. A cylindrical reflector was made from sheet metal and rivets. An N-type coaxial connector was placed along the side of the reflector. A hole was drilled in the base of the reflector so that the bolt could protrude. The base of the helix was then glued to the reflector.

After construction, the feed wire was carefully soldered from the end of the helix to N-type connector after being covered with teflon tubing for insulation. The wire was left long to allow impedance adjustment.

The power combiner used is shown in Figure 4.2.1-3. It is capable of combining four 50-Ohm loads into one 50-Ohm output.

4.2.2 Experimental Procedure

Table 4.2.2-1 lists the procedures followed for the laboratory and field experiments.

A network analyzer was used to measure helix and helical array impedance in the laboratory. During this process, plots of the impedance spirals (impedance as a function of frequency on the Smith chart) for the helices were made on a plotter. The loss of the cables

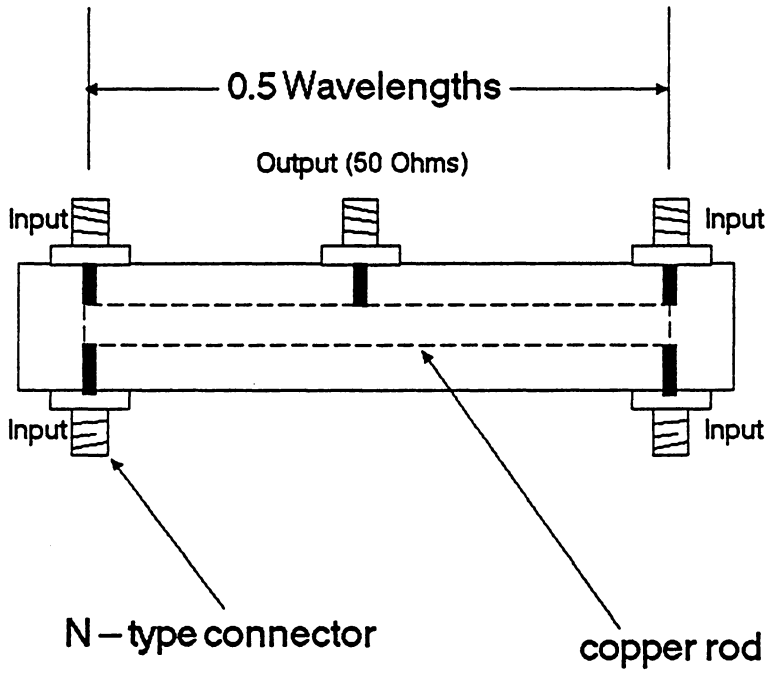

Figure 4.2.1 – 3: The Power Combiner Provides a 50 Ohm Output

Table 4.2.2 – 1: Experimental Procedure

Test Type	Goal	Procedure
Laboratory	Adjust impedance of helices and obtain impedance spirals	1. Attach calibrated network analyzer to helix. 2. Iteratively adjust feed wire and observe impedance to obtain desired impedance characteristic. 3. Repeat for all helices, recording VSWR and impedance as a function of frequency.
Laboratory	Verify operation of power combiner	1. Connect helices that have similar impedance characteristics to the four input ports. 2. Connect the output port to the network analyzer. 3. Observe VSWR over 1.0 to 2.0 GHz.
Laboratory	Measure loss of cables and power combiner	1. Attach two power combiners together with four coaxial cables of known loss. 2. Connect the power combiner arrangement to the noise figure meter ports. 3. Measure loss, subtract cable losses, and divide by two to get power combiner loss.

Table 4.2.2 – 1: Experimental Procedure (continued)

Test Type	Goal	Procedure
Test Range	Make observations for a particular helix (parasitic, extended length, extended reflector, etc.)	1. Mount standard gain horn on pedestal and make calibration measurement for gain at desired frequency. 2. Remove standard gain horn and mount the ground plane The helix is mounted in the center hole and directly connected to the test range coax. 3. Iteratively trim length and measure axial ratio. 4. Orient antenna with pedestal and rotate to take desired field pattern cut.
Test Range	Observe effect of phasing on two elements	1. Attach two helices to ground plane. Connect to two ports of power combiner. Terminate other two input ports with 50 – Ohm precision loads. Connect output port to test range coax. 2. Iteratively rotate helixes with respect to each other and observe changes in gain and pattern.

Table 4.2.2 – 1: Experimental Procedure (continued)

Test Type	Goal	Procedure
Test Range	Observe effect of element spacing on mutual coupling	1. Place one helix in center hole of ground plane. Connect to test range coax. 2. Place four helices, each terminated with 50 – Ohm precision loads, in the nearest four diagonal slots. 3. Make sure all helices are oriented for the same phase (visually inspect) 4. Take gain and pattern measurements. 5. Repeat for all element spacings
Test Range	Observe effect of element spacing on four element prototype helical array	1. Attach four helices to the ground plane in the four nearest diagonal slots. 2. Connect the helices to the power combiner input ports. 3. Connect test range coax to power combiner output 4. Make sure of proper phasing. 5. Take gain and pattern measurements 6. Repeat for all element spacings

and power combiner used in the tests was found using a commercial noise figure meter.

The pattern testing took place at a local test range (VEGA Laboratories in Vienna, Virginia) over a two day period. Gain measurements were performed by comparison to a standard gain horn. This test range was on the roof of the VEGA facility. VEGA engineers assured the author that the range was acceptable for testing the helical array configurations at the desired frequencies (approximately 1 GHz to 2 GHz), and that reflections off the surface of the roof had been quantified and would not present a problem.

4.3 Results

Experimentation produced several interesting results that both validate and, in some cases refute, the open literature. The following paragraphs describe these results.

4.3.1 Impedance Spirals

Figure 4.3.1-1 shows the impedance as a function of frequency on a Smith chart ("impedance spirals") of a typical helical element as measured in the laboratory. The obvious similarity to the impedance characteristic presented in the literature [40] validates this experiment. The impedance moves in large circles as the frequency

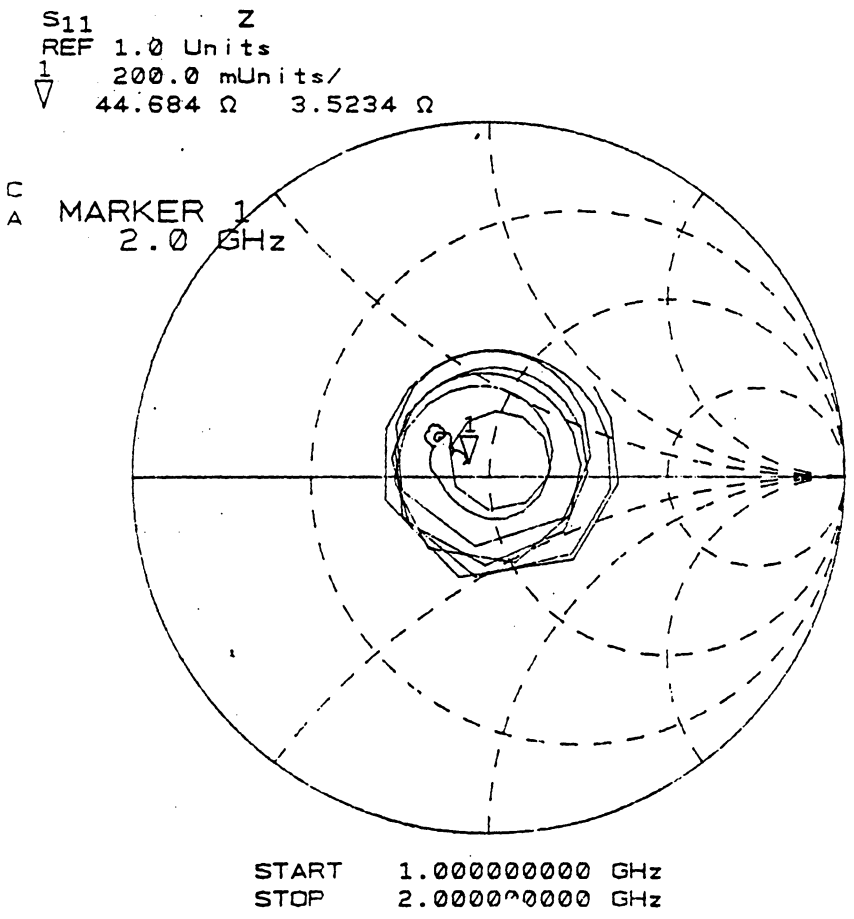

Figure 4.3.1 – 1: Measured Impedance Spiral of Typical Helix

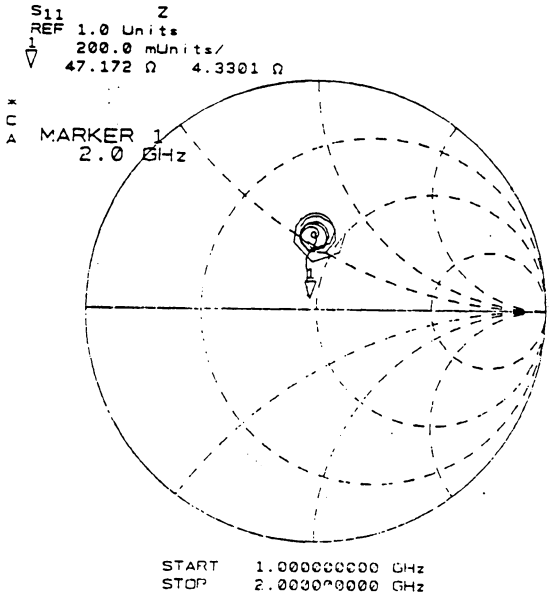

Feed wire far from ground

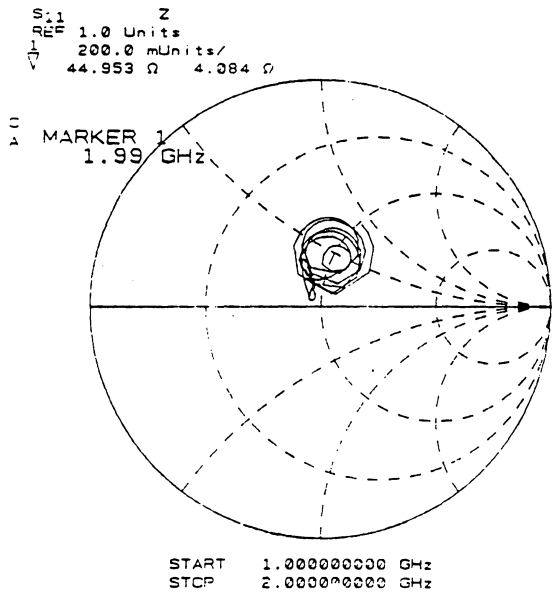

Feed wire close to ground

Figure 4.3.1 – 2: Effect of Feed Ajustment on Impedance Spirals

increases. When the helix reaches the axial mode of operation, the impedance on the Smith chart moves in tight spirals near the real axis.

As seen in Figure 4.3.1-2, the overall character of the impedance spiral was sensitive to the adjustment of the feed. Therefore, great care was taken when adjusting the feeds using the "Fox Method" (described in Section 3.2.2) prior to test range experimentation. To ensure proper operation at the test range, the VSWR of four similar helices, connected to a power combiner via short coaxial cables, was tested. Figure 4.3.1-3 shows the success of this test, with VSWR low over a wide bandwidth.

4.3.2 Field Patterns

Figure 4.3.2-1 shows the field pattern of helical element #6 in an array of helices. Axial ratio was reduced by iteratively trimming the end of the helix and observing the change. The axial ratio in the center of the main lobe generally varied from 1 dB to 2 dB. This is in agreement with the findings of others as noted in earlier in Section 3.1.3.4. The sidelobe level was approximately -10 dB, also in agreement with the published figures as stated in Section 3.1.3.2.

However, three observations refute generally accepted helix characteristics:

1. The frequency at which gain was maximum, f_{max}, was 1.3 ± 0.025 GHz. This corresponds to a C_λ of 0.964 for the three inch diameter helix, not 1.1 as expected.

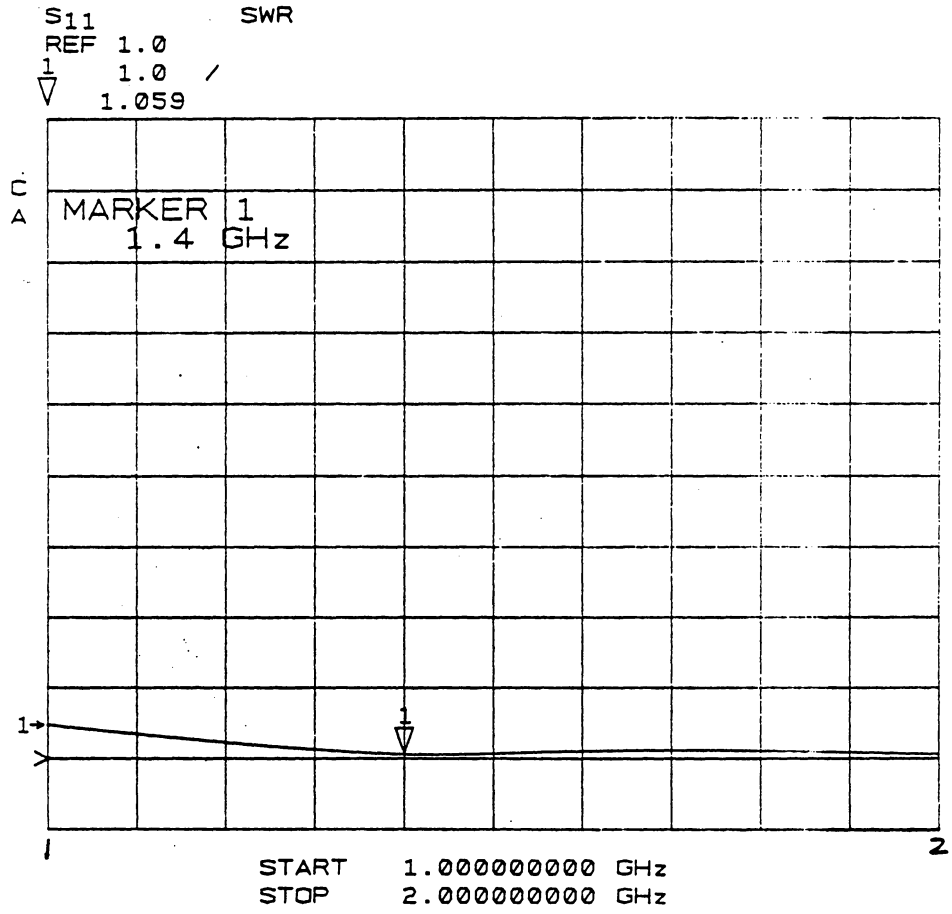

Figure 4.3.1 – 3: SWR of Four Helixes Through Power Combiner

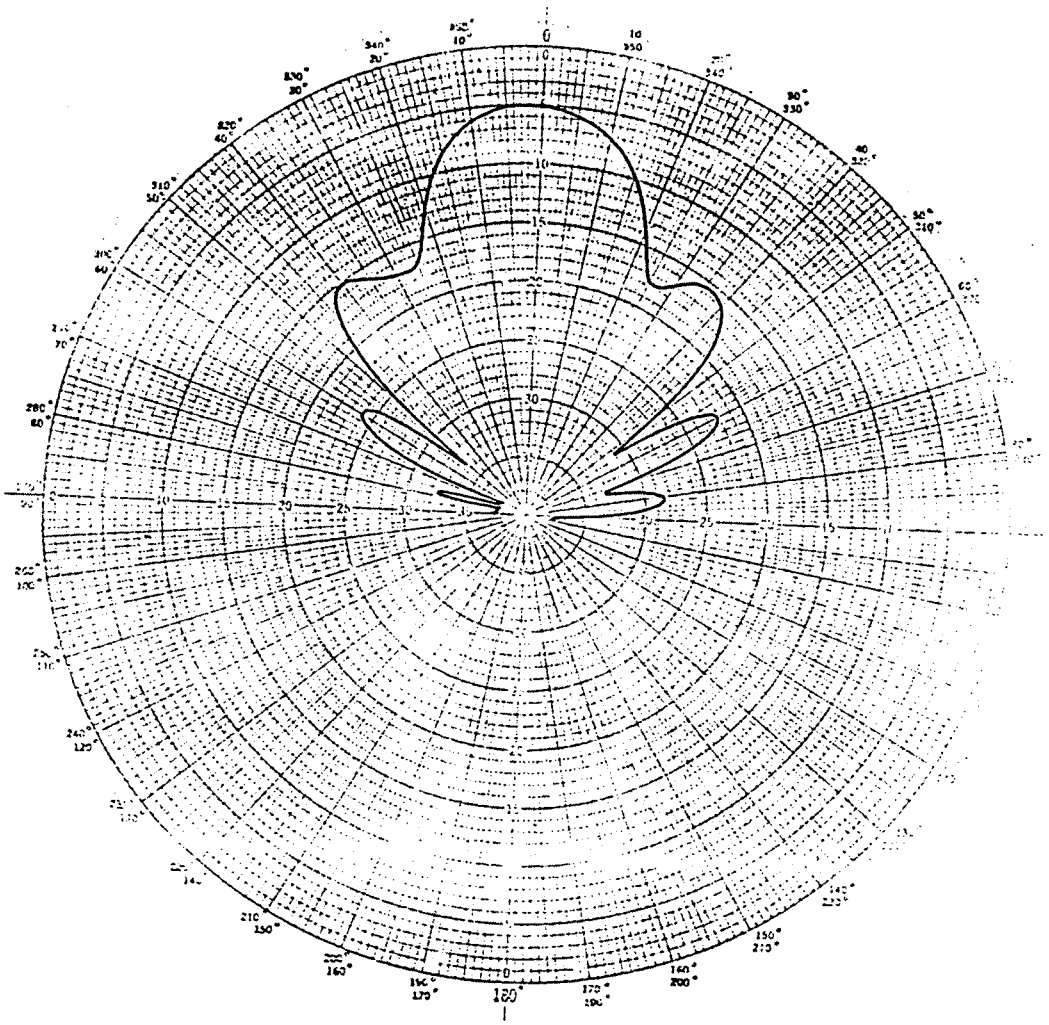

Figure 4.3.2 – 1: Typical Helix Field Pattern Taken From Testing (Test Helix #6)

2. The 3 dB bandwidth, BW, approximately 200 MHz (BW_Z=15 %), was much smaller than reported values which were as high as BW_Z=70 %. This bandwidth was determined by sweeping the frequency (of the signal generator/transmitter) and observing that frequency which produced maximum gain, and the frequencies on the high and low side of this frequency at which the gain was 3 dB lower than maximum gain.

3. The gain was as high as 15.9 dBi (helix #7); this value is significantly higher that predicted using even the more modern quasi-empirical formula of King and Wong discussed in Section 3.1.3.1. The anticipated gain is calculated below using equation (3.1.3.1-1) using the dimensions of helix #7.

   D=0.0762 m
   λ=0.2308 m
   N=18 turns
   NS (length) =1.0 m
   α=12.5°

$$G = 8.3\ (1.1333)\ (3.23)\ (1) = 30.397 = 14.83\ dB$$

The data in Appendix B shows the variation of the field pattern of helix #1 over a wide frequency range. There exists a noted similarity to the results reported in the literature (see Section 3.1.3.5).

A very long helix, (helix #9), was tested to see if gain would increase. As seen in Figure 4.3.2-2 , the pattern became distorted and the gain actually decreased. This may have been due to:

1. The presence of the T_2 wave
2. The attenuation of the T_1 wave near the end of the helix
3. A large reflection from the end of the helix
4. A shift in the frequency of operation

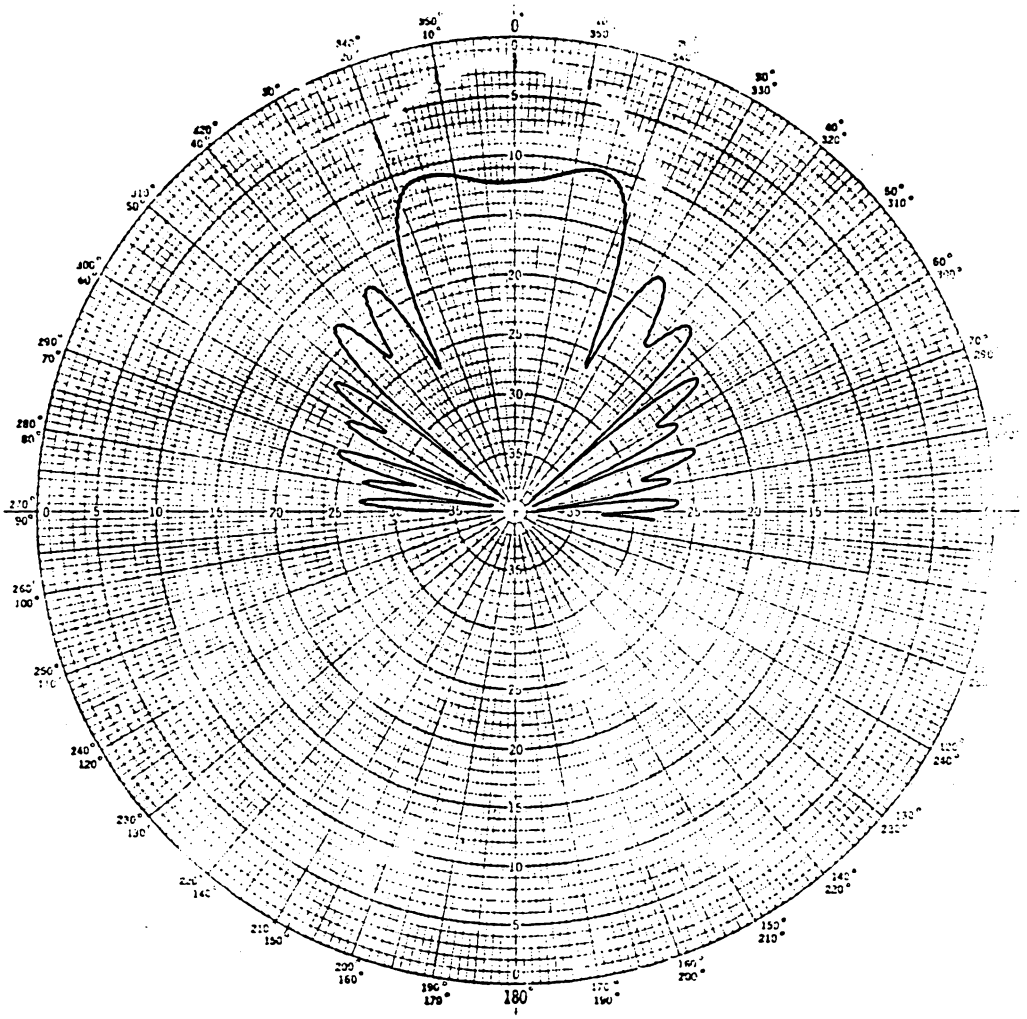

Figure 4.3.2 – 2: Field Pattern of Very Long Helix (Test Helix #9)

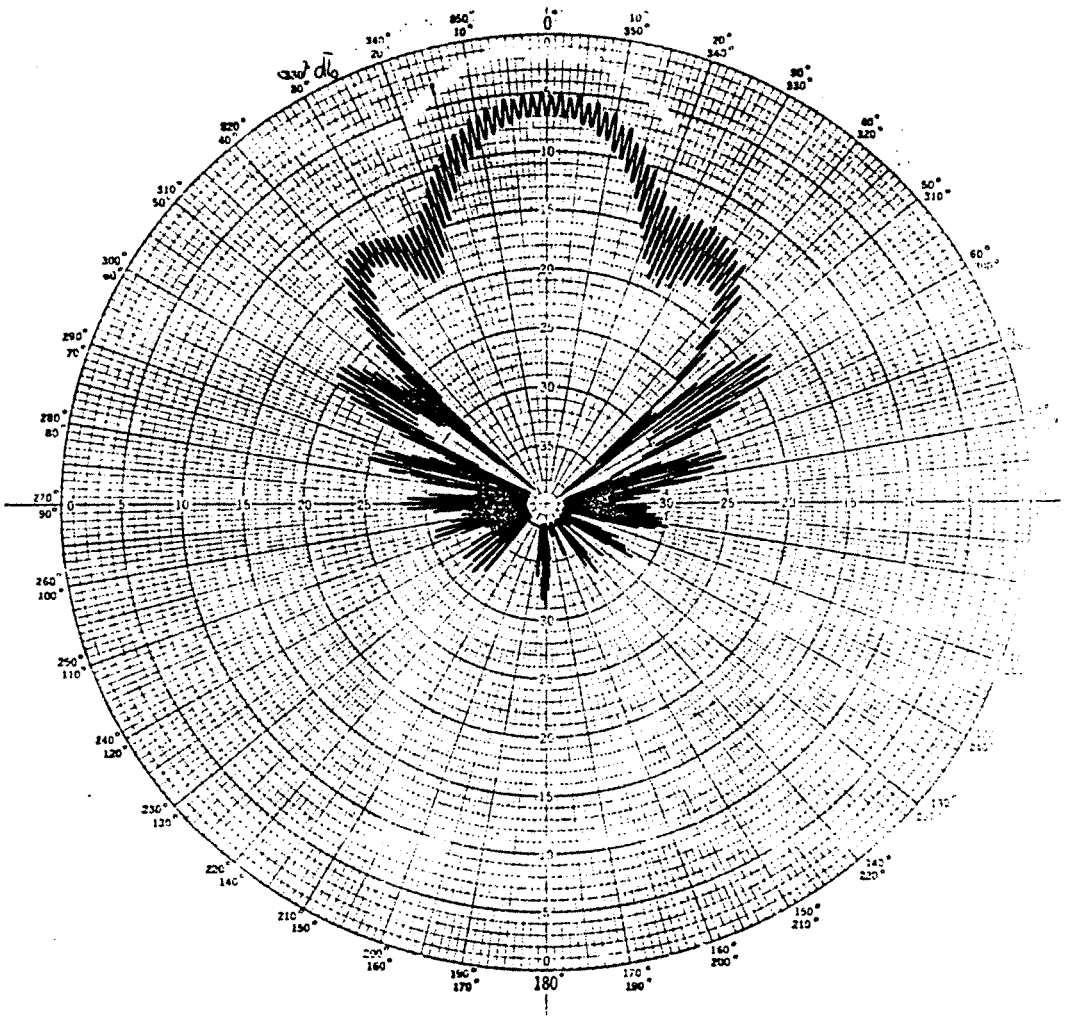

Figure 4.3.2 – 3: Field Pattern of Helix with Parasitic Winding (Test Helix #8)

Lastly, a parasitic winding was added to helix #8 to increase the forward gain. However, gain actually decreased, due to improper winding of the passive element. Figure 4.3.2-3 shows the resulting pattern.

4.3.3 Mutual Coupling

The specified procedure in Table 4.2.2-1 was followed to obtain a curve of forward gain versus element spacing with test configuration IV. Since the surrounding four elements were passive (terminated by 50-Ohm precision loads), the loss in gain can be solely attributed to the presence of mutual coupling[22]. Figure 4.3.3-1 shows the resulting data. This contrasts greatly with the results of others with low gain helical elements[22,32]. Apparently, for high-gain helical elements, the effects of mutual coupling are significant even for spacings as large as two wavelengths.

As a follow-on experiment, the length of the cylindrical reflector was doubled (helix #10). However, the gain of the element decreased and the pattern became distorted. This was perhaps due to suppression of the T_1 wave responsible for the axial mode of operation. Figure 4.3.3-2 shows the resulting field pattern.

4.3.4 Four Element Array

Before this test, two elements were arrayed to test the sensitivity of array performance to phasing using configuration II. Simply by

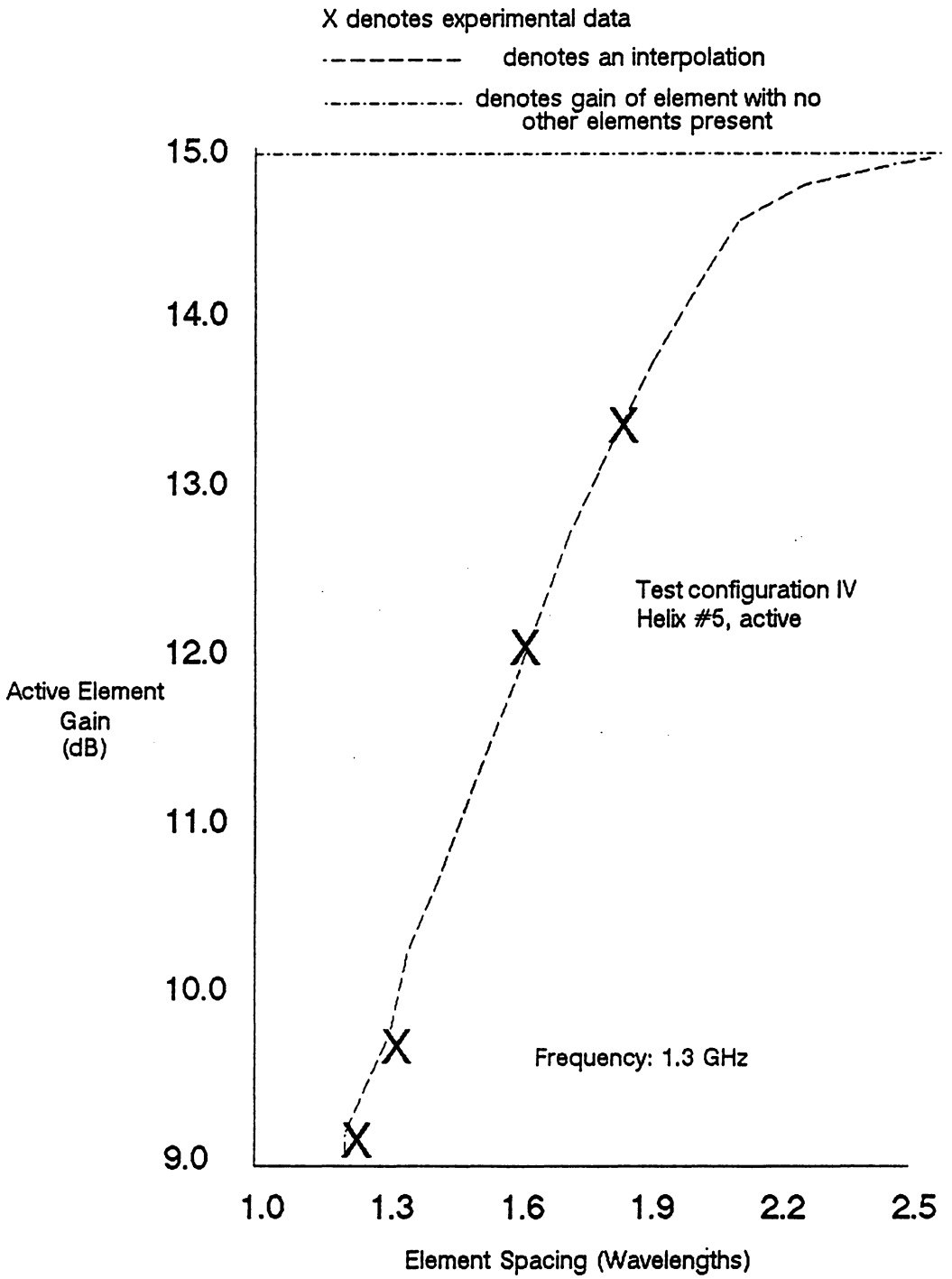

Figure 4.3.3 – 1: Gain versus Element Spacing for Helix with Induced Mutual Coupling

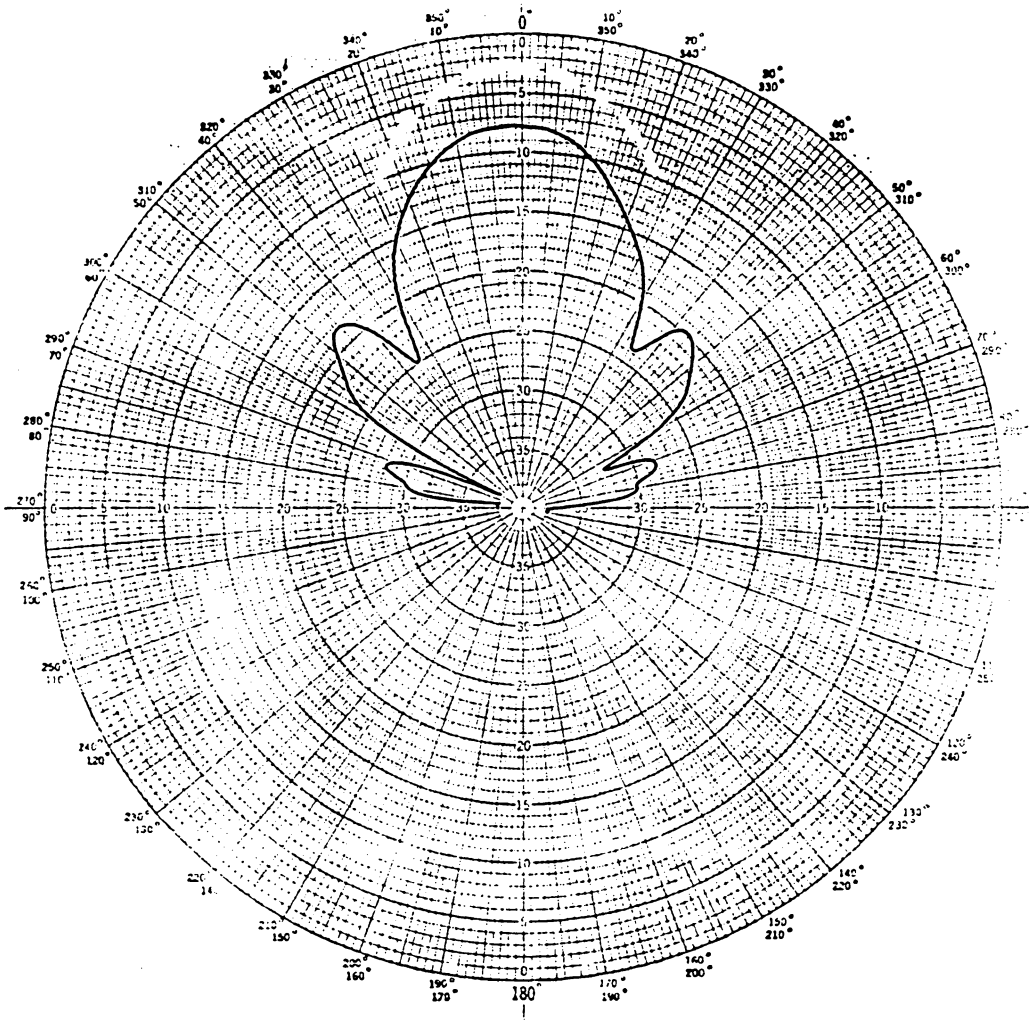

Figure 4.3.3 – 2: Field Pattern of Helix With Extended Reflector (Test Helix #10)

visually aligning the first turn of the helix, proper phasing was achieved. Figure 4.3.4-1 illustrates the relationship between mechanical rotation of the helix, and the electrical phase. For example, rotating a helix 45 mechanical degrees with respect to a reference helix will change the relative electrical phase by 45 electrical degrees [21]. After determining that phasing could be accomplished through this technique, the four element array was constructed (configuration III).

Following the procedure in Table 4.2.2-1, a curve of array gain as a function element spacing was generated. Figure 4.3.4-2 shows this curve. At two wavelength spacing, the array gain indicates that the "dB per doubling" figure is approximately 2.8 dB. That is, if a helix with a 14 dBi forward gain, then the gain of a two element array would be,

$$G_{array} = 14 + 2.8 = 16.8 \text{ dBi},$$

and a four element array would have a gain of,

$$G_{array} = 14 + 2.8 + 2.8 = 19.6 \text{ dBi}.$$

Unlike the curves in the literature [32,33], the gain versus element spacing characteristic here is not strictly monotonic. A small peak exists at 1.2 wavelengths spacing. The data points were measured several times to ensure accuracy. The reason for this anomaly at small spacings is unknown.

Key:

——→ points to start of first turn of helix
- - - - - → points to reference (the start of the first turn of a chosen helix in an array)

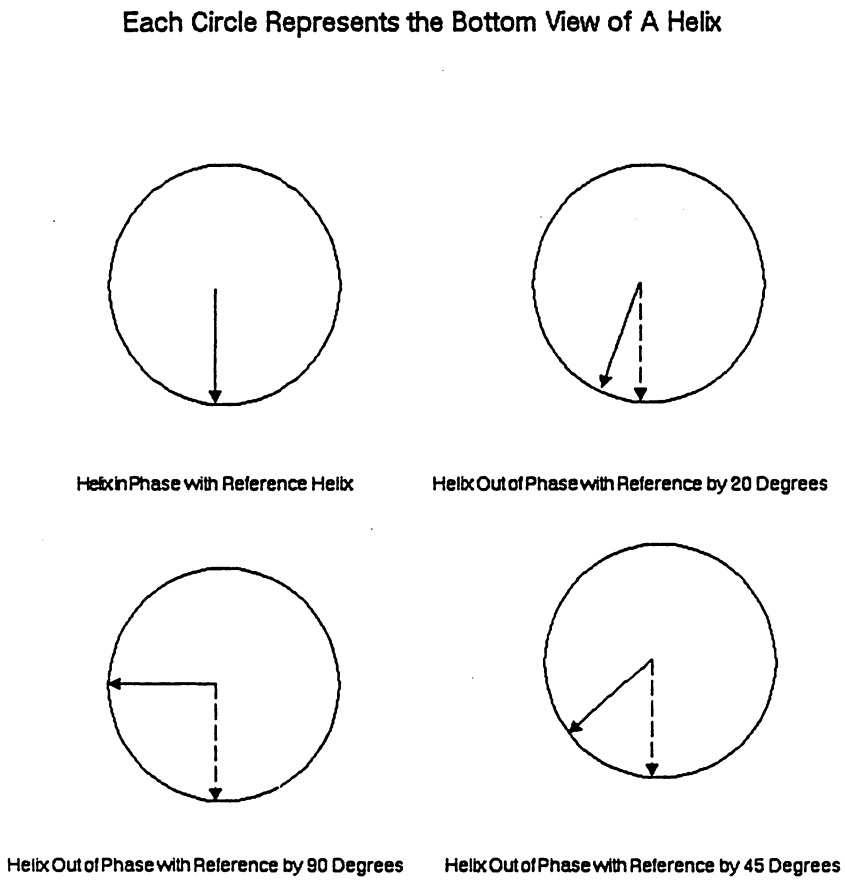

Figure 4.3.4 – 1: Mechanically Phasing the Helical Array Elements

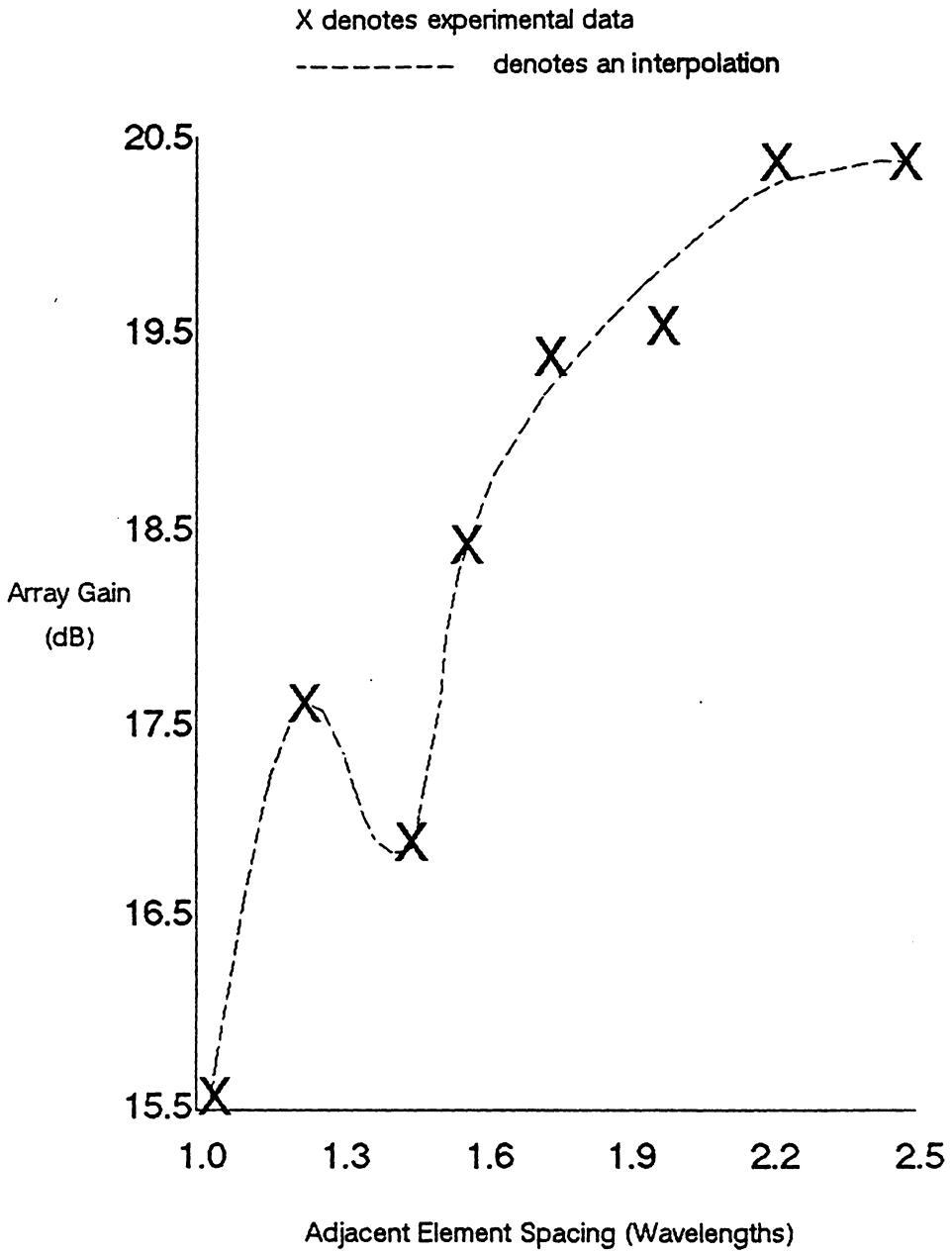

Figure 4.3.4 – 2: Gain versus Element Spacing for Prototype Array

4.3.5 Error Analysis

It should be mentioned that the repeatability of the data was excellent. However, the accuracy of the field pattern measurements was limited by the measuring device to 0.25 dB. The inaccuracies in the impedance testing were negligible.

Since the power combiner provided no isolation, it theoretically increased the overall mutual coupling in the field tests. However, since the SWR characteristic measured in the laboratory was good, it is likely that the effect of the power combiner on test results was small.

The parasitic winding was improperly wound. It should have been wound starting at the side opposite from the start of the active winding[1,5].

Chapter 5: Simulation Program, HEMAN

5.0 Simulation HEMAN

The HElical Mobile ANtenna simulation (HEMAN) uses measured or theoretical element patterns to calculate array patterns and antenna noise. This short, but useful program was written by the author to calculate the figure-of-merit, G/T, for a hypothetical array based on patterns stored in a data base. This G/T does not include the noise temperature of the electronics (preamplifier and receiver). In other words, $T=T_{sys}$. The data base points (angle and gain) taken from element patterns were typed into the computer file from the data in one degree increments. The simulation uses a coordinate transformation subroutine written for past projects at Unisys Corporation in Reston, Virginia. This transformation is necessary to transfer the coordinates of the temperature environment (earth and sky) to the coordinates of the array. A good discussion of this problem is given in [39].

5.1 Basis

The algorithm used in this simulation is given in Figure A-1 of Appendix A. This simulation is based on the Pattern Multiplication Method (PMM) and a simplified noise model. Reference [47] gives a

detailed discussion of the pattern multiplication method. The data input to the program is the pattern of a single element. This input is stored in a file. Alternatively, the user may elect to use the ideal model of a helix, for purposes of comparison. The E-field expression used for modeling the ideal helix is shown in equations (5.1-1) and (5.1-2)[45].

$$E = \sin\left(\frac{\pi}{2N}\right)\cos\theta\frac{\sin[(N/2)\psi]}{\sin[\psi/2]} \qquad (5.1\text{-}1)$$

$$\text{where } \psi = 2\pi\left[\frac{S}{\lambda}(1-\cos\theta)+\frac{1}{2N}\right] \qquad (5.1\text{-}2)$$

In this option, the user specifies the physical dimensions of the helix. However, this model possess beamwidths that are much larger than beamwidths of real helices (in the literature and in this work) , so it was not used to generate quantitative data.

The program then prompts the user for:

- Array size (assumed to be square, N by N), N^2
- Interelement spacing, d_{ele}
- Elevation angle above the horizon (antenna is set pointing in this direction for temperature calculations)

Equation (2.1-2) was used to compute the antenna noise temperature. The output of the pattern multiplication method is a field pattern.

This field pattern is then integrated to compute $G(\theta,\phi)$. It is also used to calculate T_A in using equation (2.1-2).

5.1.1 Assumptions

The following assumptions were employed in the HEMAN simulation:

- Mutual coupling is neglected. However, by entering pattern data that were taken with mutual coupling effects present (test configuration IV, helix #5), the program will approximate the radiation pattern and gain of a the actual array.
- A simplified noise model was assumed. The sky noise, T_{sky}, was considered homogeneous (6 Kelvin). The noise temperature of the earth, T_{earth}, was taken to be a constant 300 Kelvin. These assumptions are valid over 1 GHz to 2 GHz.
- The program is, in a sense, frequency invariant. The frequency of operation is implicit in the input data pattern or, in the case of the theoretically generated pattern, expressed in terms of wavelengths (e.g. circumference, element spacing, etc.)

5.1.2 Purpose

The three primary purposes of the HEMAN simulation are to:

1. Validate Experimentation
2. Generate G/T Curves
3. Predict Performance of Large Arrays

In short, a validated HEMAN simulation can be used in conjunction with minimal antenna range testing to create, design, and develop a portable ground station antenna using helices.

5.2 Output

The simulation generates output in several forms:

- o Curves(G/T versus elevation angle)
- o A 1-dimensional output is plotted in polar format so that a comparison with the experimentation and the literature can be made.
- o Data(gain and noise temperature)

As the program is now written, a system command file must be used to generate the G/T versus elevation curve. The appendix shows a sample run.

5.3 Results

The results of the simulation validate the experimental results presented in Section 4.3. Specifically, three series of runs were made to do this:

1. A pattern taken for helix #3 in test configuration I was used as input(see Figure 5.3-1). **Note that this means mutual coupling is completely neglected for this series of runs.** The HEMAN simulation was run with this input over the full range of element spacings given in figure 4.2-1 for configuration III. The result is a curve of gain versus element spacing with mutual coupling neglected.

2. The patterns taken in the mutual coupling experiment (helix #5, configuration IV) were used as input to generate a curve of gain versus element spacing. These active element patterns contain mutual coupling effects. Due to the differences in geometry (Figure 5.3-2)the amount of mutual coupling is overestimated by this method. However, the resulting curve will still give

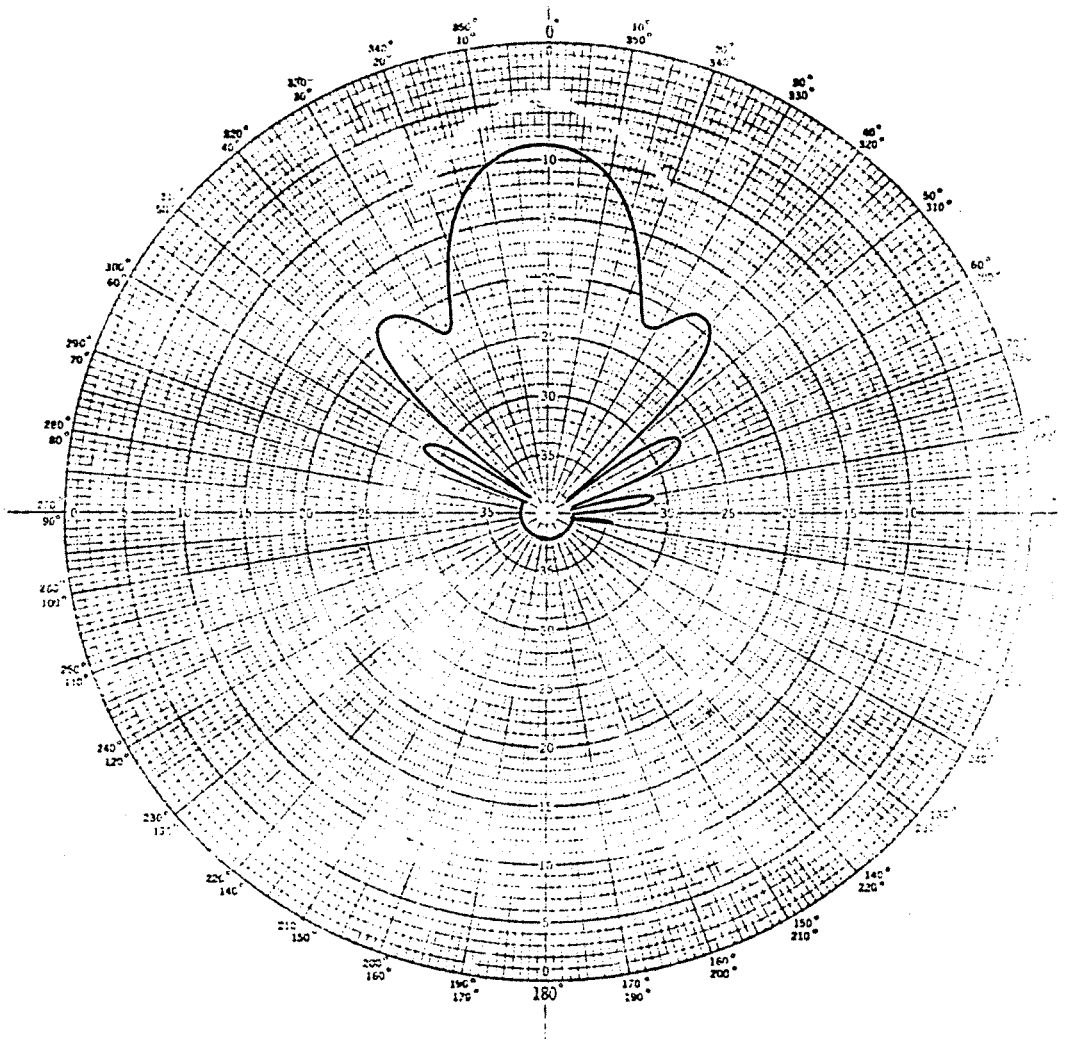

Figure 5.3 – 1: A Typical Pattern Used for Input to HEMAN Simulation (Test Helix #3)

Key: X – active element
O – passive element, terminated with 50 Ohms

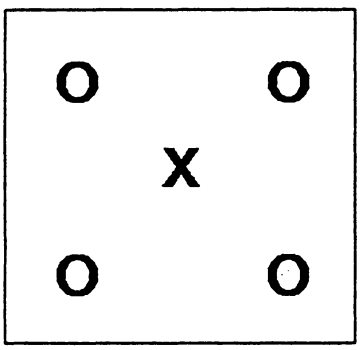

Actual Geometry Used
in Mutual Coupling Experiment

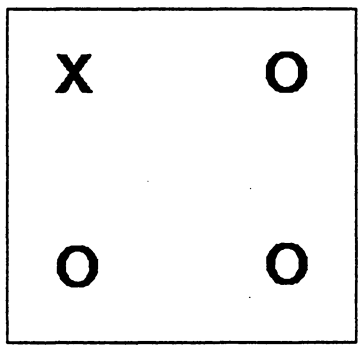

Ideal Geometry
for Modeling Mutual
Coupling in 2 x 2 Array

Figure 5.3 – 2: Improvement in Test Back Plane Geometry

meaningful results for the larger element spacings. This method was used to conserve test time on the antenna range.

3. A patterns taken for helix #5, configuration IV was used as input. The simulation was the run for the same configuration IV element spacings that took place during the test. The simulation generated the pattern at each element spacing for the purpose of comparing the general character with the results of the experiment.

Figure 5.3-3 shows the results for run series #1 and #2. The results of the experiment are presented for comparison. The curve without mutual coupling is, as expected, higher than the measured data except for large element spacings where mutual coupling was shown to be weak. The curve with mutual coupling well approximates the measured data. This implies that the HEMAN simulation can be used in conjunction with a single element field pattern to accurately predict array gain.

Figure 5.3-4 shows the results of run series #3 along with the corresponding experiment patterns. The patterns are quite similar for nearly all element spacings. This implies that HEMAN can not only predict the gain of an array, but also predict sidelobe characteristics.

Note that the similarity in the simulation and experiment patterns decreases for the element spacings less than 1.4 wavelengths where mutual coupling occurs. The effect of mutual coupling would seem to distort the pattern somewhat, particularly the sidelobes.

While some assumptions were made in the above analysis regarding mutual coupling, the method of array performance prediction has been

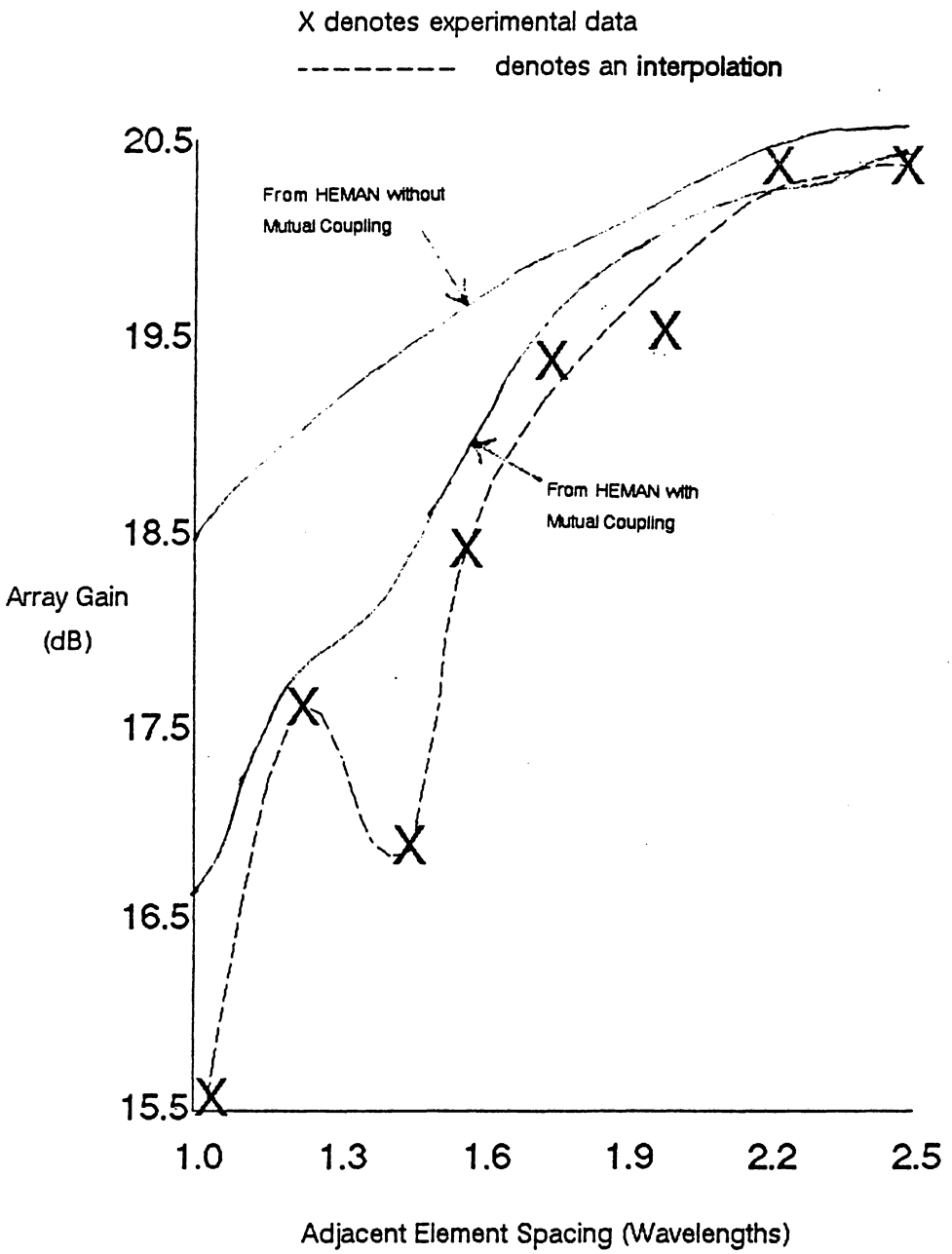

Figure 5.3 – 3: Projected Gain versus Spacing With and Without Mutual Coupling

2.46 Wavelength Spacing

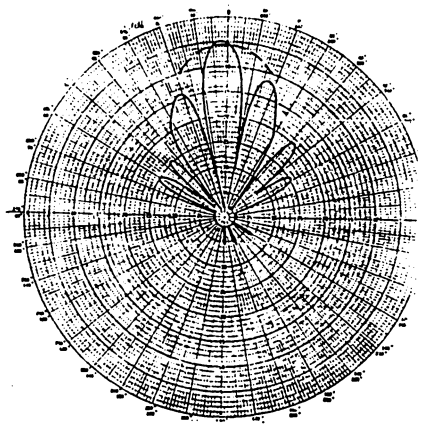

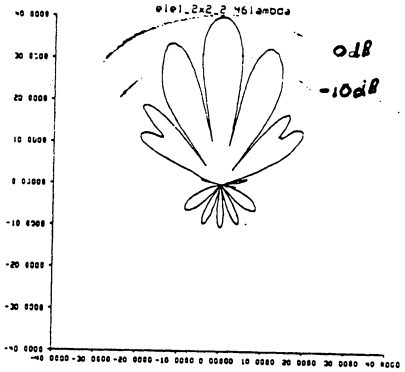

2.18 Wavelength Spacing

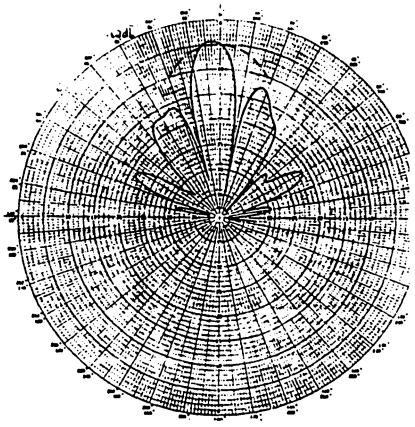

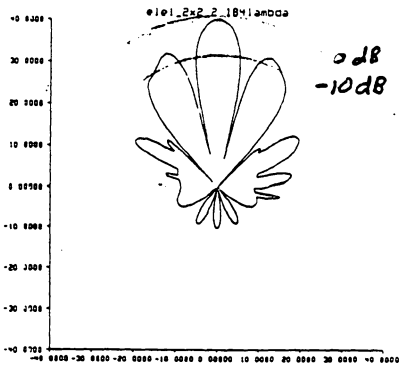

Frequency: 1.3 GHz

Figure 5.3 – 4: Comparison of Experiment and HEMAN Patterns for Various Spacings

1.92 Wavelength Spacing

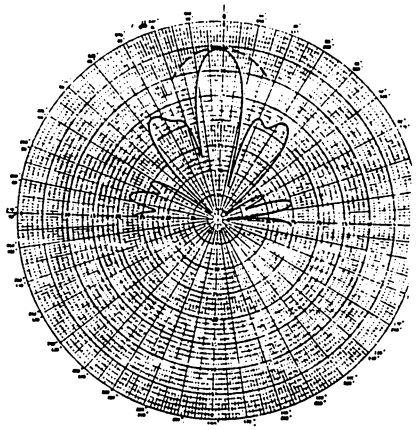

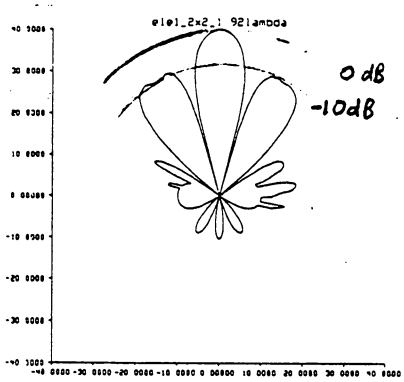

1.73 Wavelength Spacing

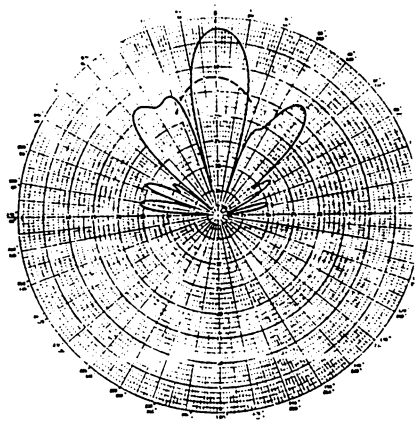

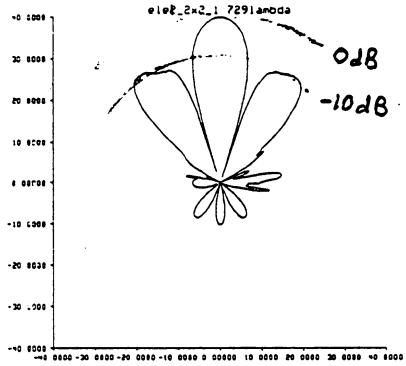

Frequency: 1.3 GHz

Figure 5.3 – 4: Comparison of Experiment and HEMAN Patterns for Various Spacings (con't)

1.55 Wavelength Spacing

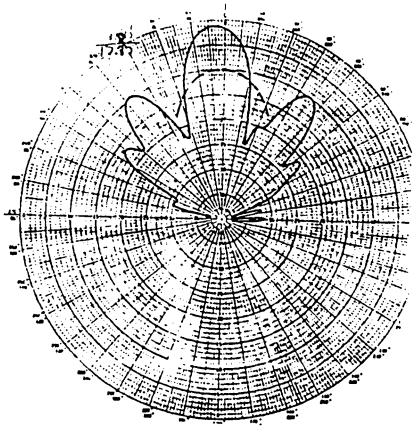

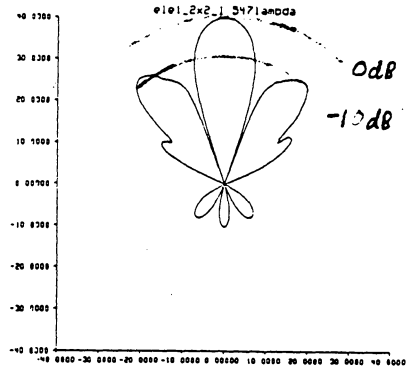

1.37 Wavelength Spacing

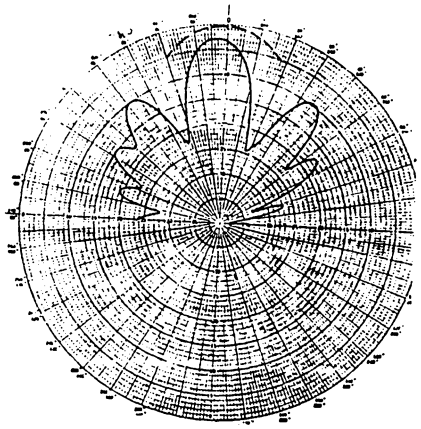

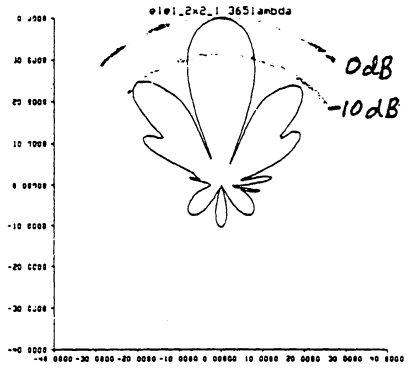

Frequency: 1.3 GHz

Figure 5.3 – 4: Comparison of Experiment and HEMAN Patterns for Various Spacings (con't)

1.18 Wavelength Spacing

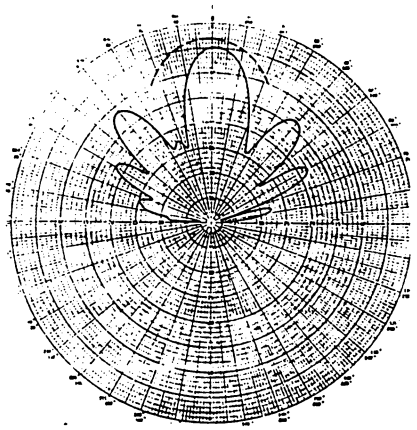

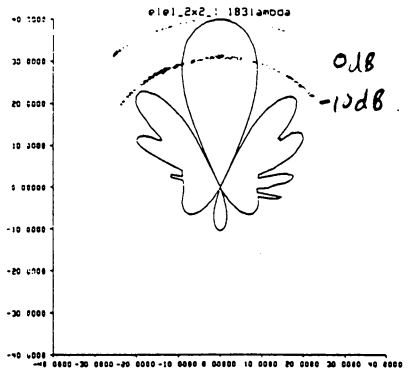

1.00 Wavelength Spacing

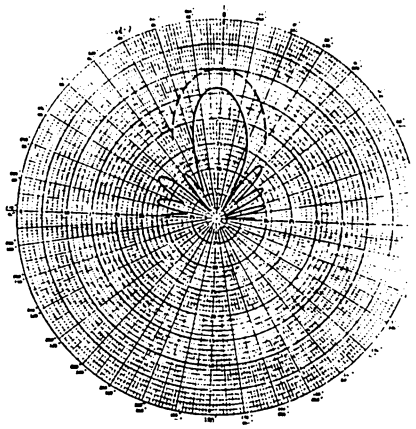

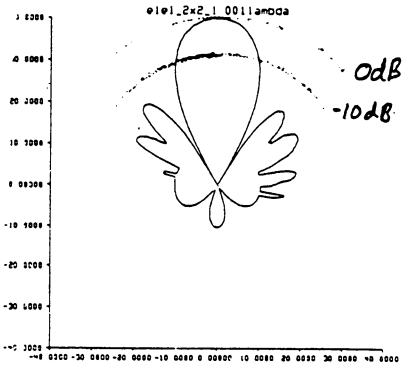

Frequency: 1.3 GHz

Figure 5.3 – 4: Comparison of Experiment and HEMAN Patterns for Various Spacings (con't)

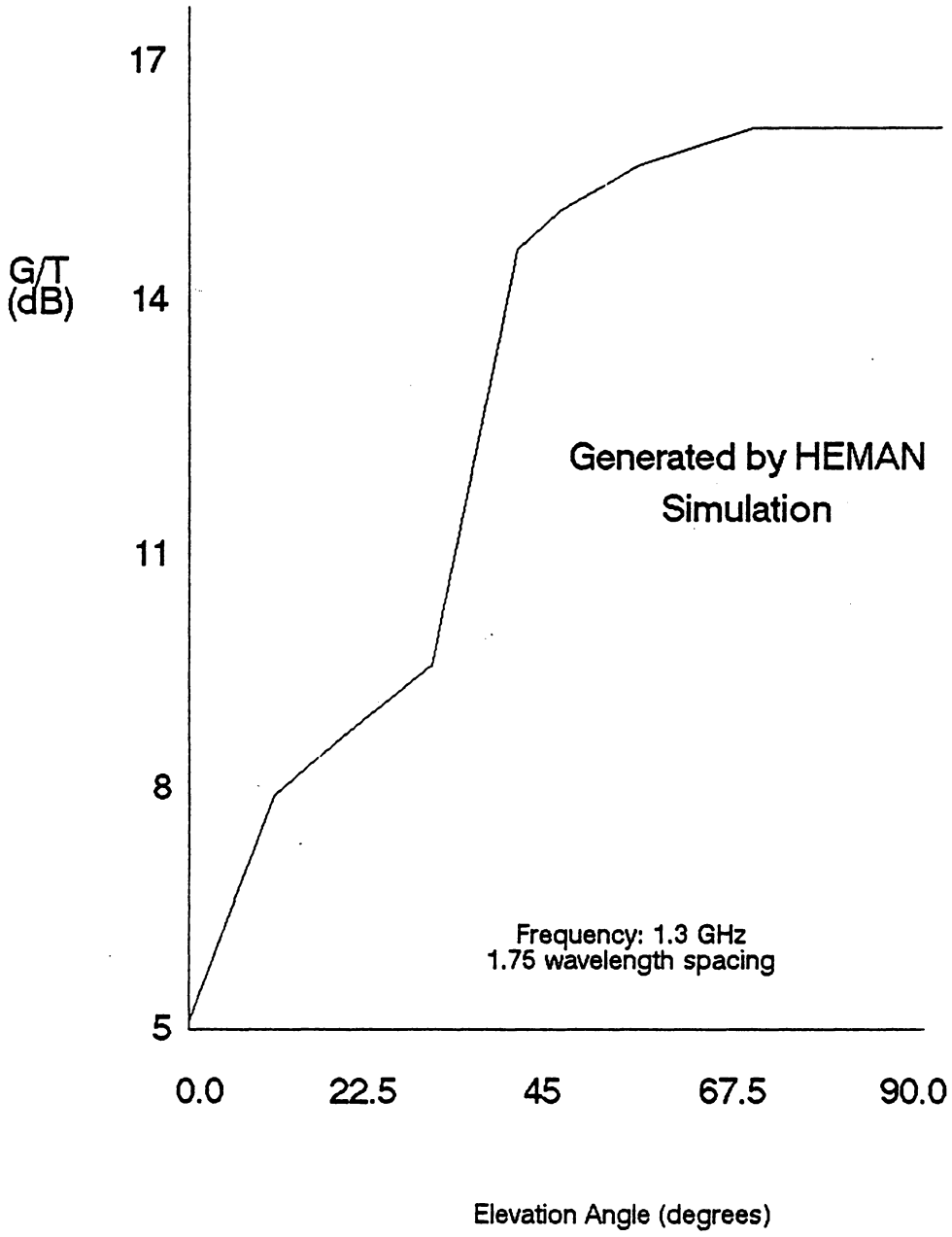

Figure 5.3 – 5: Projected G/T versus Elevation for 16 Element Helical Array

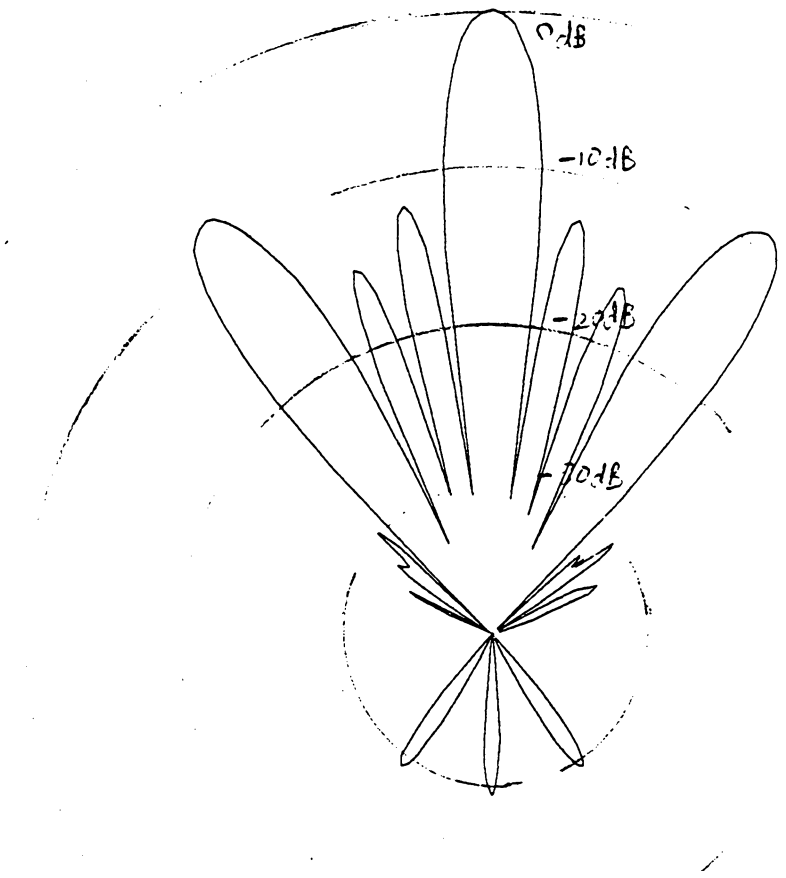

Figure 5.3 – 6: Predicted Field Pattern for 16 Element Helical Array

shown to be viable. With this in mind, the simulation was again used, this time to generate curves of G/T versus elevation angle for a 16 element (4x4 square) helical array with an element spacing of two wavelengths. Figure 5.3-5 shows the resulting curve. As previously mentioned, this curve can now be used to determine the communication window for any given satellite-to-earth link for a 16 element (4x4 square) helical antenna whose dimensions at 1.3 GHz are 5 feet by 5 feet (backplane) by 3.28 feet (helix length). Figure 5.3-6 shows the predicted field pattern.

Chapter 6: Summary

6.0 Summary

This work shows the helical array is a viable portable ground station antenna. This was done by:

1. building a test-bed array (test configuration III) from information in the literature
2. testing the test-bed array and helical elements using test configurations I, II, III, and IV
3. simulating the results using minimal test data (a single element pattern as input) with (configuration IV), and without (configuration I) mutual coupling

Several of the findings of other workers have been verified, while other results contradict widely held figures.

This work also has given a general background that can be used to understand some of the underlying principles in the operation of a helical antenna such as the three traveling waves, T_0, T_1, and T_2. Also, possible modifications to the helix have been presented.

6.1 Conclusions

Several conclusions can be drawn from this work:

1. This work and the work of others has shown the helical array to be a potential portable ground station antenna. This work was perhaps the first to examine a high-gain helical array in some detail. The helical array performance was not degraded because of handling during transportation to the antenna test range.

2. Mutual coupling is an effect that must be minimized. If the mutual coupling of an array is reduced, the required element spacing, and hence the overall array size likewise decreases.

3. The method of inputting a test range pattern for a single helix into a simulation to predict array performance is valid. The effects of mutual coupling need not be incorporated directly in the program, but rather can be included by testing the helix used for input in a similar environment (surrounded by passive elements, each terminated by a precision load as in test configuration IV).

6.1.1 G/T versus Elevation Angle

The sidelobe level is important when calculating the noise temperature of an array. Several supplemental runs on the HEMAN simulation show that noise temperature can be greatly reduced by suppressing the sidelobe level. Figure 6.1.1-1 shows the G/T for a conical helix array (the conical helix is discussed in Section 3.3.6).

The HEMAN simulation can be used to design a helical array to meet a satellite downlink requirement. Given a curve of required G/T, the designer need only test individual elements and run the simulation in an iterative fashion to find the most volumetrically efficient helical antenna that will satisfy the operational requirements.

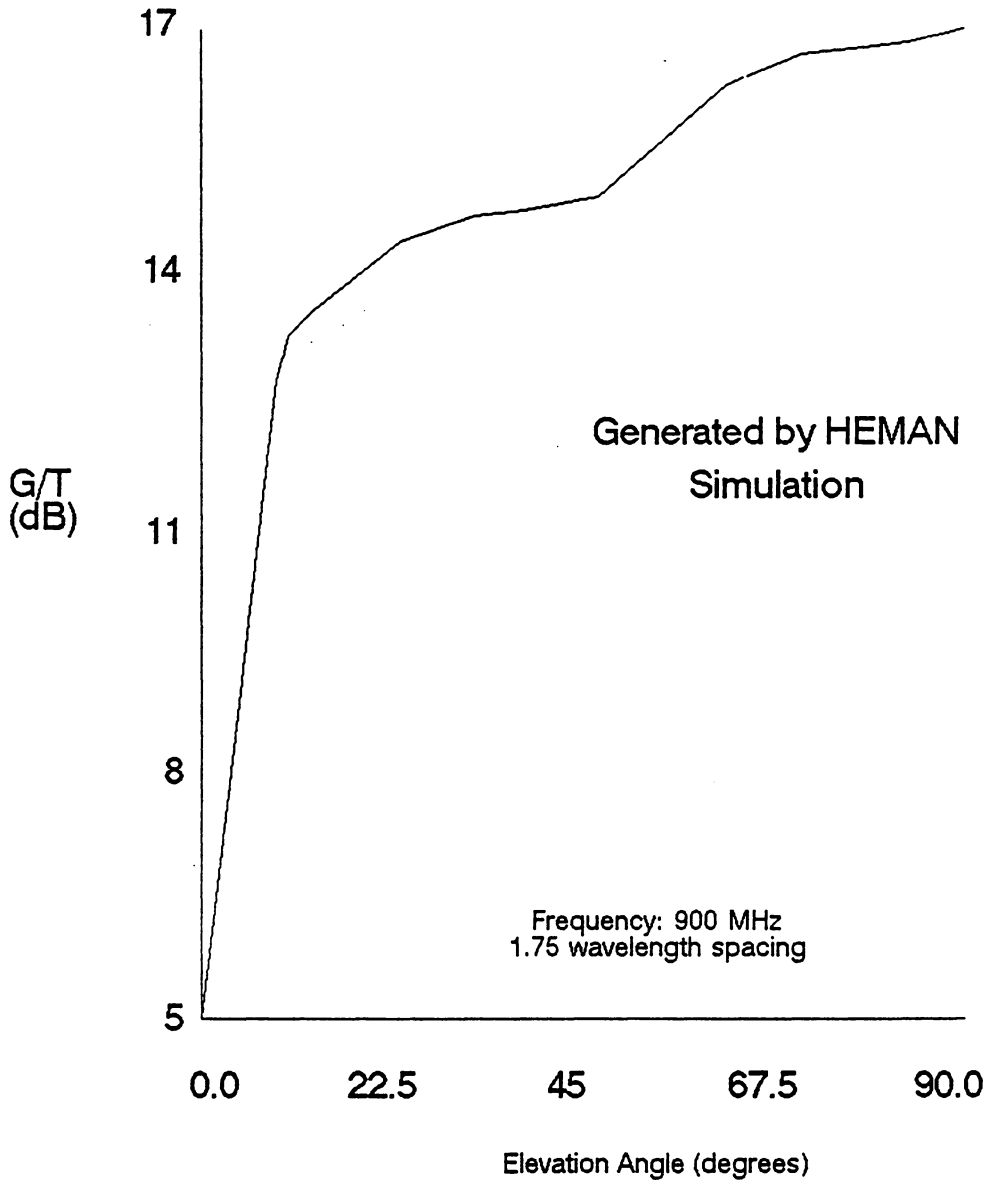

Figure 6.1.1 – 1: Projected G/T versus Elevation for 16 Element Conical Helix Array

6.1.2 Mutual Coupling

For the helical elements built for the experiments in the work, an element spacing of greater than two wavelengths ensures the designer that mutual coupling effects will not seriously degrade performance. As was shown in Section 4.3.4 there exists an anomaly at element spacings near 1.4 wavelengths that may exist because of mutual coupling effects, although the results of others [33,34] indicate that mutual coupling in a high-gain array environment is monotonic.

6.1.3 Impedance Matching

As anticipated, impedance matching the helix to 50 Ohms was a simple adjustment. In addition, feed performance proved insensitive to mechanical perturbation (during transport to the test range, and during testing). The builder must take care, however, to make certain the impedance characteristics of the helical elements in an array are similar so that the power combiner output will be constant over a desired bandwidth. This process, while time consuming (10 minutes per helix) is not complex or difficult.

6.1.4 Performance Parameters

The best observed gain for a test-bed helix (helix #7) was 15.9 dB. This is larger than any uniform helix reported to date in the

literature. This suggests that more work must be done to better characterize the gain of a single helix. Until this is done, it would seem that the use of a test range to optimize helix performance is necessary.

The gain of an array is reduced by mutual coupling and by the overlap of the effective apertures. Since both of these two effects are functions of element spacing, and both increase as element gain increases, the minimum size of the array is determined by the required G/T. Given the helices constructed for this work, a "dB per element doubling" of 2.8 dB should be used for an element spacing of two wavelengths. Due to inaccuracies in the gain data, this figure may be off by approximately 0.1 dB.

The typical sidelobe level was -10 dB and the axial ratio ranged from 1 to 2 dB (see Section 4.3.2). These results agree with the findings of others. However, the bandwidth of the helical antenna was found to be only $BW_{\%}$=15 %, much lower than anticipated. This may be due to the attenuation of the T_1 wave as the helix becomes long (approximately four to five wavelengths).

6.1.5 Pattern Variation with Frequency

The pattern of the helix changes with frequency. The pattern can become distorted outside the bandwidth. The value of C_λ for which gain

is a maximum was found to be 0.964, not the often quoted 1.1. This means that the size and weight of the helix is smaller than anticipated.

6.1.6 Helix Modifications

The use of a conical helix is recommended. The sidelobe level is very low (-20 dB) and the gain is only about 0.1 dB lower than a uniform cylindrical helix of the same length. The axial ratio is also very impressive (less than 1 dB) and the bandwidth reportedly increases. The use of reflector is also recommended to reduce the effects of the T_0 wave. It is unclear what reflector dimensions are optimum.

6.2 Future Work

More work is required to optimize the helical array. The G/T for the four element prototype presented in this work was not maximized at the test range. Available techniques, some of which have been presented, should be incorporated into the design to increase helical element, and overall array, gain. The next design should reduce noise temperature by using active elements and tailoring the array pattern.

Testing should be more extensive. Results of the simulation require validation in the field using the full scale portable ground station antenna.

6.2.1 Active Elements

Even in the 1970's, the price of Low Noise Amplifiers (LNA's) was prohibitive ($20,000). However, advances in low noise solid state technology has reduced the price of LNA's by an order of magnitude. For example, an L-band LNA with 34 dB gain and noise figure of 0.8 dB can be purchased for only $1500.

It is feasible to design low noise "active" arrays; that is, each element of the array has an LNA. Figure 6.2.1-1 shows this concept. This effectively negates the noise contributed by the feed network, cabling, and RF hardware.

However, several problems exist that require resolution:

- o Possible Undesirable Standing Waves in Combiners
- o Phase Matching LNA's
- o Amplitude Matching LNA's

More work is necessary to determine the severity of these issues and to suggest possible solutions.

6.2.2 Test Refinements

Much can be learned through further testing. For example, the conical helix should be studied to quantify the effects of mutual

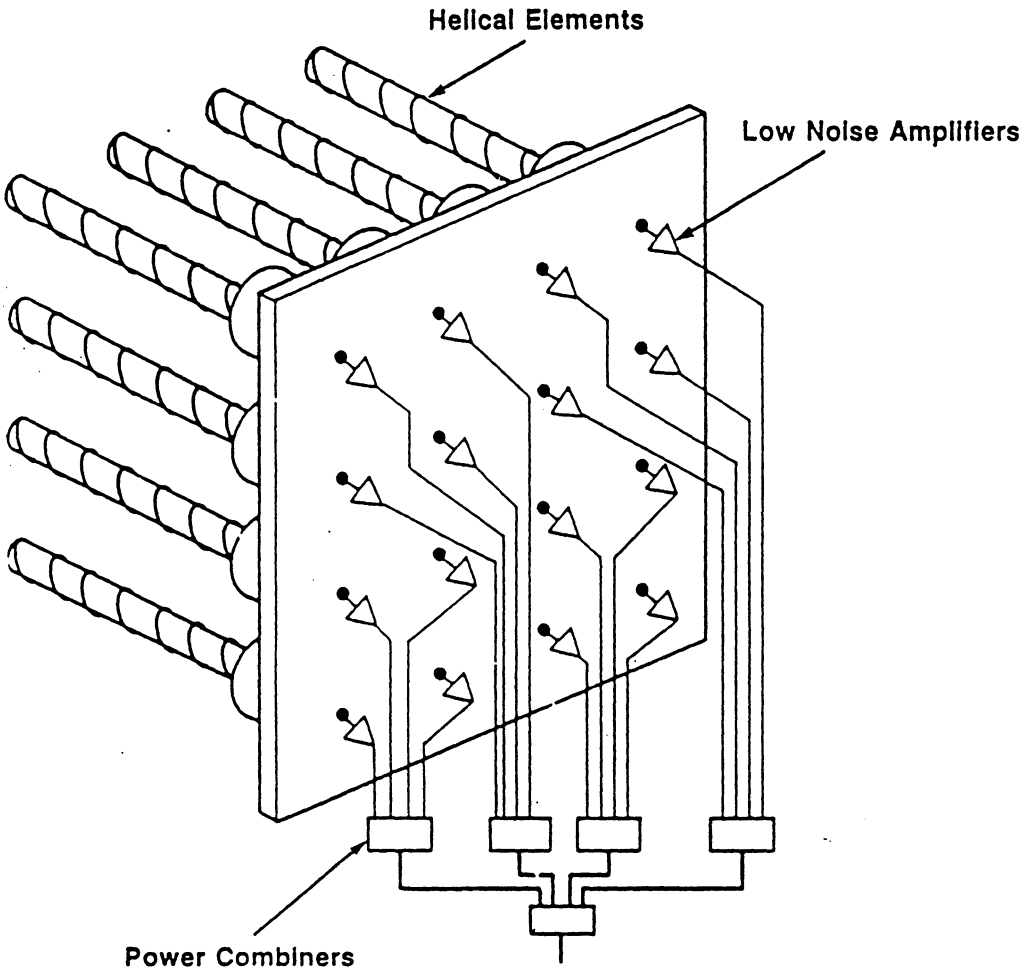

Figure 6.2.1 – 1: Use of a Low Noise Amplifier at Each Helical Array Element

coupling and to verify the findings of others. Also, gain as a function of axial length must be quantified for all helix modifications.

The single element pattern that is to be used in the simulation should be placed in an environment similar to its location in the array. For example, Figure 6.2.2-1 shows a satisfactory configuration for accurately including the effects of mutual coupling for a square four element array.

Power combiners with high port-to-port isolators should be incorporated into the next helical array design. It is likely that this will reduce the flow of energy between elements thereby reducing mutual coupling.

Larger arrays should be tested. Mutual coupling will be more severe in this case. In addition, a large array, (for example, 16 elements) is a more realistic antenna for high performance satellite systems.

Other potential tests could include:

- o Parasitic Windings
- o Different Test Frequencies
- o Multiple (Active) Helix Windings
- o Dielectric Cores

Key: X – active element

O – passive element, terminated with 50 Ohms

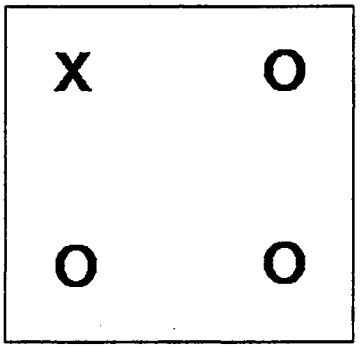

Ideal Geometry for Modeling Mutual Coupling in 2 x 2 Array

Figure 6.2.2 – 1: Geometry Can Be Improved to Better Model Mutual Coupling

6.2.3 Current Distribution

At present the current distribution along the helix has only been experimentally determined[9]. No theoretical solution has yet been derived without making limiting assumptions (only two or three modes present on the helix). Even experimental measurements have made these assumptions[9,12]. A more precise model of the current distribution on a helix would make simulations more accurate. Since it is possible to generate field patterns given the current distribution, the simulation written in this work can be modified to accept such input.

6.2.4 Mutual Coupling

Many techniques exist to reduce mutual coupling in a helical array. The most promising three techniques are:

1. Reduction through mechanically placing adjacent helices out of phase (this reduces mutual coupling) and electronically bringing the signals in-phase with phase-shifters
2. Reduction through element gain
3. Optimization of reflector dimensions

These methods must be implemented and adequately tested before the designer can use them with confidence.

7.0 References

[1]Hisamatsu Nakano, Yuji Samada, and Junji Yamauchi, "Axial Mode Helical Antennas," IEEE Transactions on Antennas and Propagation, pp.1143-1148;September 1986.

[2]T.S.M. Maclean and R.G. Kouyoumjian, "The Bandwidth of Helical Antennas," IRE Transactions on Antennas and Propagation, pp.379-386;December, 1959.

[3]J.L. Wong and H.E. King, "Broadband Quasi-Taper Helical Antennas," IEEE Transactions on Antennas and Propagation, pp.72-78;January 1979.

[4]John D. Kraus, Antennas, McGraw Hill, New York, 1950.

[5]Hisamatsu Nakano, Toshinobu Yamane, Junji Yamauchi, and Yuji Samada, "Helical Antenna with Increased Power Gain," IEEE Antenna and Propagation Symposium, pp.417-420;1984.

[6]Howard E. King and Jimmy L. Wong, "Characteristics of 1 to 8 Wavelength Uniform Helical Antennas," IEEE Transactions on Antennas and Propagation, pp.291-296;March 1980.

[7]J.L. Wong and H.E. King, "Empirical Helix Antenna Design," APS International Symposium Digest for Antennas and Propagation ,pp.366-368;1982.

[8]Thomas E. Tice and John D. Kraus, "The Influence of Conductor Size on the Properties of Helical Beam Antennas," Proceedings of the IEE, p.1296; November 1949.

[9]James A. Marsh, "Current Distributions on Helical Antennas," Proceedings of the IRE, pp.668-675;June, 1951.

[10]Rodney G. Vaughan and J. Bach Andersen, "Polarization Properties of the Axial Mode Helix Antenna," IEEE Transactions on Antennas and Propagation, pp.10-20;January 1985.

[11]K.F. Lee and P.F. Wong, "Directivities of Helical Antennas Radiating in the Axial Mode," IEE Proceedings, pp.121,122;April 1984.

[12]Cheng Donn, "A New Helical Antenna Design for Better On- and Off-Boresight Axial Ratio Performance," IEEE Transactions on Antennas and Propagation, pp.264-267;March 1980.

[13]D.J. Angelakos and D. Kajfez, "Modifications on the Axial-Mode Helical Antenna," Proceedings of the IEEE, p.558;May 1967.

[14]H. Nakano, J. Yamauchi, and S. Iio, "Tapered Backfire Helical Antenna with Loaded Termination," Electronics Letters, pp.158,159;February 1982.

[15]Alan G. Cha, "Wave Propagation on Helical Antennas," IEEE Transactions on Antennas and Propagation, pp.556-560;September, 1972.

[16]Kai Fong Lee, Principles of Antenna Theory, John Wiley and Sons, New York, 1984.

[17]Joe M. Cadwallader, "Easy 50-Ohm Feed for a Helix," QST, pp.28,29;June 1981.

[18]John D. Kraus, "A 50-Ohm Input Impedance for Helical Beam Antennas," IEEE Transactions on Antennas and Propagation, pp.913;November 1977.

[19]Dennis R. Murphy, "More on 50-Ohm Helix Feed," QST, pp.54-55;December 1981.

[20]B.A. Munk and L. Peters, Jr., "A Helical Launcher for the Helical Antenna," IEEE Transactions on Antennas and Propagation, pp.362,363;May 1968.

[21]Hisamatsu Nakano, Nobuyoshi Asaka, and Junji Yamauchi, "Short Helical Antenna Array Fed From a Waveguide," IEEE Transactions on Antennas and Propagation, pp.836-840;August 1984.

[22]Vishwani D. Agrawal and Gary G. Wong, "A High Performance Helical Element for Multiple Access Array on TDRSS Spacecraft," IEEE Antenna and Prpagation Symposium, pp.481-484;1979.

[23]Nizar Sultan, Malcolm Moody, Jabez Whelpton and Charles Hodgson, "Novel Broadband Double Pitch Cylindrical Helical Antenna for Satellite and Ground Applications," IEEE Antenna and Propagation Symposium, pp.162,163;1984.

[24]H. Nakano, T. Mikawa, and J. Yamauchi, "Monofilar Conical-Helix Antenna with Low Pitch Angle," IEE Proceedings, pp.379-382;December 1984.

[25]H. Nakano and J. Yamauchi, "Radiation Characteristics of Helix Antenna with Parasitic Elements," Electronics Letters, pp.687-688;August 1980.

[26]T.S.M. Maclean, "An Engineering Study of the Helix," Proceedings of the IRE, pp.112-116;January, 1963.

[27]J.V. Surutka and B.D. Popovic, "The Measurement of Self and Mutual Impedances in a Four-Element Antenna Array," IEEE Transactions on Antennas and Propagation, pp.576-578;July 1967.

[28]Arthur C. Ludwig, "Mutual Coupling, Gain , and Directivity of an Array of Two Identical Antennas," IEEE Transactions on Antennas and Propagation, pp.837-841;November 1976.

[29]A.R. Stratoti and E.J. Wilkinson, "An Investigation of the Complex Mutual Impedance Between Short Helical Array Elements," IRE Transactions on Antennas and Propagation, pp.279,280;July 1959.

[30]Jean-Pierre Daniel and C. Terret, "Experimental Verification of the Reduced Mutual Coupling Between Monopoles Using Appropriate Loads," IEEE Transactions on Antennas and Propagation, pp.737-739;September 1975.

[31]J. Bach Andersen, H.A. Lessow, and H. Schjaer-Jacobsen, "Coupling Between Minimum Scattering Antennas," IEEE Transactions on Antennas and Propagation, pp.832-835;November 1974.

[32]T. Shiokawa, Y. Karasawa, and H. Yokoi, "A Shipbourne Helical Array for Maritime Satellite Communication," Second International Conference on Antennas and Propagation, pp. 303-307; 13-16 April 1981.

[33]H.E. King and J.L. Wong, "Directivity of a Uniformly Excited NxN Array of Directive Elements," IEEE Transactions on Antennas and Propagation, pp.401-404;May 1975.

[34]H. Nakano, N. Asaka, J. Yamauchi, "Radiation Characteristics of Short Helical Antenna and Its Mutual Coupling," Electronics Letters, pp.202-203;March 1984.

[35]John D. Kraus, "Helical Beam Antennas for Wide-Band Applications," Proceedings of the IRE, pp.1236-1242;October, 1948.

[36]H. Nakano and J. Yamauchi, "Characteristics of Modified Spiral and Helical Antennas"

[37]Charles C. Kilgus, "Shaped-Conical Radiation Pattern Performance of the Backfire Quadrifilar Helix," IEEE Transactions on Antennas and Propagation, pp.392-397;May 1975.

[38]A.R. Neureuther, P.W. Klock, and R. Mittra, "A Study of the Sheath Helix with a Conducting Core and its Application to the Helical Antenna," IEEE Transactions on Antennas and Propagation, pp.203-210;March 1967.

[39]J. Dijk, H.H.H. Groothuis, and E.J. Maanders, "Some Improvements in Antenna Noise Temperature Calculation," IEEE Transactions on Antennas and Propagation, pp.690-692;September 1970.

[40]R. Johnson and H. Jasik, Antenna Engineering Handbook, McGraw Hill, New York, 1987.

[41]Thomas A. Milligan, Modern Antenna Design, McGraw Hill, New York, 1985.

[42]Kai-Fong Lee, Ping-Fai Wong, and Kang-Fong Larm, "Theory of Uniform and Quasi-Taper Helical Antennas," IEEE Transactions on Antennas and Propagation, pp.1017-1021;September, 1982.

[43]Keith R. Carver, "The Helicone-A Circularly Polarized Antenna with Low Sidelobe Level," Proceedings of the IEEE, p.559;May 1967.

[44]J.L. Yen, "Coupled Surface Waves and Broadside Arrays of End-Fire Antennas," IRE Transactions on Antennas and Propagation, pp.296-304;May 1961.

[45]Constantine A. Balanis,Antenna Theory, Harper & Row, Publishers, New York, 1982.

[46] R. Stephen Smith,"Analysis and Design of Microstrip Array Antennas, Including Mutual Coupling," Virginia Polytechnic Institute and State University Masters Thesis;June 1986.

[47] Warren L. Stutzman and Gary A. Thiele, Antenna Theory and Design, pp.134-141, John Wiley and Sons, Inc., 1981.

Appendix A

Computer Listing of Simulation/Sample Run/Algorithm

```
SAMPLE RUN OF PROGRAM HEMAN


 Single element selection
 ------------------------
 0 - Ideal helix model
 1 - Experimental data #30
 2 - Experimental data #31
 3 - Experimental data #29
 4 - Experimental data #35
 5 - Literature data
 6 - Experimental data #34

 *TYPE "-1" to Exit Program*

Enter single element option: 1
Enter array size N (as in NxN): 4
Enter the spacing (in wavelengths): 2
Enter degrees above the horizon: 10
Enter axis of rotation in degrees: 0
Enter number of increments in integration:10
 Noise Temperature in degrees Kelvin =    62.55306
 Estimated Gain (in dB) =    26.04053
 G/T =    8.078049     dB
Create a Plot of the Array Pattern(y/n)?n



 Single element selection
 ------------------------
 0 - Ideal helix model
 1 - Experimental data #30
 2 - Experimental data #31
 3 - Experimental data #29
 4 - Experimental data #35
 5 - Literature data
 6 - Experimental data #34

 *TYPE "-1" to Exit Program*

Enter single element option: -1

FORTRAN STOP
```

```
c
c       PROGRAM HEMAN
c
c       This program uses as input a two dimensional antenna pattern and outputs
c       the following:
c                       o  Forward gain of a square array specified by the user
c                       o  Noise temperature for a particular elevation angle
c                       o  G/T for a particular elevation angle
c                       o  A file containing the array radiation pattern which
c                          can be plotted in a 3-D format.
c
        Include 'ASim.Declare'
        Include 'ASim.Common'
        character*20 tab
        character*3 plot_ok
        Integer dummy,i,plot_number,num_columns
        real min_value(10)
c
c       initialize constants
c
        index_number=0
        tab='                    '
        Pi = 2.0 * acos(0.0)
        num_columns=2           !number of columns in gain file
c
c       open output file
c
        open (unit=22,file='GAIN.dat',status='unknown')
c
        write(22,*)num_columns
c
c       Read data file (contains pattern in "arbitrary" decibels)
c
                Open (Unit=20, file='Exp_new.dat',
     1                         status='old', READONLY)
c
c       read first line
c
                read (20,*)
c
c       read the data from ExpData.prn
c
                do i=0,360
                        read (20,*) dummy, APdata(1,i), APdata(2,i),APdata(3,i),
     1                                     APdata(4,i), APdata(5,i),APdata(6,i)

c
c       find the minimum data point for each plot so that they can be
c       normalized for calculations
c
                        do plot_number=1,6              !change to be generic
                        min_value(plot_number)=10000.   !big number
c
                        if(APdata(plot_number,i).lt.min_value(plot_number)) then
                                min_value(plot_number)=APdata(plot_number,i)
                        end if
c
                        end do
c
                end do
c
c               Normalize the data in decibels
c
                do plot_number=1,6
                        do i=0,360
                        APdata(plot_number,i) =
```

```
     $                    min_value(plot_number) - APdata(plot_number,i)
                        enddo
                enddo
c
c       close the data file
c
        Close (Unit=20)
c
        do while(APopt.ne.-1)
c
c       Print main menu
c
        write(*,'(/,/,/)')
        write (*,*) tab,'Single element selection'
        write (*,*) tab,'------------------------'
        write (*,*) tab,'0 - Ideal helix model'
        write (*,*) tab,'1 - Experimental data #30'
        write (*,*) tab,'2 - Experimental data #31'
        write (*,*) tab,'3 - Experimental data #29'
        write (*,*) tab,'4 - Experimental data #35'
        write (*,*) tab,'5 - Literature data'
        write (*,*) tab,'6 - Experimental data #34'
        write (*,*)
        write (*,*) tab,'*TYPE "-1" to Exit Program*'
        write (*,*)
        write (*,'(A,A,$)') tab,'Enter single element option: '
c
c       get element selection
c
        read (*,*) APOpt
c
c       execute unless -1 is selected in which case the program terminates
c
        if(APopt.ne.-1) then
c
c       If the "ideal" helix is selected, get parameters from user
c
        if (APOpt.EQ.0) then
                write (*,'(A,A,$)') tab,
     $            'Enter the helix circumference (in wavelengths): '
                read (*,*) Circum
                write (*,'(A,A,$)') tab,
     $            'Enter the number of turns in one helix: '
                read (*,*) Turns
                write (*,'(A,A,$)') tab,'Enter the pitch (in degrees): '
                read (*,*) Pitch
c
c       convert pitch angle to radians
c
                Pitch = Pitch*Pi/180.0
c
        endif
c
c       Get input from user
c
        write (*,'(A,A,$)') tab,'Enter array size N (as in NxN): '
        read (*,*) N
        write (*,'(A,A,$)') tab,'Enter the spacing (in wavelengths): '
        read (*,*) Space
        write (*,'(A,A,$)') tab,'Enter degrees above the horizon: '
        read (*,*) PtEl
        write (*,'(A,A,$)') tab,'Enter axis of rotation in degrees: '
        read (*,*) PtAz
c
c       adjust elevation and azimuth angles.  This program sets zenith to
c       zero degrees elevation, so a conversion from the user input is
```

```
c       required.
c
        PtEl = (Pi/2.)-PtEl*pi/180.
        PtAz = PtAz*pi/180.
c
c       enter the number or integration increments
c
        write (*,'(A,A,$)') tab,'Enter number of increments in integration: '
        read (*,*) IntRes
c
c       calculate forward gain, noise temperature, and G/T for the array
c
        Call Analysis
c
c       Ask if plot is desired. If so, then create a plot file
c
        write(*,'(A,A,$)')tab,'Create a Plot of the Array Pattern(y/n)?'
        read(5,'(A)')plot_ok
        if(plot_ok.eq.'Y'.or.plot_ok.eq.'y'.or.plot_ok.eq.'yes'.or.
     $     plot_ok.eq.'YES') then
c
c       create a 2-D plot file
c
                Call Plot_2d
c
        end if
c
c
        endif                           !end of execution IF statement
c
        end do                          !End of main loop
c
c       PROGRAM TERMINATES
c
c       close output file
c
        close(unit=22)
c
        Stop
        End
c
c
        Function AP(Az,El)
c
        Include 'ASim.Declare'
        Include 'ASim.Common'
c
        real RealPtr, APLow, APHi
        integer Ptr
        real Yap, HoldAP
c
c       if ideal helix is selected, then calculate HOLDAP accordingly
c
        if (APOpt.EQ.0) then
                Yap = Pi*(Circum*tan(pitch)*(1-cos(El))+(1.0/(2.0*Turns)))
                HoldAP = sin(Pi/(2.0*Turns))*cos(El)*(sin(Turns*Yap)/sin(Yap))
        else
                RealPtr = El*180.0/Pi
                ptr = Int (RealPtr)
                APlow = 10.0**(APdata(APOpt,ptr)/10.0)
                APhi  = 10.0**(APdata(APOpt,(ptr+1))/10.0)
                HoldAP = ((RealPtr-ptr) * (APhi-APlow)) + APlow
                HoldAP = SQRT (HoldAP)
        endif
c
        AP = HoldAP
```

```
Return
End

Function AF(Az,El)

Include 'ASim.Declare'
Include 'ASim.Common'

real a,b,c,d
real Y,Yx,Yy
integer NbyN
real HoldAF

NbyN = N*N

Y = Space*Pi*sin(El)
Yx = Y * cos(Az)
Yy = Y * sin(Az)

a = sin(float(N)*Yx)
b = sin(float(N)*Yy)
c = sin(Yx)
d = sin(Yy)

if (c*d.NE.0.0) then
        HoldAF = (a*b)/(c*d*float(NbyN))
elseif (c.NE.0.0) then
        HoldAF = a/(c*float(N))
elseif (d.NE.0.0) then
        HoldAF = b/(d*float(N))
else
        HoldAF = 1.0
end if

AF = HoldAF

Return
End

Function NT(Az,El)

Include 'ASim.Declare'
Include 'ASim.Common'

Real HoldNT
Real X, Y, Z
Real Xs, Ys, Zs
Real AzS, ElS, dummy

Call AzElR_XYZ (Az, El, 1., X, Y, Z)
Call XYZRotation (PtAz, PtEl, 0.0, X, Y, Z, Xs, Ys, Zs)
Call XYZ_AzElR (Xs, Ys, Zs, AzS, ElS, Dummy)

if ((ElS.LT.(Pi/2.)).OR.(ElS.GE.(3.*Pi/2.))) then
        HoldNT = 6.0
else
        HoldNT = 300.0
endif
c
NT = HoldNT
c
Return
End
c
Subroutine Analysis
```

```
      Include 'ASim.Declare'

      Real    GxTSinEl, GxSinEl, X(500), Wx(500), Y(500), Wy(500)
      Real    LGauss, DoubNI
      Real    Ans1, Ans2
      EXTERNAL GxTSinEl, GxSinEl
      Real    RefGain, Gain, RefPtr, Ptr,G_over_T
      Include 'ASim.Common'
      character*20 tab

      tab='                    '

      Call LGauss (X, Wx, IntRes, 999)
      Call LGauss (Y, Wy, IntRes, 999)

      Ans1 = DoubNI (GxTSinEl, 0.0, 2.0*Pi, 0.0, Pi, IntRes, IntRes,
     1                X, Wx, Y, Wy, 6, 6)
      Ans2 = DoubNI (GxSinEl, 0.0, 2.0*Pi, 0.0, Pi, IntRes, IntRes,
     1                X, Wx, Y, Wy, 6, 6)

      write (*,*) tab,'Noise Temperature in degrees Kelvin = ',Ans1/Ans2
      write (*,*) tab,'Estimated Gain (in dB) = ',10.0 * Log10(4.*Pi/Ans2)

      calculate G/T

      G_over_T=10.0*log10((4.*Pi/Ans2)/(Ans1/Ans2))
      write (*,*) tab,'G/T = ',G_over_T,' dB'

      write data to data file

      write(22,*)-PTel*180./pi+90,Ans1/Ans2,
     $ 10.0 * Log10(4.*Pi/Ans2),G_over_T
      index_number=index_number+1
      write(22,*)space,10.0 * Log10(4.*Pi/Ans2)

      Return

 99   write (*,*) ' Error in LGauss routine.'
      Return
      End

      Real Function GxTSinEl(Az, El)
      Include 'ASim.Declare'
      Include 'ASim.Common'

      GxTSinEl = ((AP(Az,El)*AF(Az,El))**2)*NT(Az,El)*Sin(El)

      Return
      End

      Real Function GxSinEl(Az, El)
      Include 'ASim.Declare'
      Include 'ASim.Common'

      GxSinEl = ((AP(Az,El)*AF(Az,El))**2)*Sin(El)

      Return
      End

      Subroutine Plot
      Include 'ASim.Declare'
      Include 'ASim.Common'

      Integer I,J
      Real    Ri, Rj, Gain
      character*20 tab
```

```
c
      tab='                    '
c
      write (*,'(A,A,$)') tab,'Enter data points in 90 degrees: '
      read (*,*) PlotRes
      Open(Unit = 11,file='asim.plot',status='unknown',form='formatted')
c
      do I = -PlotRes,PlotRes
c
            do J=-PlotRes,PlotRes
c
            Ri = float(I)/float(PlotRes)
            Rj = float(J)/float(PlotRes)
c
            if ((Rj.NE.0.0).OR.(Ri.NE.0.0)) then
                  Az = atan2 (Ri, Rj)
                  El = Pi * sqrt(Rj*Rj+Ri*Ri) /2.0
            else
                  Az = Pi/2.0
                  El = 0.0
            endif
c
            Gain = 10.0*log10((af(Az,El) * ap(Az,El))**2)
            if (Gain.LT.-40.0) Gain = -40.0
            if (El.GT.(Pi/2.0)) Gain = -40.0
            write (11,*) Gain
            end do
      end do
      Close (Unit=11)
c
      Return
      End

      Subroutine Plot_2D
      Include 'ASim.Declare'
      Include 'ASim.Common'
c
      integer number_of_columns
      Real    Gain,el_rad,az_rad
      character*20 tab
c
      tab='                    '
c
      write (*,'(A,A,$)') tab,'Enter azimuth cut in degrees: '
      read (*,*) Az
      Open(Unit = 12,file='heman.plot',status='unknown',form='formatted')
c
      number_of_columns=2
      write(12,*)number_of_columns
      az_rad=pi/180.*az
c
c     do plot
c
      do el=0.,360.
            el_rad=el*pi/180.
c
c     calculate gain at the specified Az,El coordinates
c
            Gain = 10.0*log10((af(Az_rad,El_rad) * ap(Az_rad,El_rad))**2)
            if(Gain.lt.-40) then
                  Gain=-40.
            endif
c
            write (12,*) (40+gain)*sin(el_rad),(40+gain)*cos(el_rad)
      end do
      Close (Unit=12)
c
      Return
      End
```

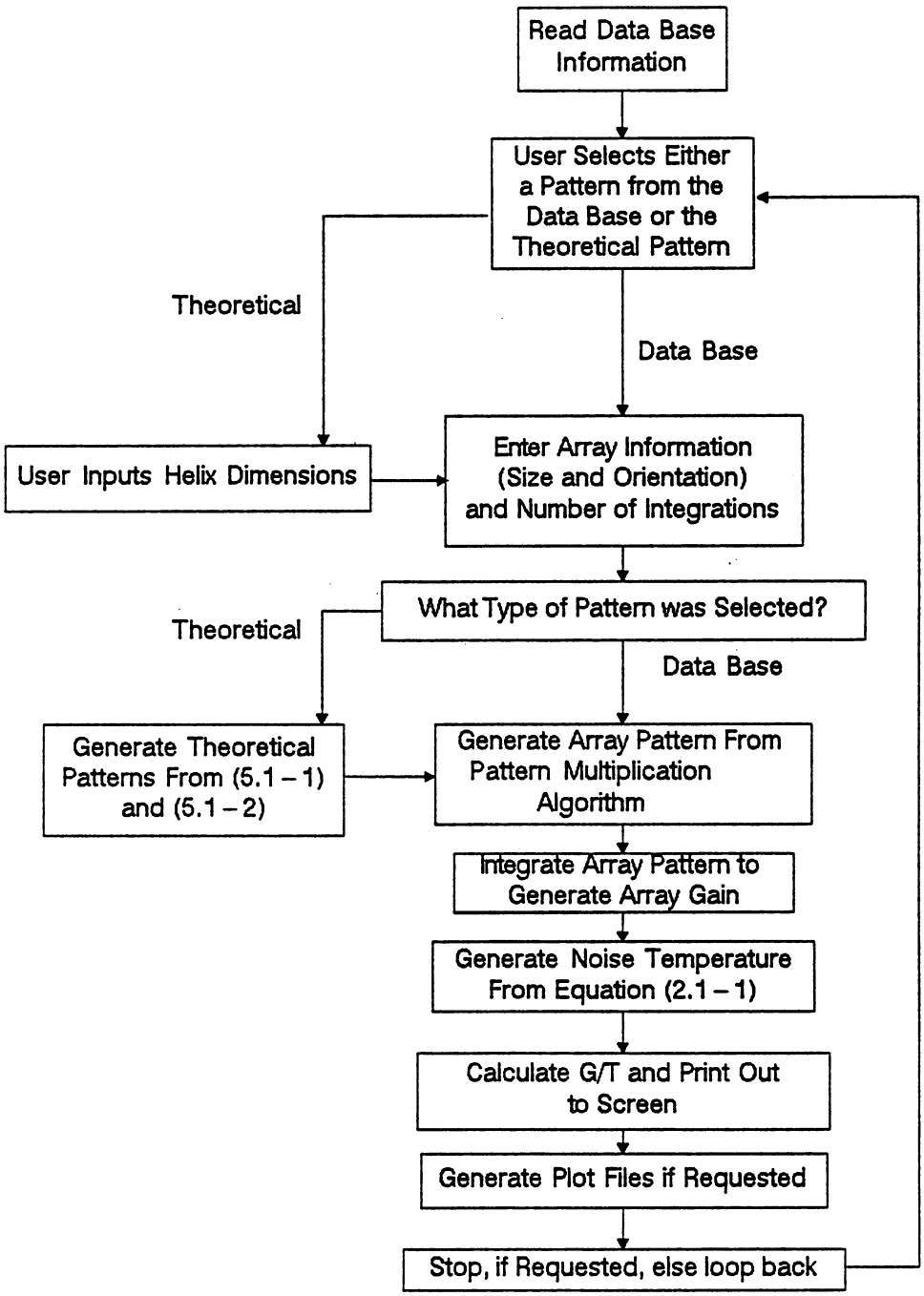

Figure A – 1: HEMAN Flowchart

Appendix B

Data: Pattern Variation Over Frequency for Helix #1, Test Configuration I

Frequency: 1.1 GHz

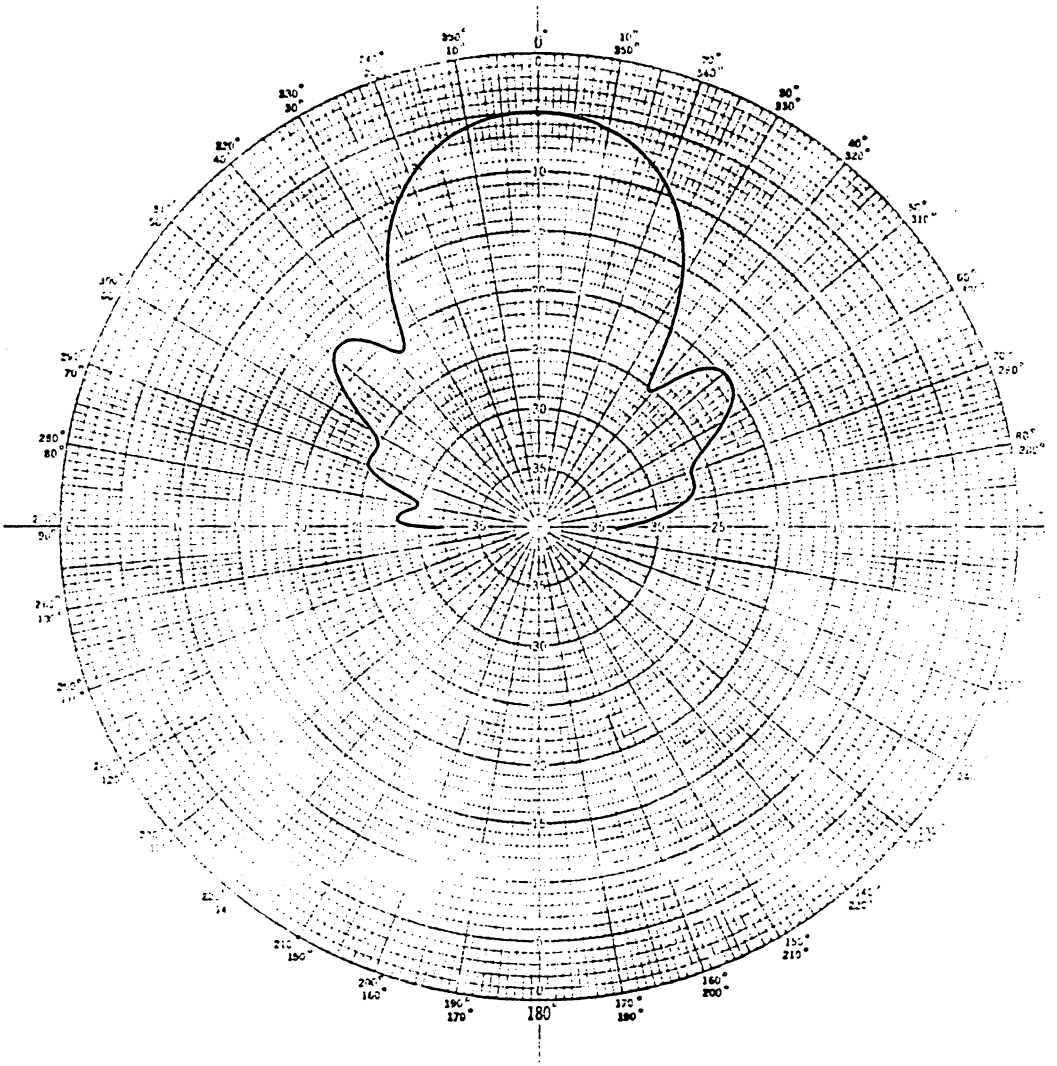

Figure B – 1 : Field Pattern of Helix #1 Over Frequency

Frequency: 1.2 GHz

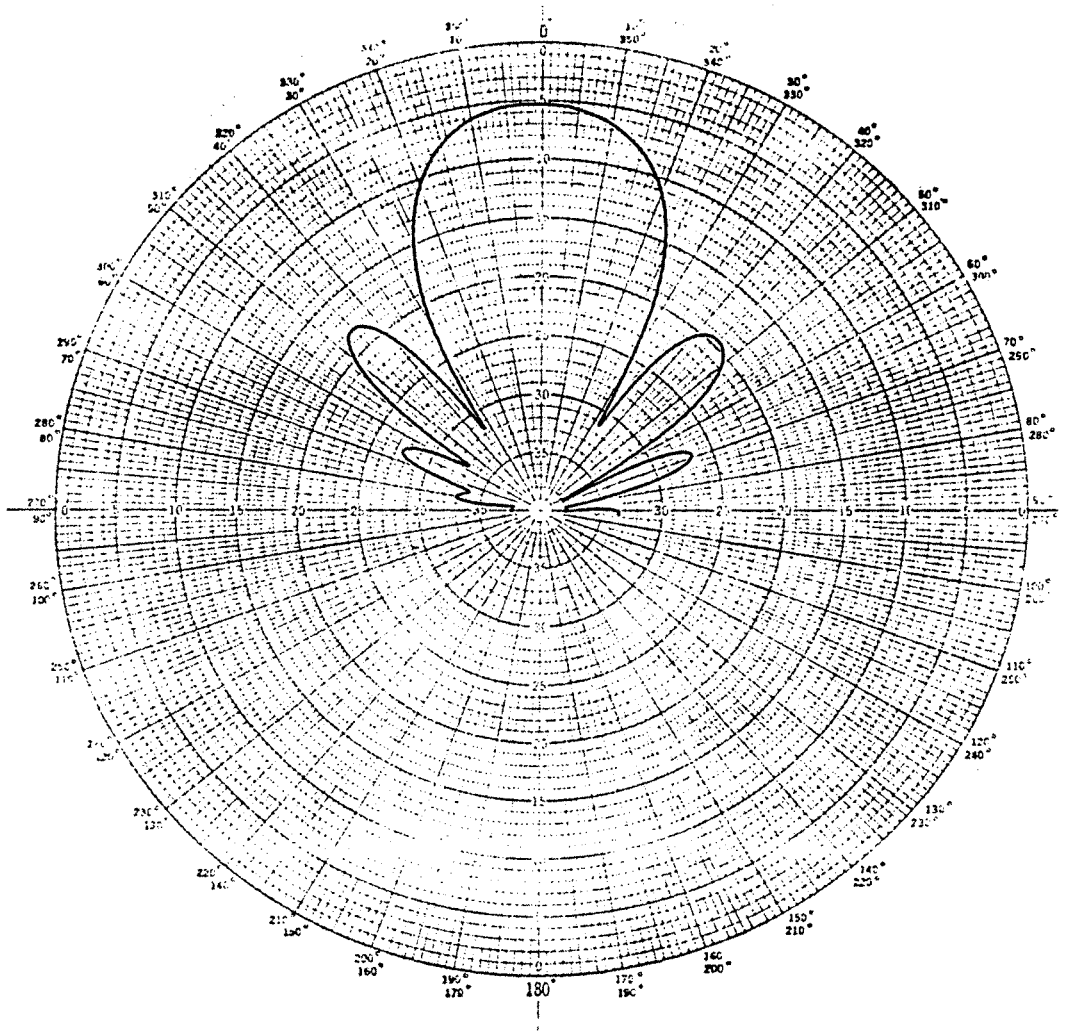

Figure B – 1 : Field Pattern of Helix #1 Over Frequency (continued)

Frequency: 1.25 GHz

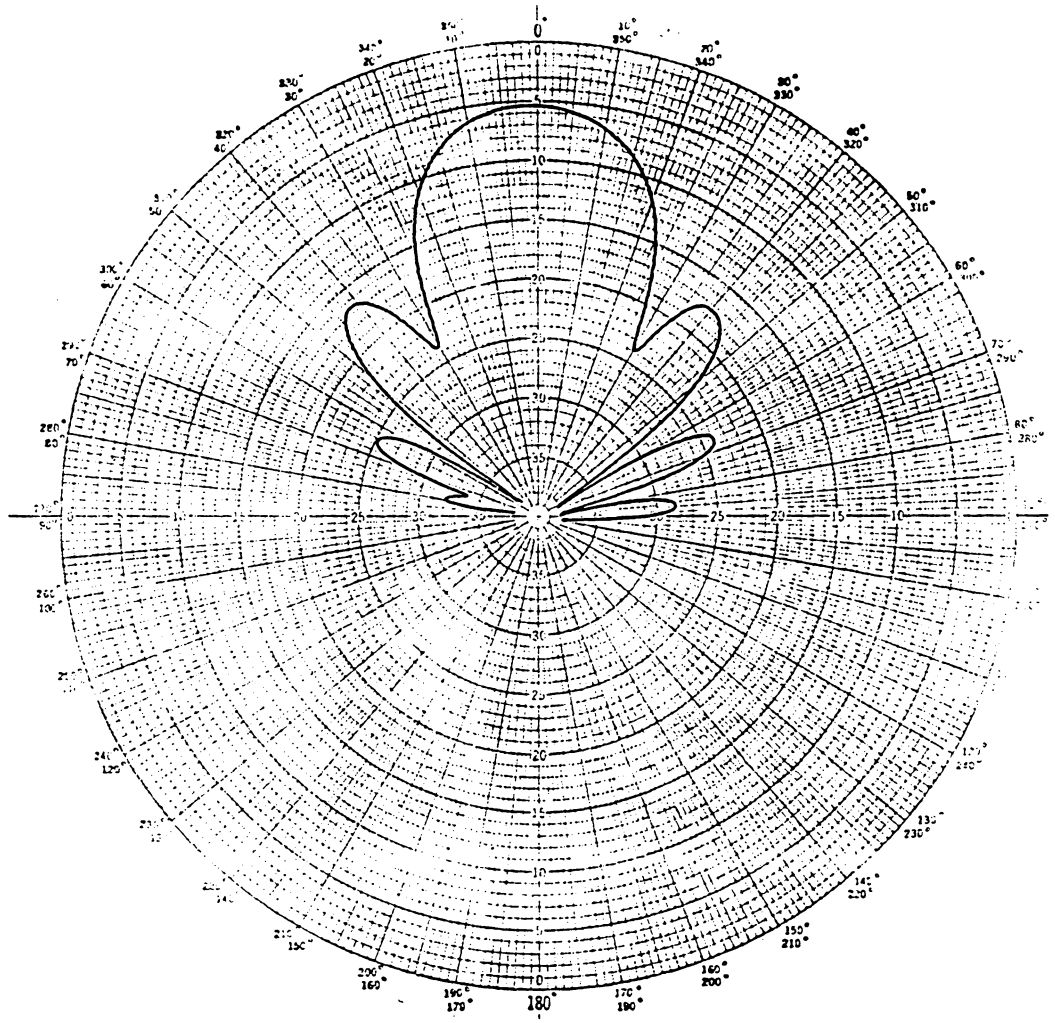

Figure B – 1 : Field Pattern of Helix #1 Over Frequency (continued)

Frequency: 1.275 GHz

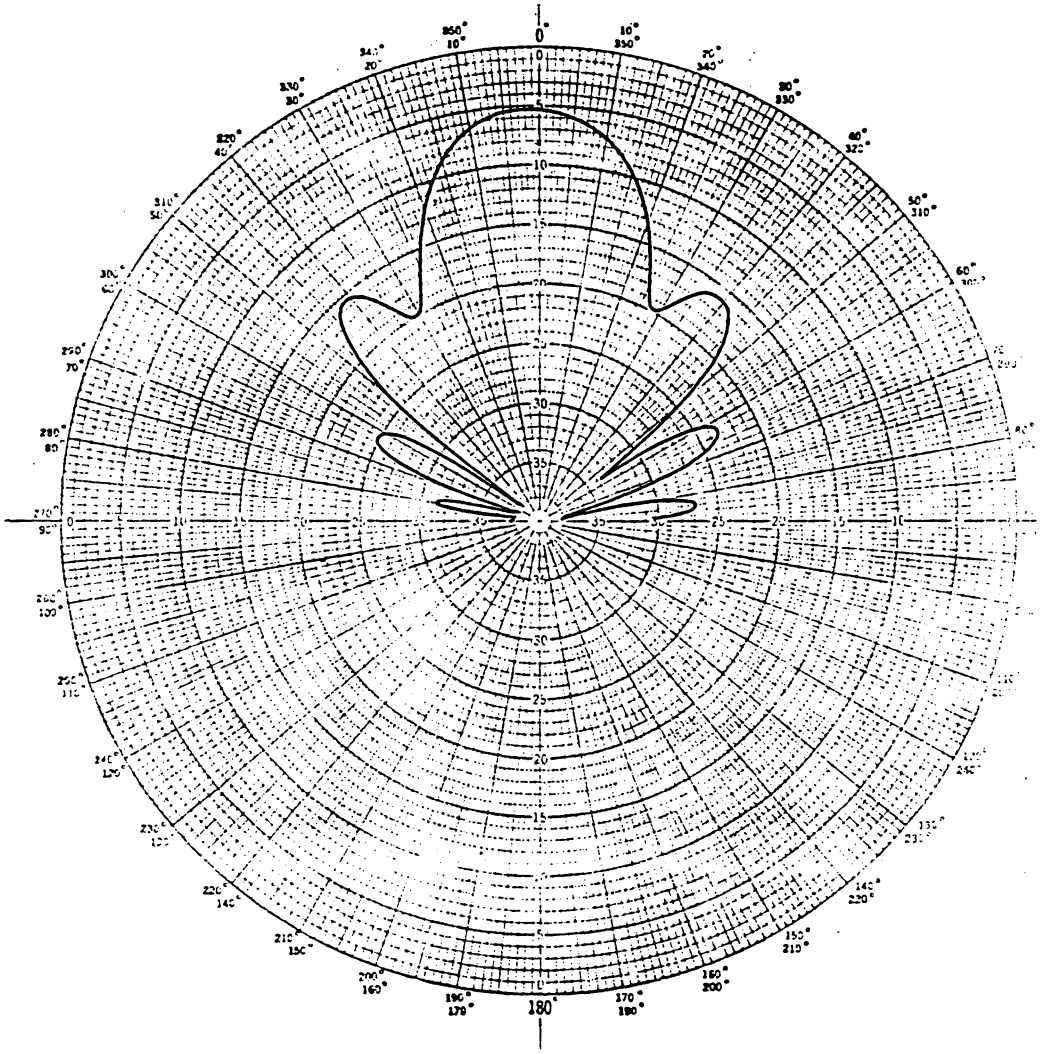

Figure B – 1 : Field Pattern of Helix #1 Over Frequency (continued)

Frequency: 1.3 GHz

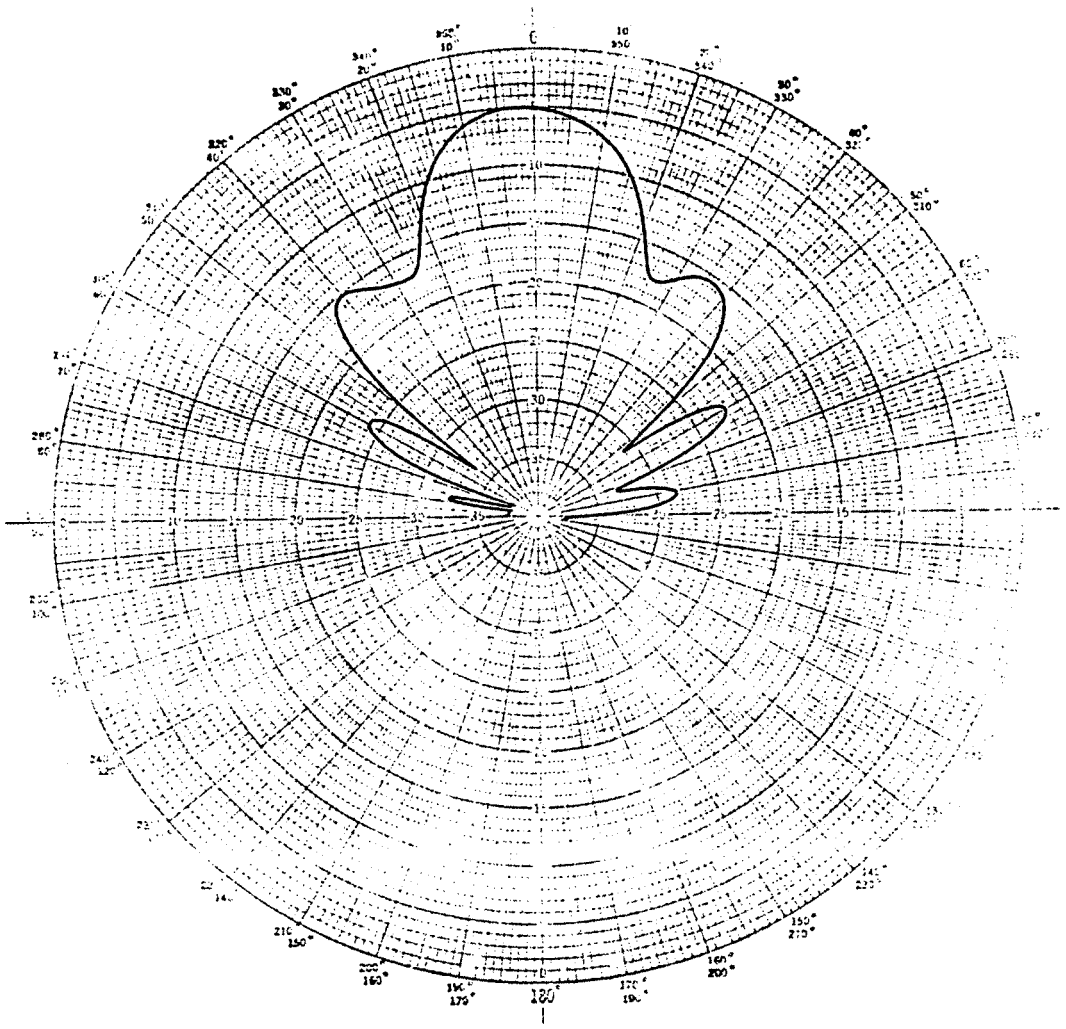

Figure B – 1 : Field Pattern of Helix #1 Over Frequency (continued)

Frequency: 1.325 GHz

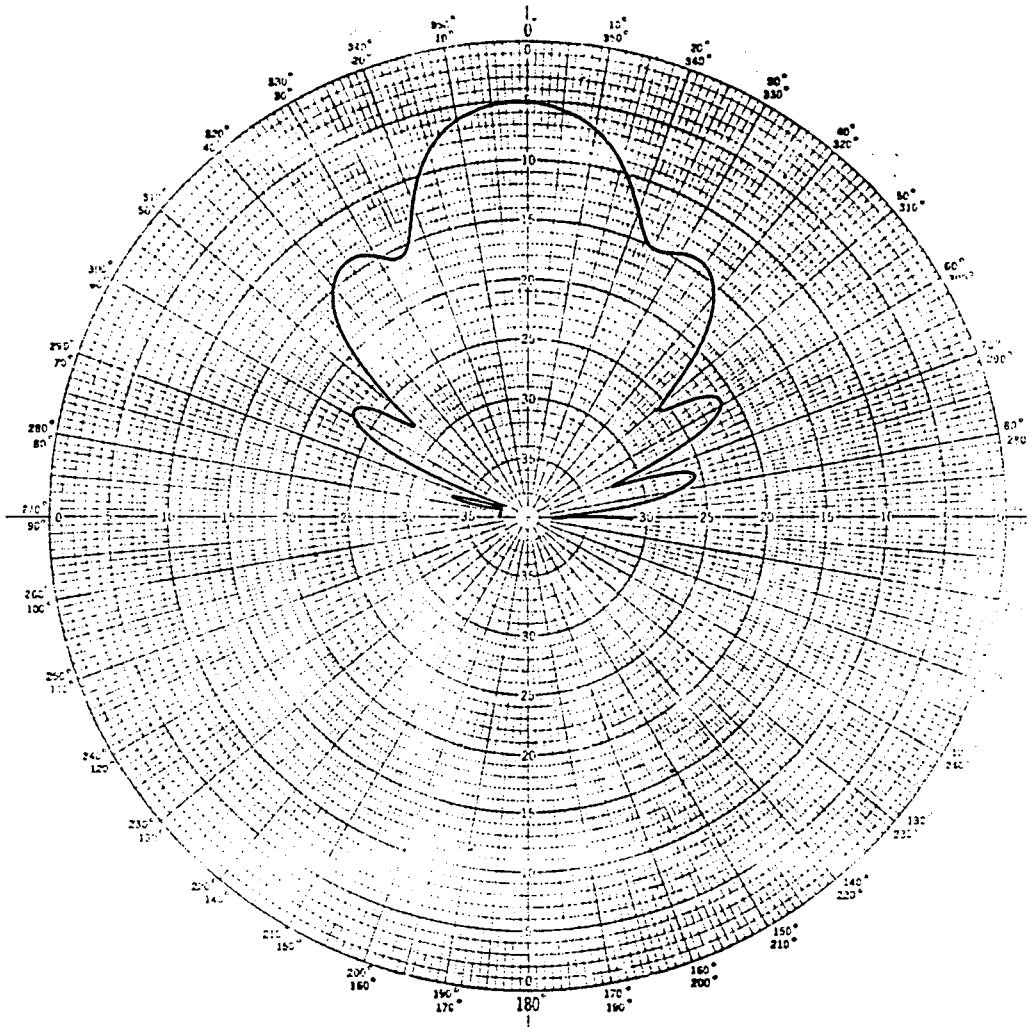

Figure B – 1 : Field Pattern of Helix #1 Over Frequency (continued)

Frequency: 1.35 GHz

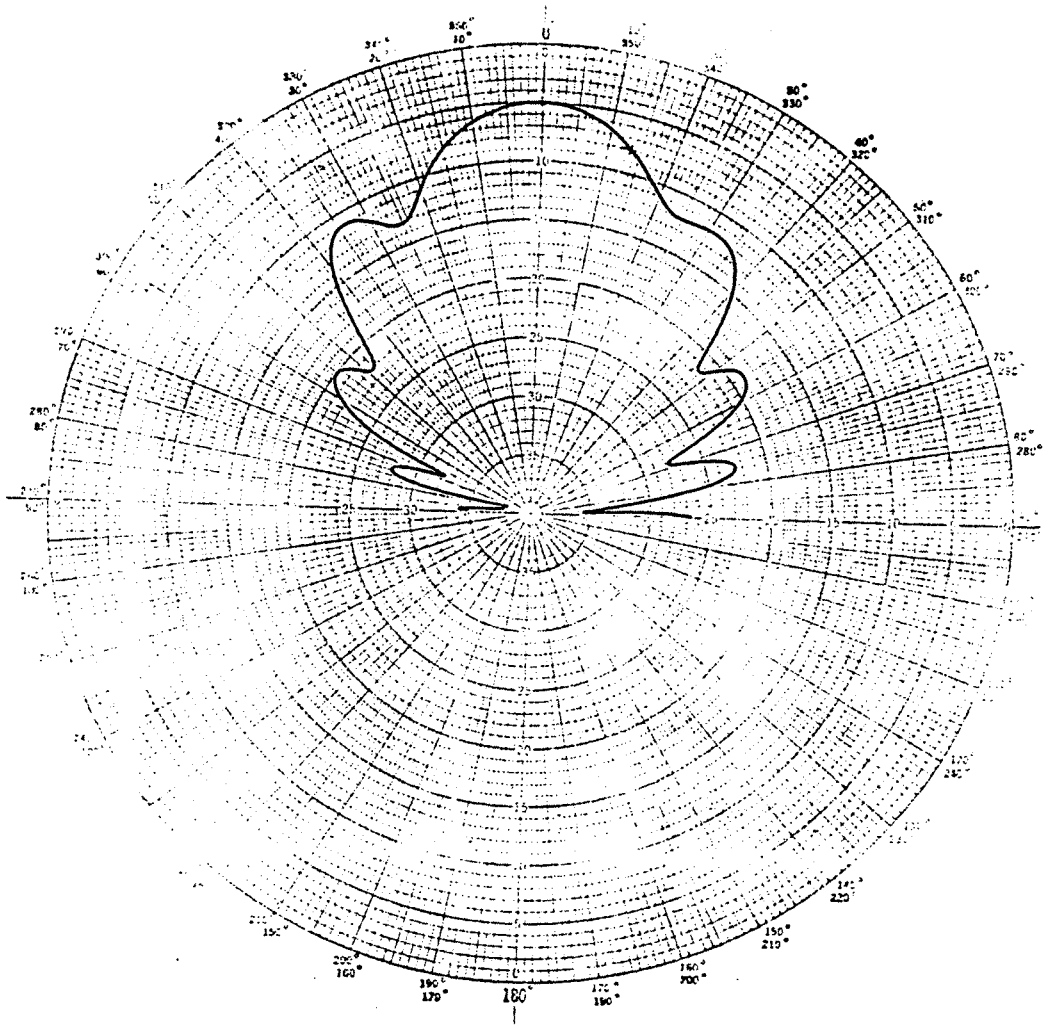

Figure B – 1 : Field Pattern of Helix #1 Over Frequency (continued)

Frequency: 1.4 GHz

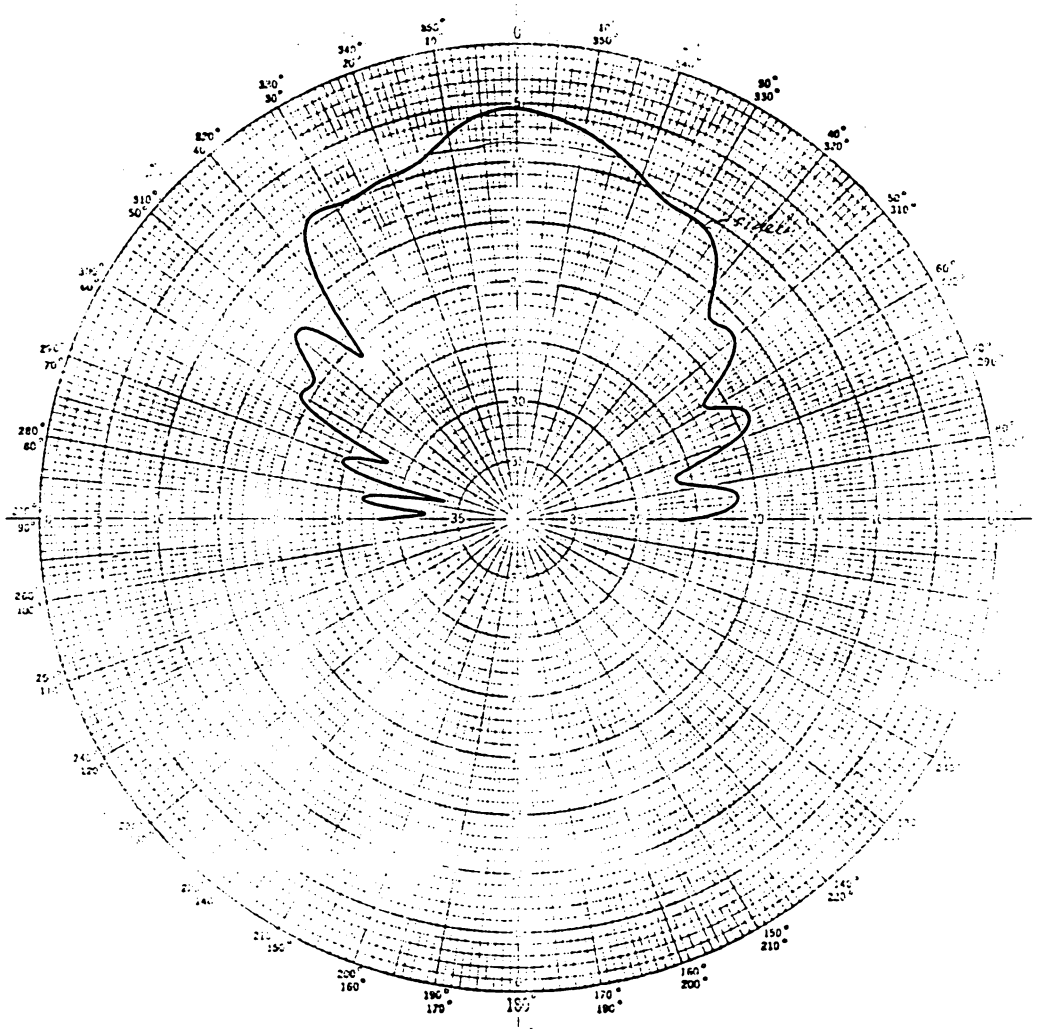

Figure B – 1 : Field Pattern of Helix #1 Over Frequency (continued)

Frequency: 1.5 GHz

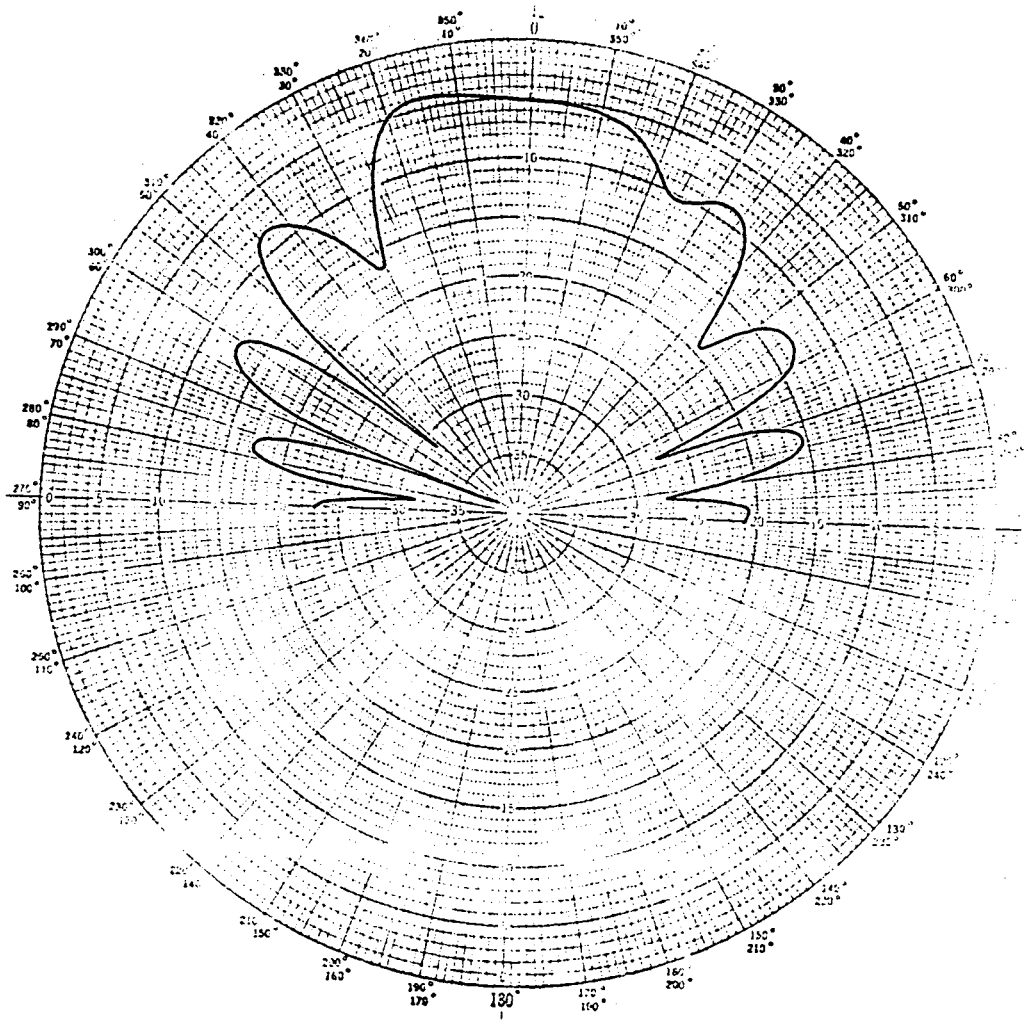

Figure B – 1 : Field Pattern of Helix #1 Over Frequency (continued)

Frequency: 1.6 GHz

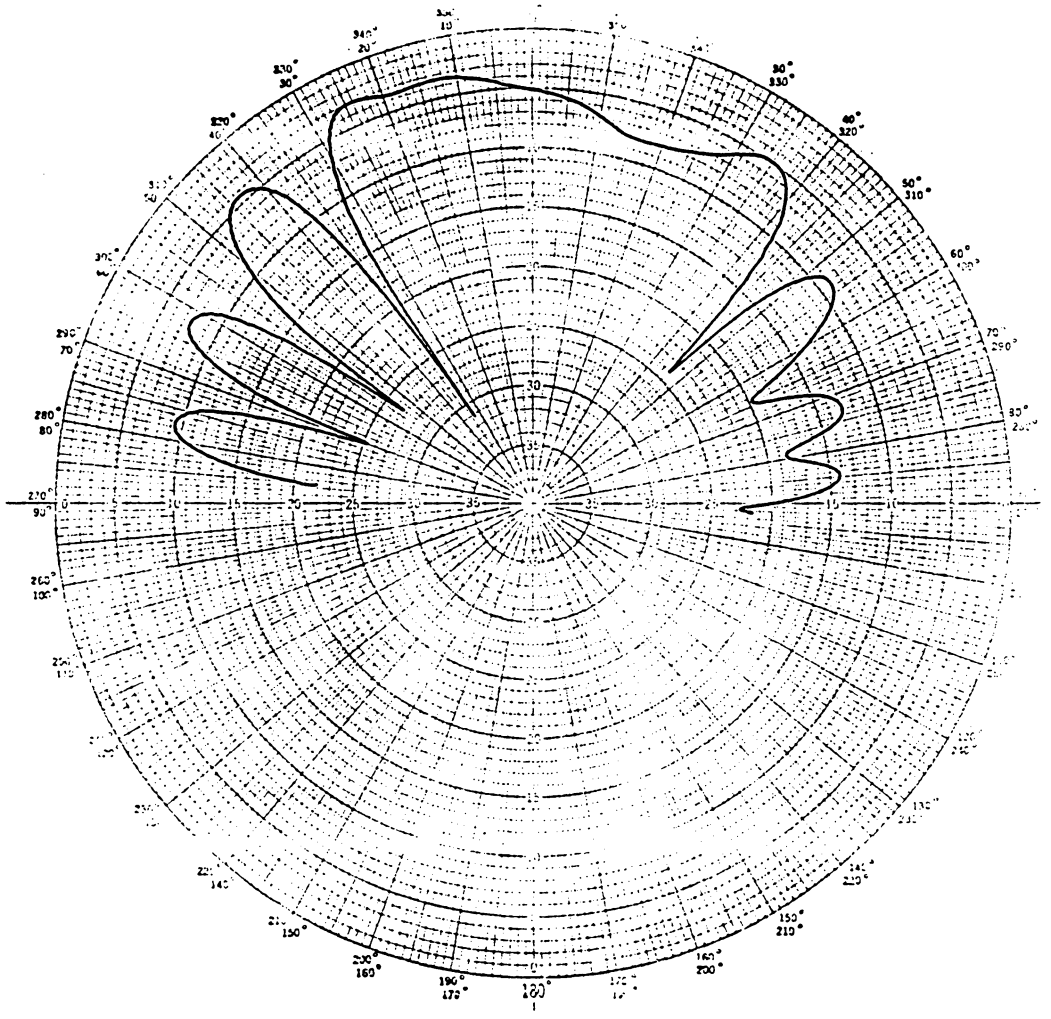

Figure B – 1 : Field Pattern of Helix #1 Over Frequency (continued)

Frequency: 1.7 GHz

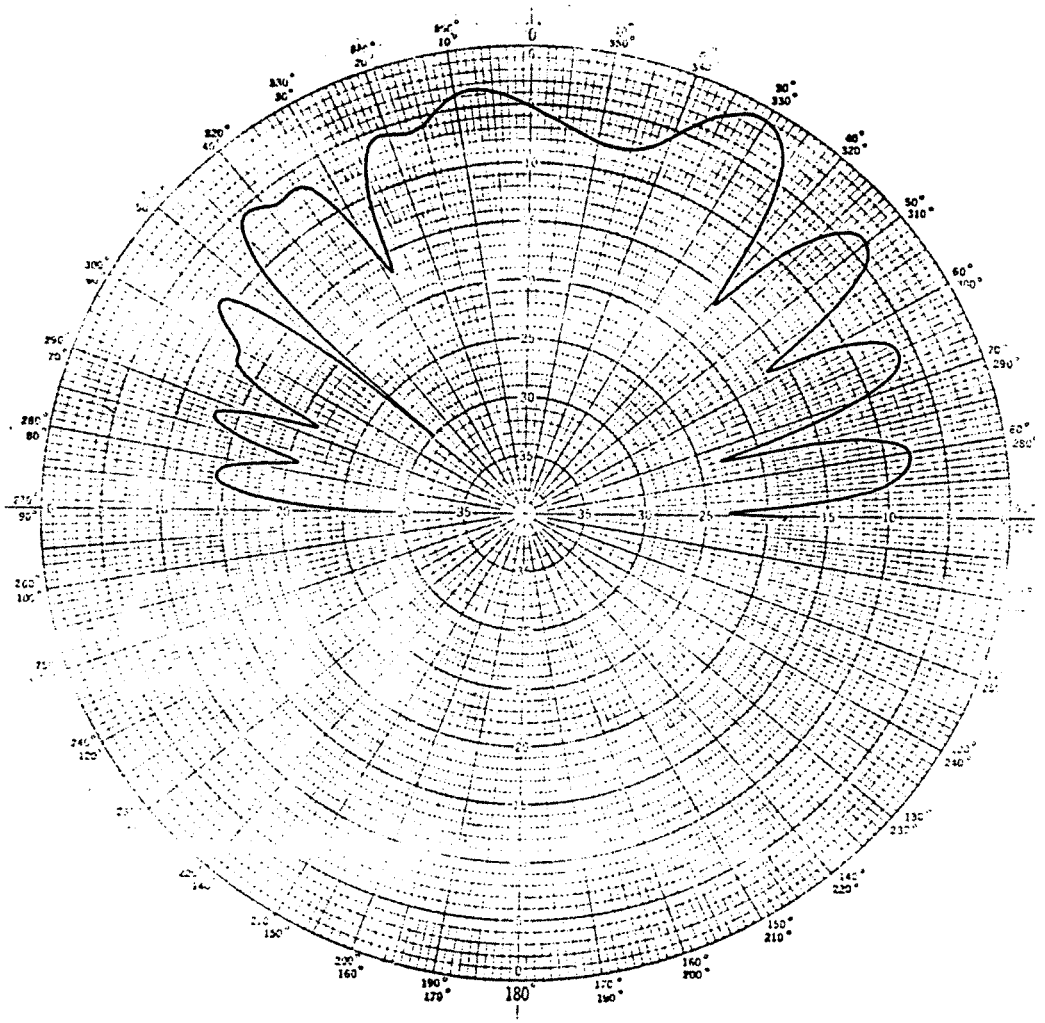

Figure B – 1 : Field Pattern of Helix #1 Over Frequency (continued)

Frequency: 1.8 GHz

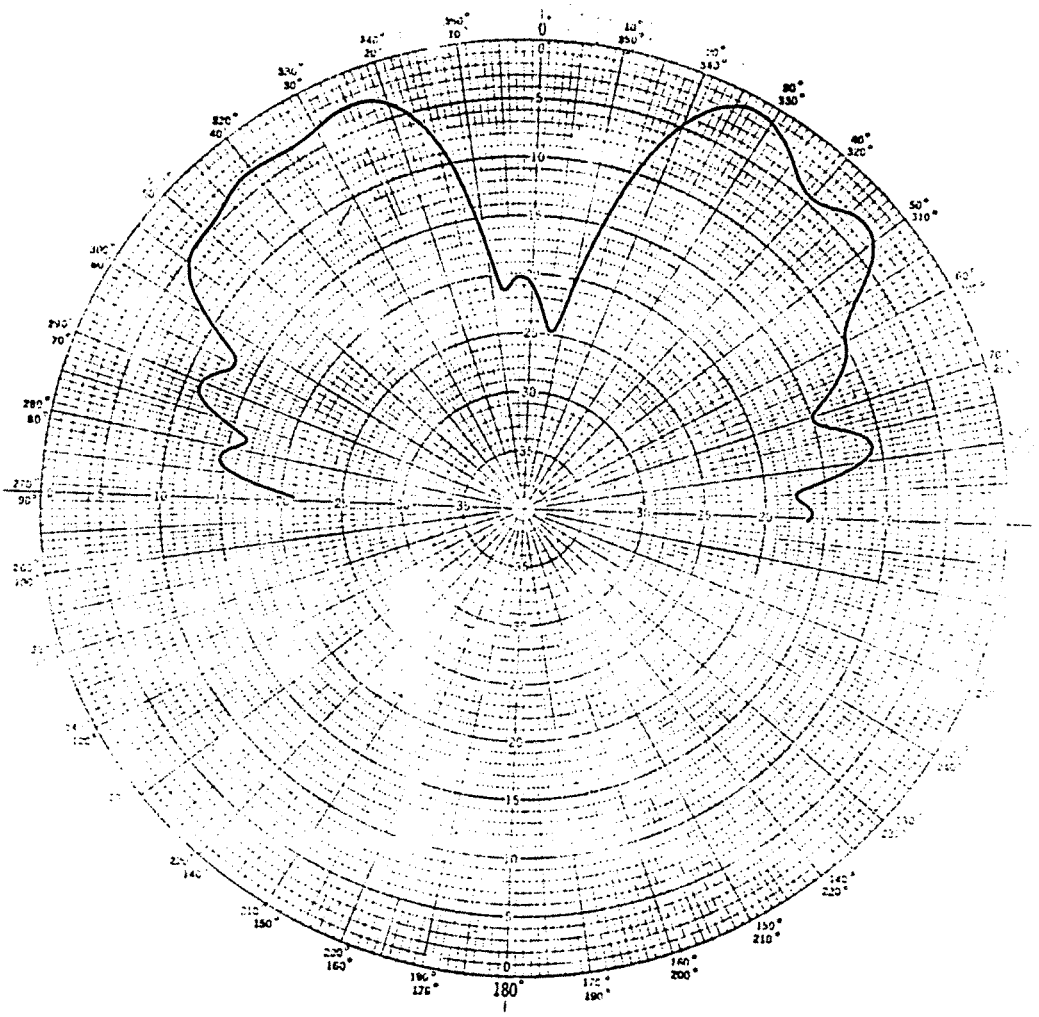

Figure B – 1 : Field Pattern of Helix #1 Over Frequency (continued)

The vita has been removed from the scanned document